

**Modeling and Control of Airport Departure Processes  
for Emissions Reduction**

by

Ioannis Simaiakis

Eng. Dipl., National Technical University of Athens (2006)

Submitted to the Engineering Systems Division  
and the Department of Aeronautics and Astronautics  
in partial fulfillment of the requirements for the degrees of

Master of Science in Technology and Policy

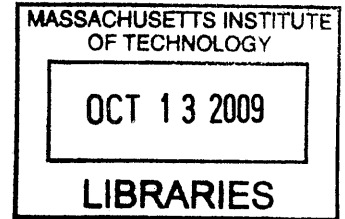
and

Master of Science in Aeronautics and Astronautics

at the

MASSACHUSETTS INSTITUTE OF TECHNOLOGY

September 2009



**ARCHIVES**

© 2009 Massachusetts Institute of Technology. All rights reserved.

Author .....

Engineering Systems Division  
and the Department of Aeronautics and Astronautics  
August 12, 2009

Certified by .....

Hamsa Balakrishnan  
Assistant Professor of Aeronautics and Astronautics and Engineering Systems  
Thesis Supervisor

Accepted by .....

David L. Darmofal  
Associate Professor of Aeronautics and Astronautics  
Associate Department Head  
Chair, Committee on Graduate Students

Accepted by .....

Dava J. Newman  
Professor of Aeronautics and Astronautics and Engineering Systems  
Director, Technology and Policy Program



# Modeling and Control of Airport Departure Processes for Emissions Reduction

by

Ioannis Simaiakis

Submitted to the Engineering Systems Division  
and the Department of Aeronautics and Astronautics  
on August 12, 2009, in partial fulfillment of the  
requirements for the degrees of  
Master of Science in Technology and Policy  
and  
Master of Science in Aeronautics and Astronautics

## Abstract

Taxiing aircraft contribute significantly to the fuel burn and emissions at airports. This thesis investigates the possibility of reducing fuel burn and emissions from surface operations through a reduction of the taxi times of departing aircraft. Data analysis of the departing traffic in four major US airports provides a comprehensive assessment of the impact of surface congestion on taxi times, fuel burn and emissions. For this analysis two metrics are introduced: one that compares the taxi times to the unimpeded ones and another that evaluates them in terms of their contribution to the airport's throughput.

A novel approach is proposed that models the aircraft departure process as a queuing system. The departure taxi (taxi-out) time of an aircraft is represented as a sum of three components: the unimpeded taxi-out time, the time spent in the departure queue, and the congestion delay due to ramp and taxiway interactions. The dependence of the taxi-out time on these factors is analyzed and modeled. The performance of the model is validated through a comparison of its predictions with observed data at Boston's Logan International Airport (BOS).

A reduction in taxi times may be achieved through the queue management strategy known as *N-Control*, which controls the pushback process so as to keep the number of departing aircraft on the surface of the airport below a specified threshold. The developed model is used to quantify the impact of *N-Control* on taxi times, delays, fuel burn and emissions at BOS. Finally, the benefits and implications of *N-Control* are compared to the ones theoretically achievable from a scheme that controls the takeoff queue of each departing aircraft.

Thesis Supervisor: Hamsa Balakrishnan

Title: Assistant Professor of Aeronautics and Astronautics and Engineering Systems



## Acknowledgments

This research was funded by the FAA under the PARTNER Center of Excellence and by NASA through the Airspace Systems Program –Airportal Program. I was also supported by the Airport Cooperative Research Program (ACRP) through a Graduate Research Award.

First, I would like to thank my research supervisor, Professor Hamsa Balakrishnan, for her guidance and support during the last two years. I would especially like to thank Professor Balakrishnan for giving me the opportunity to work on such an exciting project. Her research interests and activities were pivotal for my decision to come to MIT for graduate studies. Professor Balakrishnan has also embraced and supported my decision to continue in the PhD track under her supervision. Professor Balakrishnan has devoted numerous hours in meetings and discussions and has urged me to pursue exciting opportunities, such as the ACRP. I am also especially grateful to Professor Balakrishnan for all the time she has devoted to make me a better academic writer and presenter.

I would like to thank Professor Odoni for all the conversations we have had and the continuous guidance he has offered me since I came to MIT. I would also like to thank Professor Hansman for his feedback he has provided on my work and the opportunity he has given me to be part of the Joint University Program sessions. I would like to thank Flavio Leo from MASSPORT for all the useful information and data he has generously offered me.

I would also like to thank all the wonderful labmates in the International Center for Air Transportation (ICAT) at MIT who made my life and work so much more joyful. My ICAT colleague Varun Ramanujam deserves special credit for all the guidance he has offered me in probability, statistics and optimization. I am also grateful to another ICAT colleague, Indira Deonandan, for the calculations on fuel burn and emissions impacts she performed for this thesis. I would like to thank my summer UROP, Max Brand, for the calculations he did on congestion and taxi times. A special thanks goes to my friend Nikolas Pyrgiotis with whom I spent together this unique winter break studying for quals. I would also like to thank another friend, Kostas Bimpikis, for all the philosophical discussions we have had on the the mission of academic research and the meaning of a PhD dissertation.

A special and huge thank-you note goes to my parents, Panagiota and Kostas, for all their support they have given me while at MIT and their life-long commitment to providing me with the best educational opportunities available. Finally, I am especially grateful to my grandparents, Vasiliki and Iraklis, who have always stood next to me and supported me in every possible way.



# Contents

<b>1</b>	<b>Introduction</b>	<b>19</b>
1.1	Organization of the thesis . . . . .	21
<b>2</b>	<b>Data Sources</b>	<b>23</b>
2.1	The Aviation System Performance Metrics (ASPM) database . . . . .	23
2.2	Flights not reported in ASPM . . . . .	24
2.3	OOOI and non-OOOI flights . . . . .	25
<b>3</b>	<b>The problem of surface congestion</b>	<b>31</b>
3.1	Introduction . . . . .	31
3.2	The notion of segments . . . . .	31
3.3	Flow analysis of the departure process . . . . .	32
3.4	Congestion metric . . . . .	34
3.5	A metric for the “sustained departure capacity” . . . . .	35
3.6	Optimal time interval for take-off rate estimation . . . . .	36
3.7	Congestion analysis for major airports in 2007 . . . . .	37
3.7.1	John F. Kennedy International Airport(JFK) . . . . .	37
3.7.2	Newark Liberty International Airport (EWR) . . . . .	40
3.7.3	Philadelphia International Airport (PHL) . . . . .	43
3.7.4	Boston Logan International Airport (BOS) . . . . .	45
3.8	Summary . . . . .	48
<b>4</b>	<b>The effect of surface congestion on taxi times</b>	<b>49</b>
4.1	Introduction . . . . .	49
4.2	The unimpeded taxi-out time metric . . . . .	49

4.2.1	Definition of unimpeded taxi-out times . . . . .	49
4.2.2	Estimation of unimpeded taxi-out times . . . . .	50
4.2.3	Example of unimpeded taxi-out time calculation . . . . .	53
4.2.4	Unimpeded taxi-out times estimation for a segment in BOS . . . . .	56
4.2.5	Unimpeded taxi-out time as a baseline . . . . .	59
4.2.6	Method description . . . . .	59
4.3	Saturation taxi time . . . . .	59
4.3.1	Definition of saturation taxi time . . . . .	59
4.3.2	Estimation of the saturation taxi time . . . . .	61
4.4	Taxi times analysis . . . . .	62
4.4.1	JFK taxi times . . . . .	63
4.4.2	EWR taxi times . . . . .	64
4.4.3	PHL taxi times . . . . .	65
4.4.4	BOS taxi times . . . . .	67
4.5	Emissions analysis . . . . .	68
<b>5</b>	<b>A queuing model of the departure process</b>	<b>71</b>
5.1	Introduction . . . . .	71
5.2	Related work . . . . .	71
5.3	Model inputs and outputs . . . . .	72
5.4	Model structure . . . . .	74
5.5	Data requirements . . . . .	76
5.6	Model development for BOS . . . . .	77
5.6.1	Unimpeded taxi time calculation . . . . .	77
5.6.2	Identification of throughput saturation points . . . . .	77
5.6.3	Modeling the runway service process . . . . .	78
5.6.4	Modeling ramp and taxiway interactions . . . . .	80
5.7	Model results . . . . .	85
5.7.1	Taxi times prediction . . . . .	85
5.7.2	Predicting runway queues and taxiway congestion . . . . .	88
5.7.3	Emissions and fuel burn prediction . . . . .	88
5.8	Model Validation . . . . .	89



5.9	A predictive model of departure operations . . . . .	92
5.9.1	Estimating the states of surface queues and taxi-out times . . . . .	92
5.10	Summary . . . . .	94
<b>6</b>	<b>Management of the pushback queue</b>	<b>95</b>
6.1	Introduction . . . . .	95
6.2	The N-Control strategy . . . . .	95
6.3	Potential benefits of N-Control . . . . .	96
6.3.1	Taxi times reduction . . . . .	96
6.3.2	Fuel burn and emissions reduction . . . . .	100
6.3.3	Strategy assessment . . . . .	102
6.4	Comparison to the saturation taxi time metric . . . . .	102
6.5	Operational challenges . . . . .	106
<b>7</b>	<b>Conclusions</b>	<b>109</b>
7.1	Summary of results . . . . .	109
7.2	Contributions of the thesis . . . . .	110
<b>A</b>	<b>Airport diagrams</b>	<b>113</b>
A.1	John F. Kennedy International Airport(JFK) . . . . .	114
A.2	Newark Liberty International Airport (EWR) . . . . .	115
A.3	Philadelphia International Airport (PHL) . . . . .	116
A.4	Boston Logan International Airprort(BOS) . . . . .	117
<b>B</b>	<b>Takeoff rate plots</b>	<b>119</b>
B.1	John F. Kennedy International Airport(JFK) . . . . .	119
B.1.1	Visual Meteorological Conditions . . . . .	119
B.1.2	Instrumental Meteorological Conditions . . . . .	123
B.2	Newark Liberty Airport (EWR) . . . . .	124
B.2.1	Visual Meteorological Conditions . . . . .	124
B.2.2	Instrumental Meteorological Conditions . . . . .	128
B.3	Philadelphia International Airport (PHL) . . . . .	130
B.3.1	Visual Meteorological Conditions . . . . .	130
B.3.2	Instrumental Meteorological Conditions . . . . .	133

B.4 Boston Logan International Airport (BOS) . . . . . 135  
B.4.1 Visual Meteorological Conditions . . . . . 135  
B.4.2 Instrumental Meteorological Conditions . . . . . 138

# List of Figures

1-1	A schematic of the airport system, including the terminal-area [21]. . . . .	20
1-2	The average departure taxi times at EWR over 15-minute intervals and the unimpeded taxi-out time (according to the ASPM database) from May 16, 2007. We note that large taxi times persisted for a significant portion of the day [14]. . . . .	21
2-1	[Left] Taxi-out time distribution of OOOI flights at BOS; [Right] Taxi-out time distribution of non-OOOI flights at BOS . . . . .	26
2-2	[Left] Taxi-out time distribution of OOOI flights at JFK; [Right] Taxi-out time distribution of non-OOOI flights at JFK . . . . .	26
2-3	[Left] Taxi-out time distribution of OOOI flights at BOS; [Right] Taxi-out time distribution of non-OOOI flights at BOS . . . . .	27
2-4	[Left] Taxi-out time distribution of OOOI flights at JFK; [Right] Taxi-out time distribution of non-OOOI flights at JFK . . . . .	27
2-5	[Left] Taxi-out time distribution of OOOI flights at BOS; [Right] Taxi-out time distribution of non-OOOI flights at BOS . . . . .	29
2-6	[Left] Taxi-out time distribution of OOOI flights at JFK; [Right] Taxi-out time distribution of non-OOOI flights at JFK . . . . .	29
3-1	Aircraft movement process as a controlled queuing system [21]. . . . .	33
3-2	Example of airport congestion . . . . .	35
3-3	Congestion under VMC during different hours of the day . . . . .	39
4-1	$\tau(i)$ vs. $N_Q(i)$ scatter . . . . .	51
4-2	$\tau(i)$ vs. $N_Q(i)$ scatter for Comair . . . . .	54
4-3	$\tau(i)$ vs. $N(t)$ scatter for Comair . . . . .	56

5-1	Integrated model of the departure process . . . . .	75
5-2	Takeoff rate as function of $N(t)$ . . . . .	79
5-3	[Left] Histogram of inter-departure times; [Right] Simplified histogram of inter-departure times. . . . .	80
5-4	Actual and modeled takeoff rate as a function of $N(t)$ , when taxiway interactions are neglected. . . . .	81
5-5	Actual and modeled $N(t)$ histogram, when taxiway interactions are neglected. . . . .	82
5-6	Actual and modeled takeoff rate as a function of $N(t)$ , when taxiway interactions are included. . . . .	84
5-7	Distributions of observed and modeled $N(t)$ . . . . .	84
5-8	Taxi-out time distributions under low ( $N \leq 8$ ), medium ( $9 < N \leq 16$ ) and heavy ( $N > 17$ ) departure traffic on the surface for configuration 27, 32   33L. . . . .	86
5-9	Taxi-out time distributions under low ( $N \leq 8$ ), medium ( $9 < N \leq 16$ ) and heavy ( $N > 17$ ) departure traffic on the surface for configuration 4L, 4R   4L, 4R, 9. . . . .	87
5-10	Taxi-out time distributions under low ( $N \leq 8$ ), medium ( $9 < N \leq 16$ ) and heavy ( $N > 17$ ) departure traffic on the surface for configuration 22L, 27   22L, 22R. . . . .	87
5-11	Estimated time spent by an aircraft transiting the taxiways and waiting in the runway queue for different levels of surface traffic. . . . .	88
5-12	Taxi-out time distributions under low ( $N \leq 8$ ), medium ( $9 < N \leq 16$ ) and heavy ( $N \geq 17$ ) surface traffic for configuration 22L, 27   22L, 22R in BOS in 2008. . . . .	91
5-13	Takeoff rate $\bar{T}_9(t+9)$ as a function of $N(t)$ for configuration 22L, 27   22L, 22R in BOS in 2008. The model was derived from a training set of data from 2007. . . . .	91
5-14	Prediction of departure throughput, average taxi-out times and departure queue lengths in each 15-min interval over a 10-hour period on July 22, 2007. The error bars denote the standard deviations of the estimates. . . . .	93
6-1	Integrated model of the <i>controlled</i> departure process . . . . .	97
A-1	JFK airport diagram[13] . . . . .	114
A-2	EWR airport diagram[13] . . . . .	115
A-3	PHL airport diagram[13] . . . . .	116
A-4	BOS airport diagram[13] . . . . .	117
A-5	Allocation of gates to airlines as of May 2008 (courtesy of MASSPORT) . . . . .	118

B-1	Takeoff rate as a function of $N(t)$ in segment (VMC; 31R -31L) . . . . .	119
B-2	Takeoff rate as a function of $N(t)$ in segment (VMC; 31L, 31R - 31L) . . . . .	120
B-3	Takeoff rate as a function of $N(t)$ in segment (VMC; 13L, 22L - 13R) . . . . .	120
B-4	Takeoff rate as a function of $N(t)$ in segment (VMC; 22L - 22R, 31L) . . . . .	121
B-5	Takeoff rate as a function of $N(t)$ in segment (VMC; 13L - 13R) . . . . .	121
B-6	Takeoff rate as a function of $N(t)$ in segment (VMC; 4R - 4L, 31L) . . . . .	122
B-7	Takeoff rate as a function of $N(t)$ in all VMC segments . . . . .	123
B-8	Takeoff rate as a function of $N(t)$ in segment (VMC; 22L- 22R) . . . . .	124
B-9	Takeoff rate as a function of $N(t)$ in segment (VMC; 31L, 4R - 4L) . . . . .	125
B-10	Takeoff rate as a function of $N(t)$ in segment (VMC; 11, 22L - 22R) . . . . .	125
B-11	Takeoff rate as a function of $N(t)$ in segment (VMC; 4R, 11 - 4L) . . . . .	126
B-12	Takeoff rate as a function of $N(t)$ in segment (VMC; 4R, 29 - 4L) . . . . .	126
B-13	Takeoff rate as a function of $N(t)$ in segment (VMC; 22L - 22R, 29) . . . . .	127
B-14	Takeoff rate as a function of $N(t)$ in segment (VMC; 22L- 22R) . . . . .	128
B-15	Takeoff rate as a function of $N(t)$ in segment (VMC; 4R - 4L) . . . . .	129
B-16	Takeoff rate as a function of $N(t)$ in segment (VMC; 26, 27R, 35 - 27L, 35) . . . . .	130
B-17	Takeoff rate as a function of $N(t)$ in segment (VMC; 9R, 17 — 8, 9L, 17) . . . . .	131
B-18	Takeoff rate as a function of $N(t)$ in segment (VMC; 9R, 35 - 8, 9L, 35) . . . . .	131
B-19	Takeoff rate as a function of $N(t)$ in segment (VMC; 26, 27R — 27L) . . . . .	132
B-20	Takeoff rate as a function of $N(t)$ in segment (VMC; 9R, 17 - 8, 9L, 17) . . . . .	133
B-21	Takeoff rate as a function of $N(t)$ in segment (VMC; 9R - 8, 9L) . . . . .	134
B-22	Takeoff rate as a function of $N(t)$ in segment (VMC; 22L, 27 — 22L, 22R) . . . . .	135
B-23	Takeoff rate as a function of $N(t)$ in segment (VMC; 4L, 4R — 4L, 4R, 9) . . . . .	136
B-24	Takeoff rate as a function of $N(t)$ in segment (VMC; 27, 32 — 33L) . . . . .	136
B-25	Takeoff rate as a function of $N(t)$ in segment (VMC; 33L, 33R — 27, 33L) . . . . .	137
B-26	Takeoff rate as a function of $N(t)$ in segment (VMC; $RC \in [5, 6, \dots, 20]$ ) . . . . .	137
B-27	Takeoff rate as a function of $N(t)$ in segment (VMC; $RC \in [10, 12, 13]$ ) . . . . .	138



# List of Tables

1.1	Taxi-out times in the United States, illustrating the increase in the number of flights with large taxi-out times between 2006 and 2007. . . . .	19
1.2	Top 10 airports with the largest taxi-out times in the United States in 2007 [32]. . .	19
2.1	ASPM departures vs. ETMSC departures in four major US airports in 2007 . . . . .	24
2.2	ASPM departures vs. OPSNET and ACI movements at four major US airports in 2007 . . . . .	25
2.3	OOOI recordings vs. total reported departures at four major US airports in 2007 . .	25
3.1	Correlation coefficient between $N$ and $\bar{T}_n(t + dt)$ for different values of $n$ and $dt$ . .	37
3.2	Reported weather conditions at JFK in 2007 . . . . .	37
3.3	Runway configurations use at JFK in 2007 under VMC . . . . .	38
3.4	Congestion analysis for JFK in 2007 under VMC . . . . .	38
3.5	Congestion analysis for JFK in 2007 under IMC . . . . .	40
3.6	Reported weather conditions at EWR at 2007 . . . . .	40
3.7	Runway configurations use at EWR in 2007 under VMC . . . . .	41
3.8	Congestion analysis for EWR in 2007 under VMC . . . . .	41
3.9	Most frequently runway configurations use in EWR in 2007 under IMC . . . . .	42
3.10	Congestion analysis for EWR in 2007 under IMC . . . . .	43
3.11	Reported weather conditions at PHL in 2007 . . . . .	43
3.12	Runway configurations use at PHL in 2007 under VMC . . . . .	43
3.13	Congestion analysis for PHL in 2007 under VMC . . . . .	44
3.14	Most frequently runway configurations use at PHL in 2007 under IMC . . . . .	44
3.15	Congestion analysis for PHL in 2007 under IMC . . . . .	45
3.16	Reported weather conditions at BOS in 2007 . . . . .	45

3.17	Runway configurations use at BOS in 2007 under VMC . . . . .	46
3.18	Congestion analysis for BOS in 2007 under VMC . . . . .	46
3.19	Most frequently runway configurations use at BOS in 2007 under IMC . . . . .	47
3.20	Congestion analysis for BOS in 2007 under IMC . . . . .	48
4.1	Unimpeded taxi time estimation in BOS segment (4L, 4R   4L, 4R, 9; VMC) . . . .	57
4.2	Congestion analysis for JFK in 2007 under VMC . . . . .	63
4.3	Congestion analysis for JFK in 2007 under IMC . . . . .	64
4.4	Congestion analysis for EWR in 2007 under VMC . . . . .	64
4.5	Congestion analysis for EWR in 2007 under IMC . . . . .	65
4.6	Congestion analysis for PHL in 2007 under VMC . . . . .	66
4.7	Congestion analysis for PHL in 2007 under IMC . . . . .	66
4.8	Congestion analysis for BOS in 2007 under VMC . . . . .	67
4.9	Congestion analysis for BOS in 2007 under IMC . . . . .	67
4.10	Fuel burn and emissions in JFK, EWR, PHL and BOS . . . . .	68
4.11	Fuel burn and emissions in JFK, EWR, PHL and BOS . . . . .	69
5.1	Runway saturation points for most frequent configurations used in BOS . . . . .	78
5.2	Parameter $\alpha$ for different BOS runway configurations . . . . .	83
5.3	Actual and modeled taxi times for different BOS segments . . . . .	85
5.4	Model predictions for segment (VMC; 22L, 27   22L, 22R) . . . . .	85
5.5	Model predictions for segment (VMC; 4L, 4R   4L, 4R, 9) . . . . .	85
5.6	Model predictions for segment (VMC; 7, 32   33L) . . . . .	85
5.7	Actual and modeled emissions for BOS segment (VMC; 22L, 27 — 22L, 22R) in 2007	89
5.8	Actual and modeled emissions for BOS segment (VMC; 4L, 4R — 4L, 4R, 9) in 2007	89
5.9	Actual and modeled emissions for BOS segment (VMC; 7, 32 — 33L) in 2007 . . . .	89
5.10	Actual and modeled taxi times for different BOS segments in 2008 . . . . .	90
5.11	Model predictions for segment (VMC; 22L, 27   22L, 22R) for 2008 . . . . .	90
5.12	Model predictions for segment (VMC; 4L, 4R   4L, 4R, 9) for 2008 . . . . .	90
5.13	Model predictions for segment (VMC; 7, 32   33L) for 2008 . . . . .	90
5.14	Evaluation of model predictions using Monte Carlo simulations. . . . .	93



6.1	Taxi-out time reduction for different values of $N_{ctrl}$ in segment (22L, 27   22L, 22R; VMC) . . . . .	98
6.2	Reduction in taxi-out time for different values of $N_{ctrl}$ in segment (4L, 4R   4L, 4R, 9; VMC) . . . . .	99
6.3	Reduction in taxi-out time for different values of $N_{ctrl}$ in segment (7, 32   33L; VMC) . . . . .	100
6.4	Fuel burn and emissions reduction for different values of $N_{ctrl}$ in segment (22L, 27   22L, 22R; VMC) . . . . .	101
6.5	Fuel burn and emissions reduction for different values of $N_{control}$ in segment (VMC; 4L, 4R   4L, 4R, 9) . . . . .	101
6.6	Fuel burn and emissions reduction for different values of $N_{control}$ in segment (VMC; 7, 32   33L) . . . . .	101
6.7	Estimated taxi time, fuel burn and emissions reduction from controlling $N(t)$ to the saturation value. . . . .	103
6.8	Estimated taxi time, fuel burn and emissions percentage reduction from controlling $N(t)$ to the saturation value. . . . .	103
6.9	Congestion analysis for BOS in 2007 under VMC using the two different metrics . . . . .	103
6.10	$N$ -control strategy evaluation . . . . .	104
6.11	Congestion analysis for BOS in 2007 under VMC using the two different metrics . . . . .	106
6.12	$N$ -control strategy evaluation . . . . .	106



# Chapter 1

## Introduction

Aircraft taxi operations contribute significantly to the fuel burn and emissions at airports. The quantities of fuel burned, as well as different pollutants such as Carbon Dioxide, Hydrocarbons, oxides of Nitrogen, oxides of Sulfur and Particulate Matter (PM) are a complicated function of the taxi times of aircraft, in combination with other factors such as the throttle settings, number of engines that are powered, and pilot and airline decisions regarding engine shutdowns during delays. In 2007, aircraft in the United States spent more than 63 million minutes taxiing in to their gates, and over 150 million minutes taxiing out from their gates [14]. In addition, the number of flights with large taxi-out times (for example, over 40 min) has been increasing (Table 1.1). Similar trends have been noted at major airports in Europe, where it is estimated that aircraft spend 10-30% of their flight time taxiing, and that a short/medium range A320 expends as much as 5-10% of its fuel on the ground [10].

**Table 1.1:** Taxi-out times in the United States, illustrating the increase in the number of flights with large taxi-out times between 2006 and 2007.

Year	Number of flights with taxi-out time (in min)						
	< 20	20-39	40-59	60-89	90-119	120-179	≥ 180
2006	6.9 mil	1.7 mil	197,167	49,116	12,540	5,884	1,198
2007	6.8 mil	1.8 mil	235,197	60,587	15,071	7,171	1,565
Change	-1.5%	+6%	+19%	+23%	+20%	+22%	+31%

**Table 1.2:** Top 10 airports with the largest taxi-out times in the United States in 2007 [32].

Airport	JFK	EWR	LGA	PHL	DTW	BOS	IAH	MSP	ATL	IAD
Avg. taxi-out time (in min)	37.1	29.6	29.0	25.5	20.8	20.6	20.4	20.3	19.9	19.7

Operations on the airport surface include those at the gate areas/aprons, the taxiway system

and the runway systems, and are strongly influenced by terminal-area operations. The different components of the airport system are illustrated in Figure 1-1. These different components have aircraft queues associated with them and interact with each other. The cost per unit time spent by an aircraft in one of these queues depends on the queue itself. For example, an aircraft waiting in the gate area for pushback clearance predominantly incurs flight crew costs, while an aircraft taxiing to the runway or waiting for departure clearance in a runway queue with its engines on incurs additional fuel costs and contributes to surface emissions.

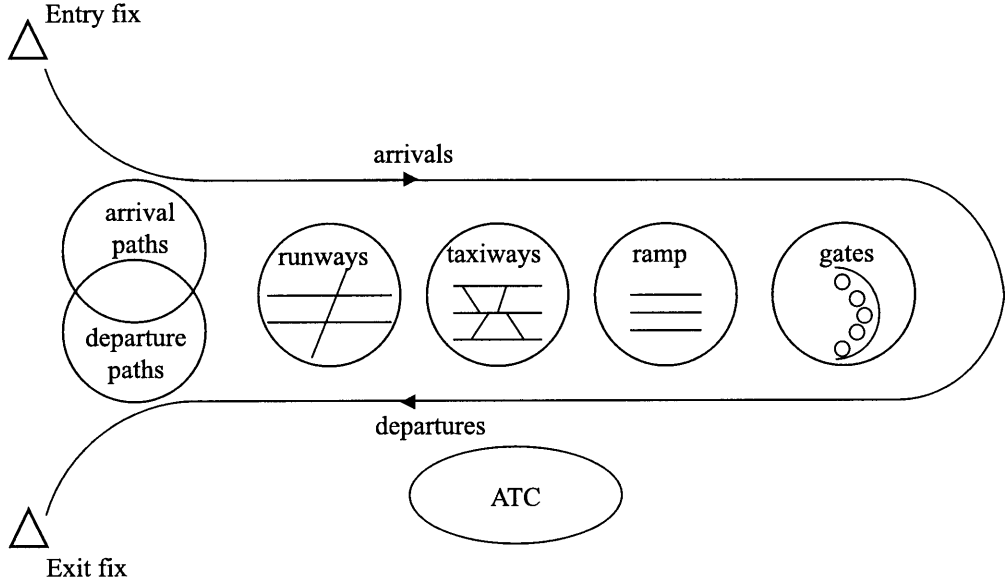


**Figure 1-1:** A schematic of the airport system, including the terminal-area [21].

The *taxi-out time* is defined as the time between the actual pushback and takeoff time. This quantity represents the amount of time that the aircraft spends on the airport surface with engines on and includes the time spent on the taxiway system and in the runway queues. As a result, surface emissions from departures are closely linked to the taxi-out times. At several of the busiest US airports, the taxi times are long, and tend to be much greater than the unimpeded taxi times for those airports (Figure 1-2). By addressing the inefficiencies in surface operations, it may be possible to decrease taxi times and surface emissions. This was the motivation for prior research on the Departure Planner [17].

It is well known that taxi-out delays are primarily caused by an imbalance between demand and capacity. Queuing theory tells us that large delays are anticipated as the demand for departures approaches the capacity of the airport. Even larger delays are expected when the demands exceeds

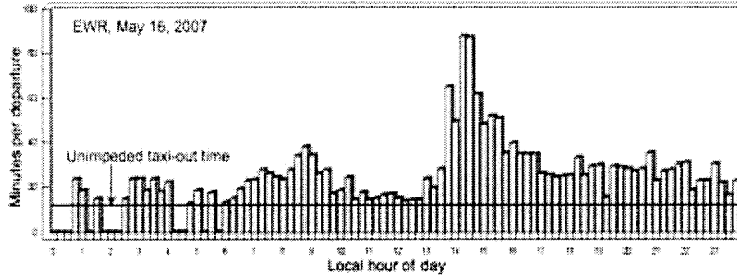


**Figure 1-2:** The average departure taxi times at EWR over 15-minute intervals and the unimpeded taxi-out time (according to the ASPM database) from May 16, 2007. We note that large taxi times persisted for a significant portion of the day [14].

capacity [11]. This mismatch often occurs during bad weather conditions: in such scenarios, the capacity of an airport can drop significantly. This is an operational constraint that is well understood and studied for departure planning (see, for example, [5]). Advanced procedures have been developed for reducing the number of the flights served so that the effective demand will not cause unacceptable delays(see, for example, [31]). At most congested airports, there are times when the demand results in large delays, even in good weather conditions. An example of this is visualized in Figure 1-2 where the average taxi times over 15-minute intervals at Newark Liberty Airport(EWR) are shown along with the unimpeded taxi time: We can observe that the the difference between the recorded taxi-out times and the unimpeded times exceeds 60 minutes during some parts of the day, although this was a good-weather day at EWR.

In this work we consider both good and bad weather conditions, or, more formally, visual and instrumental meteorological conditions. We attempt to reduce the taxi-out times and the resultant emissions, which result from the imbalance of departure demand and the capacity of an airport under stable and known weather conditions.

## 1.1 Organization of the thesis

This section provides a brief outline of the organization of the thesis.

In Chapter 2, we introduce the data sources used in this work. In Chapter 3, we present and analyze departure data from four major US airports, and illustrate that the airports suffer from surface congestion in both good and bad weather conditions. We quantify the levels of congestion, and in Chapter 4, we calculate the impact of congestion on taxi-out times and the corresponding emissions. We also estimate the extent to which taxi times could be reduced by controlling surface congestion.

In Chapter 5, we describe quantitatively how queues form on the surface, and what factors lead to increased taxi-out times. We develop a queuing model of the departure process, and validate this model in terms of its ability to predict taxi-out times and the aircraft flows at Boston Logan International Airport (BOS).

In Chapter 6, we consider a previously-proposed approach toward reducing taxi-times and emissions at airports, *N-control*, which limits the build up of queues and congestion on the airport surface through improved queue management [6]. We then explain how the model developed in Chapter 5 can be used to determine the impacts of *N-control*, and estimate the potential benefits and implications of this approach. We also do a preliminary comparison of *N-control* and a more complicated strategy that would control for the length of the takeoff queue of each aircraft.

## Chapter 2

# Data Sources

### 2.1 The Aviation System Performance Metrics (ASPM) database

As outlined in Chapter 1, in this work we are primarily concerned with analyzing and predicting taxi-out times. For analyzing the current operations, and building and validating a model, we make use of the Aviation System Performance Metrics (ASPM) database, which is maintained by the Federal Aviation Administration (FAA). This database provides a wealth of information on the performance of the busiest 77 airports in the United States [14].

For the purposes of this thesis we make use of the following pieces of information:

- From the ASPM module giving information about “individual flights”:
  1. Actual pushback time time of each flight
  2. Actual takeoff time of each flight
  3. Actual taxi-out time of each flight
  4. Flight code (airline and flight number) of each flight
  
- From the ASPM module giving information about the “airport”:
  1. Runway configuration in use
  2. Reported meteorological conditions

The data used in the subsequent chapters of the thesis are from this source unless otherwise noted.

## 2.2 Flights not reported in ASPM

The airports that we study also serve a small number of flights that are not present in the ASPM databases. These include certain air taxi operations, general aviation and military flights. We assume that this is a small number of flights. Establishing the exact number of departures that took off during a year from a particular airport is not a straightforward task. For example, ASPM gives different estimates if one counts the total number of departures in the “individual flights” mode and in the “airport” mode.

Another FAA database is the Enhanced Traffic Management System Counts (ETMSC). According to the FAA, ETMSC contains data derived from the Air Traffic Airspace Lab’s Enhanced Traffic Management System, and does not represent the official traffic counts for the National Airspace System [15]. In Table 2.1 we compare the ASPM counts with the ETMSC. We can see that ASPM data account for between 93% and 96 % of the ETMSC.

**Table 2.1:** ASPM departures vs. ETMSC departures in four major US airports in 2007

Airport	ASPM departures	ASPM fraction of ETMSC departures	ETMSC departures
JFK	210049	93.87%	223,754
EWR	209010	96337%	216,885
PHL	232583	95.24%	244,216
BOS	183071	92.95%	19,949

Since ETMSC does not represent the official counts according to FAA, we investigate this issue further by assuming that the total number of departures served from an airport during a year equals half of the total number of movements at the airport. The Operations Network (OPSNET) database [16] gives the total number of movements recorded in a US airport during a certain period of time. Table 2.2 gives a comparison of the ASPM departure counts to half of the total number of movements as reported in OPSNET. Assuming that half of the movements were departures, we can see that ASPM contains 90 – 95% of the total number of departure operations. Finally, we note that the OPSNET numbers for the total number of movements do not match the estimates that the Airport Council International (ACI) [1] provides. In fact, the OPSNET numbers are larger from a handful to up to a few thousand flights, depending on the particular facility, as seen in Table 2.2.



**Table 2.2:** ASPM departures vs. OPSNET and ACI movements at four major US airports in 2007

Airport	ASPM departures	ASPM fraction of half of OPSNET movements	OPSNET movements	ACI movements
JFK	210049	91.96%	456,835	446.348
EWR	209010	94.60%	441,908	435.691
PHL	232583	93.09%	499,683	499,653
BOS	183071	91.11%	401,890	399,537

### 2.3 OOOI and non-OOOI flights

According to the ASPM documentation [27], the information regarding the departing flights within the ASPM database is organized into two categories: The OOOI and the non-OOOI flights. Several airlines provide data on gate pushback (gate-out or OUT), takeoff (wheels-off or OFF), landing (wheels-on or ON) and gate arrival (gate-in or IN), collectively known as OOOI, times for most of their flights. These airlines are often called OOOI carriers. This data is automatically recorded by their aircraft equipped with ACARS sensors and is processed by Aeronautical Radio, Incorporated (ARINC). For the flights of the OOOI carriers with unavailable information, and for flights of non-participating carriers, the ASPM database calculates the OOOI information, and in particular the pushback time, the take-off time and the taxi-out time, which are of interest to us, in the following manner:

1. The takeoff time is calculated using the Departure message (DZ).
2. The taxi-out time is calculated using the median taxi-out time of the airport, for the day and hour the departure took place.
3. The pushback time is computed by subtracting the taxi-out time from the takeoff time.

In Table 2.3, we list the counts of OOOI and non-OOOI flights at JFK, EWR, PHL and BOS airports in 2007.

**Table 2.3:** OOOI recordings vs. total reported departures at four major US airports in 2007

Airport	Total departures	OOOI recordings	OOOI fraction of total departures
JFK	210049	137917	65.66
EWR	209010	163464	78.21
PHL	232583	116092	49.91
BOS	183071	129183	70.56

Unfortunately, the ASPM documentation [27] does not provide sufficient detail on the taxi-out time calculation. Specifically, there is evidence that the estimated median for non-OOOI flights is adjusted or truncated. Figure 2-1, which depicts the taxi-out distributions for OOOI and non-OOOI flights at BOS, in 2007, illustrates these effects. The same phenomenon is also apparent in Figure 2-2. These trends suggest that the taxi-out time estimates of non-OOOI flights are truncated. For example, at BOS, there is a spike at 12 minutes and a smaller spike at 59 minutes. At JFK, there is a spike at 17 minutes and another spike at 59 minutes.

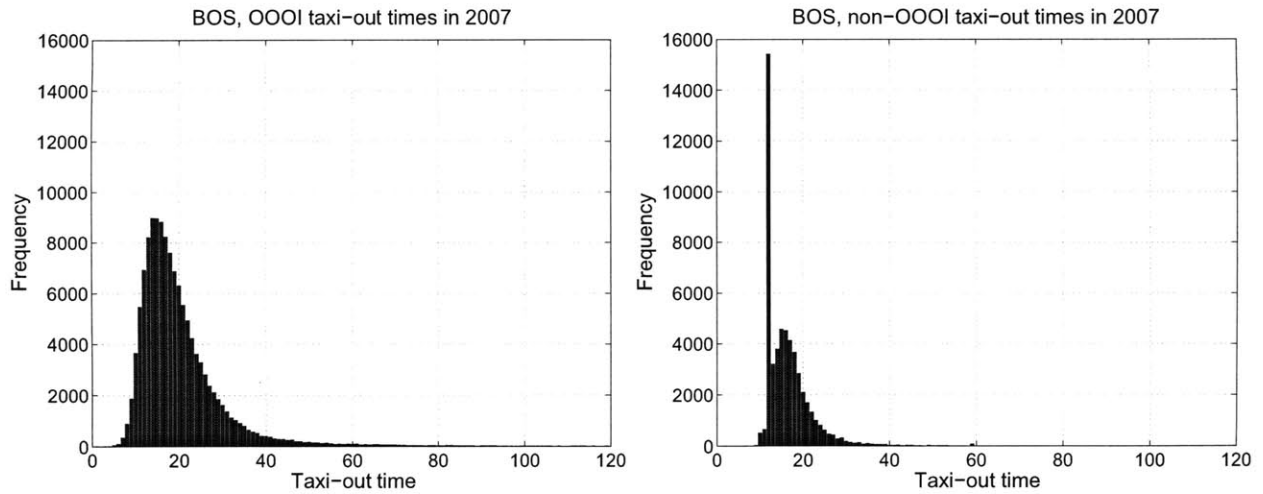


**Figure 2-1:** [Left] Taxi-out time distribution of OOOI flights at BOS; [Right] Taxi-out time distribution of non-OOOI flights at BOS

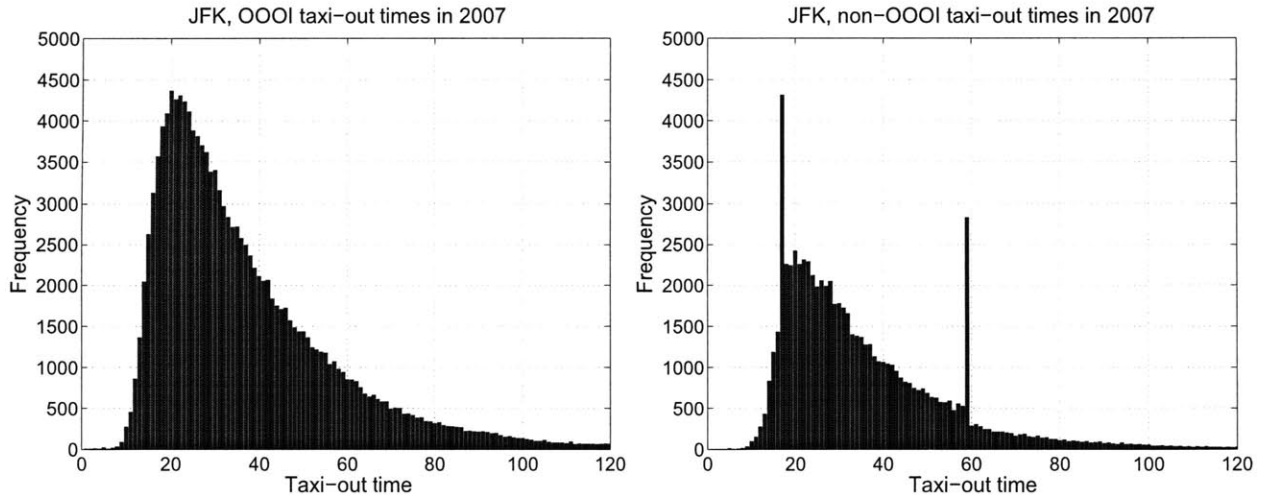


**Figure 2-2:** [Left] Taxi-out time distribution of OOOI flights at JFK; [Right] Taxi-out time distribution of non-OOOI flights at JFK

We repeated the calculation of the taxi-out time of the non-OOOI flights using as the estimator of a non-OOOI flight the median taxi-out time of the OOOI-flights that took off in some time interval surrounding its take-off time. The distribution we obtain is very different from the ones in Figures 2-1 and 2-2. The spikes fade away irrespective of the time interval we chose. The distributions of the taxi-times of the non-OOOI flights compared to the ones of the OOOI flights that result when using as an estimator of the taxi times of the OOOI flights the median taxi times of the OOOI flights that took off in the one hour centered in the takeoff time of the non-OOOI flight can be seen in Figures 2-3 and 2-4.

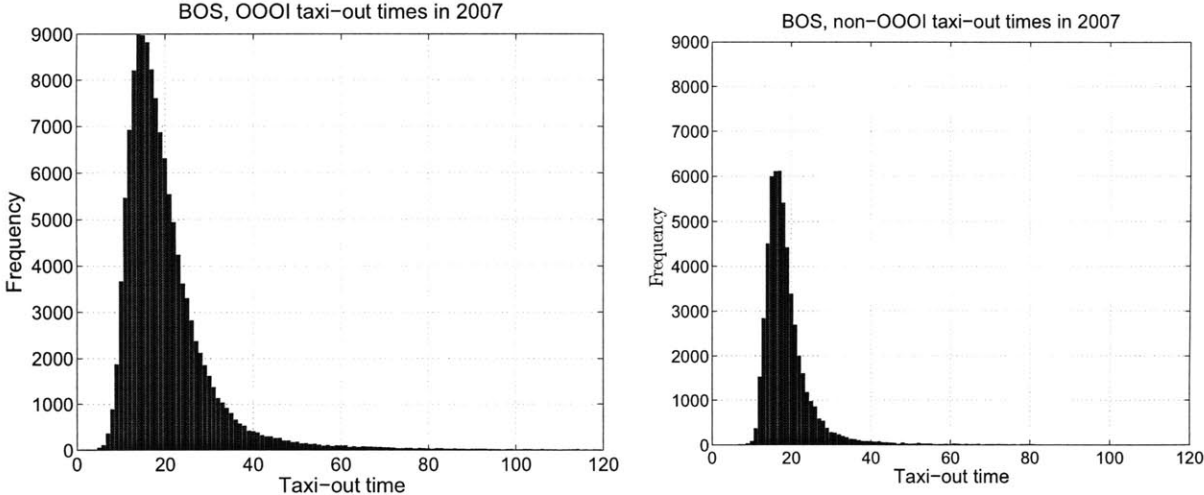


**Figure 2-3:** [Left] Taxi-out time distribution of OOOI flights at BOS; [Right] Taxi-out time distribution of non-OOOI flights at BOS

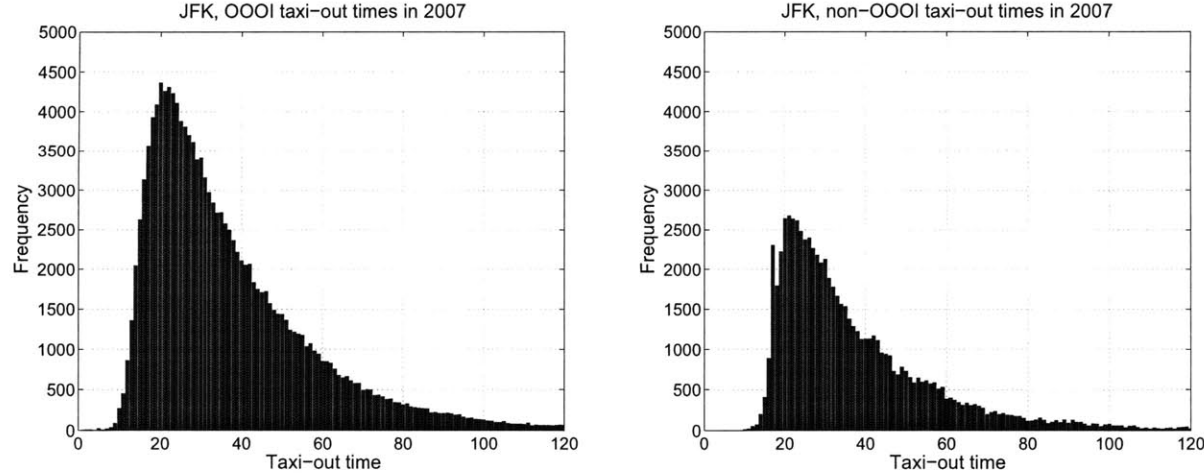


**Figure 2-4:** [Left] Taxi-out time distribution of OOOI flights at JFK; [Right] Taxi-out time distribution of non-OOOI flights at JFK

Furthermore, the estimated median for taxi-out times may not always be appropriate. The median estimate attaches less importance to outliers, and is especially useful when there are measurement errors. In this case, it is often difficult to distinguish between measurement or reporting errors, outliers because of operational reasons<sup>1</sup>, abnormal operations because of very heavy congestion, and delays because of downstream restrictions (such as ground stops, ground delays, or in-trail restrictions).

It is reasonable to expect that the taxi times of non-OOOI flights in a given time interval are similar to those of the OOOI flights for the same interval. We therefore recompute the taxi-out time of the non-OOOI flights using the following method: The taxi time of every non-OOOI flight  $i$  is estimated as the mean taxi time of the OOOI flights which made use of the same runway configuration as  $i$  and took off within 7 minutes before or after the takeoff time of  $i$ . We make use of the runway configuration information, since this is readily available and it is well known that there is limited correlation in the taxi time of flights departing from different runway configurations. The results of this modification to the ASPM database are depicted in Figures 2-5 and 2-6 for BOS and JFK. As desired, when compared to Figures 2-1 and 2-2, the spikes are removed and the distributions look much more like the ones of the OOOI flights.

For all the airports analyzed in this study, we recompute the taxi time and the pushback time following the above method.

---

<sup>1</sup>For example, a flight with an unusually long taxi time caused by a mechanical problem

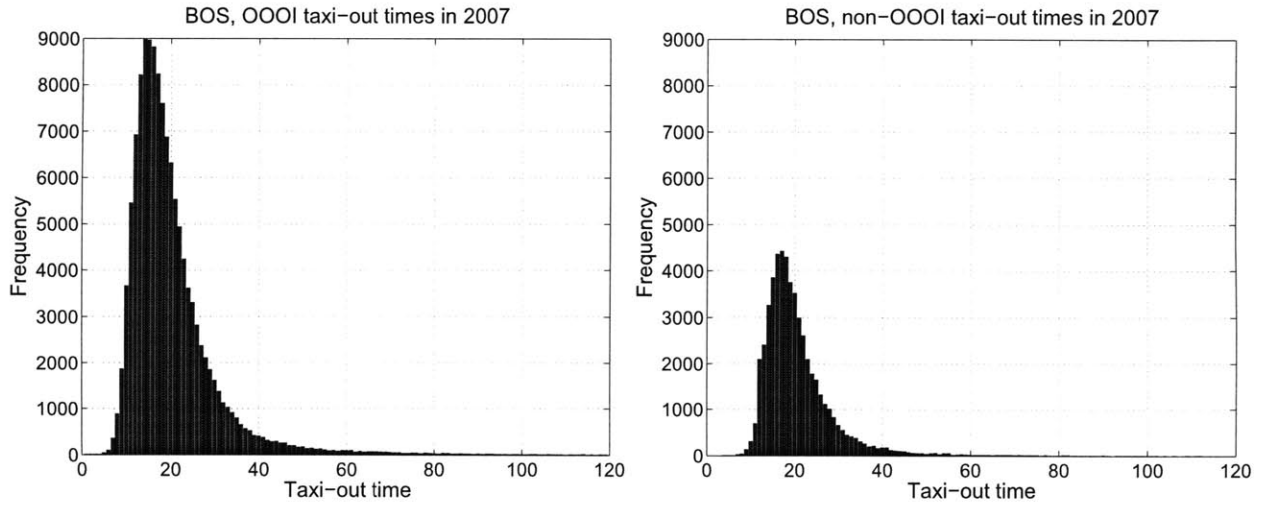


**Figure 2-5:** [Left] Taxi-out time distribution of OOOI flights at BOS; [Right] Taxi-out time distribution of non-OOOI flights at BOS

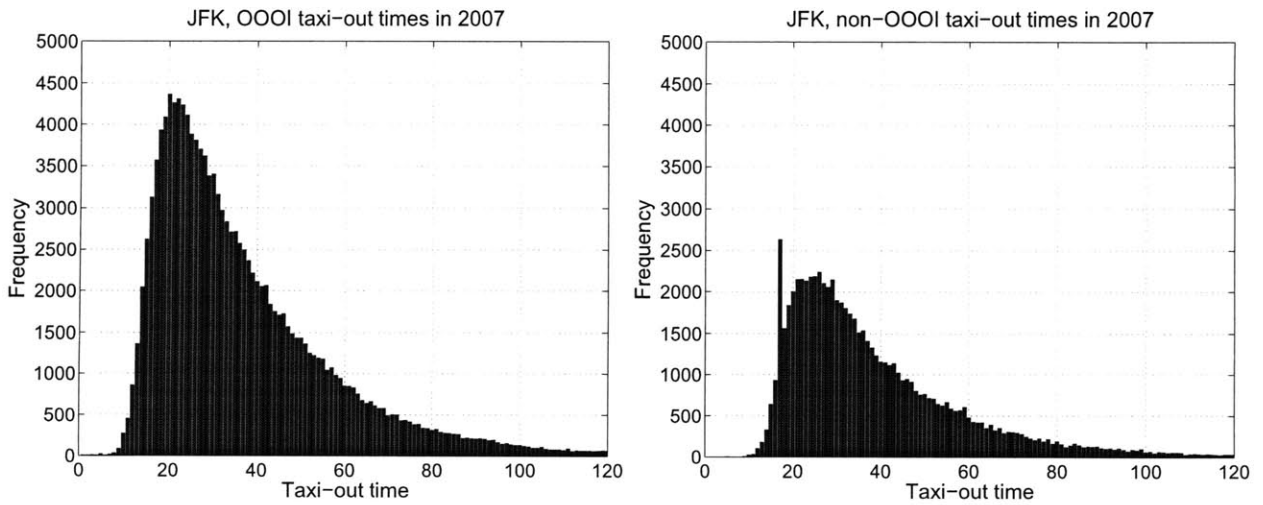


**Figure 2-6:** [Left] Taxi-out time distribution of OOOI flights at JFK; [Right] Taxi-out time distribution of non-OOOI flights at JFK



## Chapter 3

# The problem of surface congestion

### 3.1 Introduction

As mentioned in Chapter 1, we hypothesize that surface emissions may be mitigated by sufficiently reducing inefficiencies on the ground. The purpose of this chapter is to identify and quantify these inefficiencies. We provide an analytic model for calculating the congestion due to departing aircraft on the surface. Subsequently we make use of this model and assess the problem of surface congestion in four major US airports, namely JFK, EWR, PHL and BOS.

### 3.2 The notion of segments

In recent work, Idris et al. [18] identified the key variables that influence the taxi time of a departing flight as being the following: runway configuration, weather conditions, downstream restrictions, gate location, and queuing delays. The results of their paper suggested that these factors would need to be accounted for independently while analyzing congestion. In their work, Pujet [29] and Andersson *et al.* [2] studied throughput and taxi-out times for each airport separately for various runway configurations/weather conditions. In doing so, Andersson *et al.* introduced the concept of the *segment*, which they defined as a particular combination of runway configuration and weather conditions [2].

Although we will not offer an in-depth description of these efforts, it is important to make note of the intuition behind their methodology: Suppose we have an airport with two different runway configurations: in the first one, a single runway is devoted to departures and in the second one, three runways are available for departures. Assuming all other parameters are equal, the airport

is expected to experience higher congestion and longer taxi-out times in the former configuration than in the latter. This is due to fact that the first configuration has a smaller departure capacity. By a similar argument, more severe weather conditions would require more stringent separation requirements and decrease throughput. In this thesis, the general weather conditions (denoted either Visual Meteorological Conditions, or Instrumental Meteorological Conditions, VMC vs. IMS) are used as surrogates for weather and downstream airspace conditions. The runway configuration is characterized by both the runways used for arrivals as well as those used for departures. Each segment is defined as a combination of the runway configuration and the general weather conditions (VMC vs. IMC). Therefore, we denote a segment as (*Weather Conditions; Arrival Runways | Departure Runways*).

### 3.3 Flow analysis of the departure process

Recall Figure 1-1, which showed the main components of the airport system. As mentioned above, each of these components could be subject to queuing delays. Idris presented an extensive analysis of the departure process and the respective queues in his PhD thesis [21]. Figure 3-1 depicts the different components of the system along with the corresponding control points for a particular runway configuration at Boston Logan International Airport (BOS).

Any queuing effect in the different components leads to longer taxi-times. Concerning the departure process, we can identify four different components where queues can form:

- Pushback
- Ramp
- Taxiways
- Runway

Conceptually, the departure process, as shown in Figure 3-1 can be described as following: First, aircraft request pushback from their gates. They must wait to be cleared for pushback; this waiting time is modeled by a queuing process (*pushback queue*). Following clearance for pushback, they enter the ramp, the taxiway system, and lastly taxi to the departure queues (denoted as *takeoff queues* in Figure 3-1). This departure queue is formed at the start of the departure runway(s). During the intervening phase, different aircraft may interact with one other. For example, aircraft



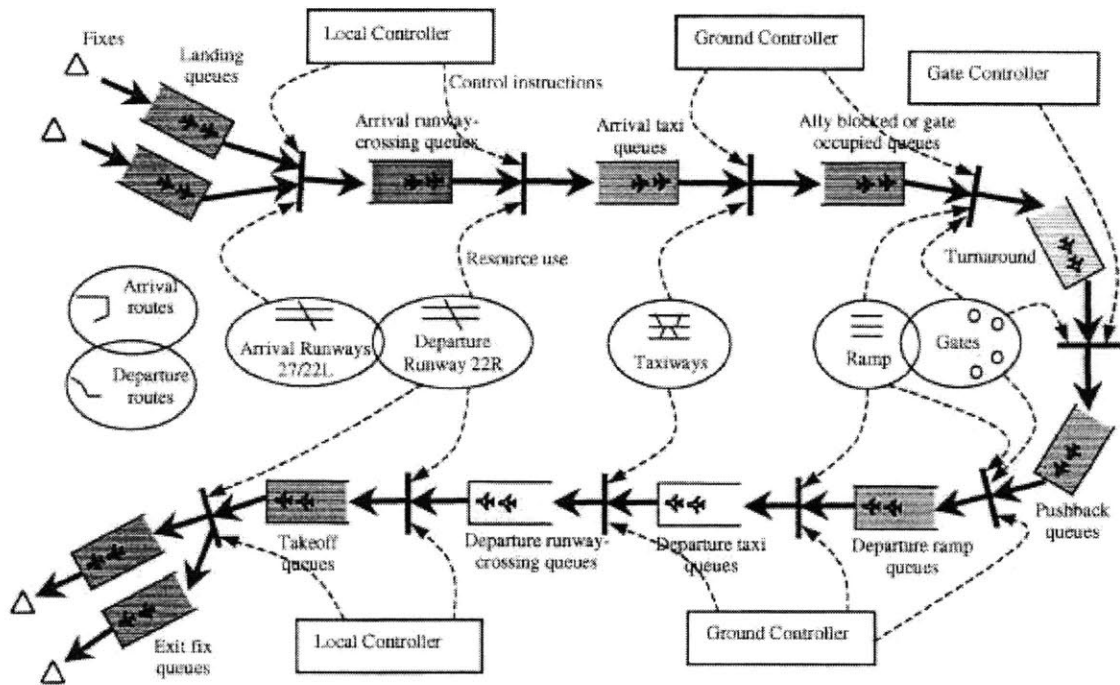


Figure 3-1: Aircraft movement process as a controlled queuing system [21].

queue to obtain access to a confined part of the ramp, to cross an active runway or to enter a taxiway segment in which another aircraft is taxiing. These spatially distributed queues that form while aircraft traverse the airport surface from their gates towards the departure queue are denoted as *departure ramp*, *taxi* and *runway-crossing queues* in Figure 3-1. After the aircraft reach the departure queue, they line up to await takeoff (the departure queue is denoted as *takeoff queue* in Figure 3-1)<sup>1</sup>.

As mentioned in Chapter 1, these queues have different characteristics and costs associated with them. This thesis will primarily focus on taxiing delays and the aircraft emissions during these periods. This narrows the queues of interest to the following, as we only consider aircraft with running engines.

- Ramp queue
- Taxi queue
- Runway-crossing queue

<sup>1</sup>The reason we use a different term than that in Figure 3-1 is because the term “takeoff queue” has a different connotation in the context of this thesis.

- Departure queue

Delays incurred at these queues are a direct consequence of congestion, and contribute to excess emissions. Therefore, to estimate the total effects of congestion from departing aircraft on the ground, we sum the waiting times in all four queues. Although this specific data is not available, it is still possible to infer these queuing delays.

In order to do this, we adopt an approach proposed by previous researchers in the area. We first define the appropriate congestion metric for our work and then assess the congestion problem of four major airports using this metric. The method is outlined in the following sections.

### 3.4 Congestion metric

The poor data resolution in the ASPM database is a recurring problem researchers must face. Shumsky and Pujet in their PhD theses proposed the following solution in an effort to solve a similar problem, namely the load of the departure queues: they used the total number of departing aircraft on the ground as a measure of the congestion [30, 28]. However, the total number of aircraft on the ground by itself, does not provide much insight into the level of congestion, since it does not say how many of the aircraft on the ground are “moving” and how many are being queued.

In order to alleviate this problem, Shumsky suggested and Pujet formalized a method that links the number of aircraft on the ground at the beginning of a time period  $t$ ,  $N(t)$ , with the take-off rate during a subsequent time period. One would expect that during times when  $N(t)$  is low, few take-offs take place. As  $N(t)$  increases, the take-off rate increases until the take-off capacity is reached. This relationship is illustrated in Figure 3-2, where the average take-off rate is shown as a function of the number of departing aircraft on the ground for a segment at Philadelphia International Airport (PHL) in 2007. The error bars show the standard deviation of the take-off rate at a particular value of  $N(t)$ .

As expected, the take-off rate increases at first, and then it saturates close to airport capacity. We observe that this segment is at capacity when there are 20 departing aircraft on the ground. We define the point where the saturation occurs as  $N^*$ . By our definition, at  $N^*$  the airport works at its full capacity: increasing the number of aircraft further will just lead to congestion and will not bring any efficiency gains. Therefore, we define the congestion area  $S$  as the values of  $N(t)$  which are greater than  $N^*$ , ( $N(t) > N^*$ ). In the congestion area, the take-off rate remains almost stable, fluctuating around the capacity of the airport.

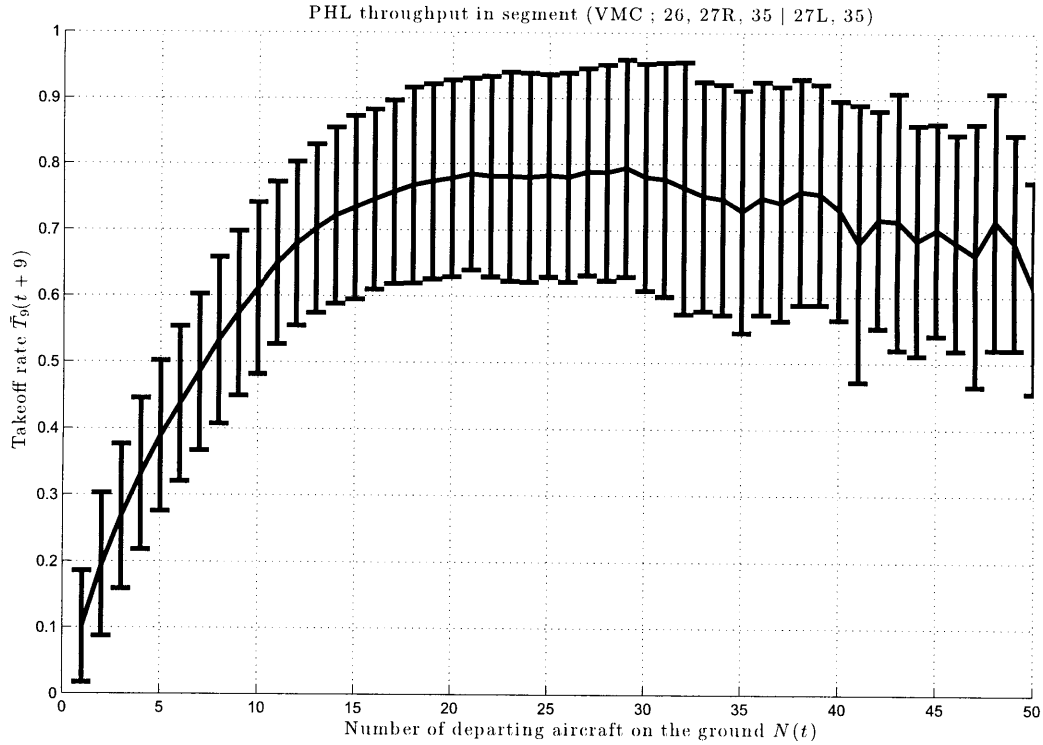


**Figure 3-2:** Example of airport congestion

Figure 3-2 illustrates a property that is very helpful regarding the problem of the poor data resolution: although we cannot know precisely the times that each aircraft spends queuing because of the congestion, we know that whenever the number of departing aircraft on the ground is larger than 20 ( $N(t) > 20$ ), the airport operates in the “saturation area”. An individual aircraft may experience queuing up also for smaller values of  $N(t)$ , but the airport on average increases its throughput by allowing more aircraft on the ground until  $N(t) = 20$ . After that point, increasing the number of aircraft does not increase the throughput (since this is saturated) , it just contributes to congestion.

The method which we follow to measure congestion for a segment of a particular airport is to sum all the times when an airport operated in the saturation area ( $N(t) > N^*$ ). The length and the effect of these saturation periods are used as a metric for the congestion of an airport.

### 3.5 A metric for the “sustained departure capacity”

The method described in Section 3.4 also provides a way to measure the “practical hourly capacity” in addition to the congestion metric. Although, defining and measuring the capacity of an airport

is not within the scope of this thesis and it is an open research question on its own [11], Figure 3-2 yields a good approximation of the departure capacity of an airport's segment. We observe that for a large span of values of  $N \geq N^*$ , the takeoff rate is around 0.79 aircraft/min. This means, that during busy periods, the observed average takeoff rate is 0.79 aircraft/min or 47 aircraft/hour. Although Figure 3-2 does not convey any information about the length of time over which this capacity can be sustained, the fact that during a year-long series of observations the takeoff rate is 47 aircraft/hour when the airport operates in the saturation area suggests that this is the maximum takeoff rate that this segment can achieve on average. Thus, it is a good estimate for the departure capacity that this segment can sustain. We do not claim that this method should be applied to measure the "sustained departure capacity" of a segment, but only that it yields a reasonable approximation for it for the purposes of this thesis.

In the context of this thesis the word "capacity" will be used to denote the capacity that a segment can sustain. This will denote the observed takeoff rate of a segment for  $N \geq N^*$ . It is calculated as the average takeoff rate observed for  $N \geq N^*$ .

### 3.6 Optimal time interval for take-off rate estimation

A subtlety, which was not discussed in Section 3.4, is the take-off rate metric. We only said that the number of aircraft on the ground is very well correlated with the take-off rate of the following time interval. In this section we discuss how to choose the length and the starting point of the time interval.

Following the approach introduced by Pujet [28], we define  $\bar{T}_n(t + dt)$  as the take-off rate over the time period  $(t + dt - n, t + dt - n + 1, \dots, t + dt, \dots, t + dt + n)$ , that is the number of aircraft that took off during the time interval  $(t + dt - n, t + dt - n + 1, \dots, t + dt, \dots, t + dt + n)$  divided by the length of the time interval that is,  $(2n + 1)$ . For each segment we calculate the values of  $n$  and  $dt$  that yield the highest correlation coefficient  $\rho_{N(t), \bar{T}_n(t+dt)}$  between  $N(t)$  and  $\bar{T}_n(t + dt)$  over a time period when this segment was in use.

Figure 3-2 displays the relationship between  $\bar{T}_n(t + dt)$  and  $\rho_{N(t), \bar{T}_n(t+dt)}$  over a year of observations. The  $y$ -axis denotes the takeoff rate,  $\bar{T}_9(t + 9)$ , so, in this case  $n = 9$  and  $dt = 9$ . These parameters were chosen because  $n = 9$  and  $dt = 9$  give on average the highest correlation coefficient at PHL for the time intervals of the year 2009 when this segment was in use.

Table 3.1 depicts the average correlation coefficient  $\rho_{N(t), \bar{T}_n(t+dt)}$  for different values of  $n$  and

$dt$  for the time intervals that this segment was in use at PHL in 2007.  $\rho_{N(t),\bar{T}_n(t+dt)}$  is calculated for the pairs  $(n, dt)$  that fulfill the condition  $n \geq dt$ . As can be seen in Table 3.1,  $\rho_{N(t),\bar{T}_n(t+dt)}$  is maximum for  $n = 9$  and  $dt = 9$ .

**Table 3.1:** Correlation coefficient between  $N$  and  $\bar{T}_n(t + dt)$  for different values of  $n$  and  $dt$

$dt \backslash n$	3	4	5	6	7	8	9	10	11	12	13
3	0.751	0.752	0.754	0.755	0.753	0.750	0.744	0.737	0.728	0.717	0.705
4		0.780	0.780	0.781	0.779	0.775	0.769	0.762	0.753	0.742	0.731
5			0.800	0.798	0.797	0.793	0.787	0.780	0.771	0.761	0.749
6				0.813	0.809	0.806	0.800	0.793	0.784	0.774	0.763
7					0.821	0.815	0.810	0.803	0.795	0.785	0.774
8						0.824	0.818	0.811	0.803	0.794	0.783
9							0.825	0.817	0.810	0.801	0.791
10								0.824	0.815	0.807	0.797
11									0.821	0.812	0.802
12										0.817	0.807
13											0.811

### 3.7 Congestion analysis for major airports in 2007

Following the steps prescribed in Sections 3.4, 3.5 and 3.6, we analyze congestion at four major airports in the USA in 2007.

#### 3.7.1 John F. Kennedy International Airport(JFK)

##### Weather conditions

Table 3.2 shows the reported meteorological conditions at JFK for 2007. One preliminary observation which can be made is that since the weather is mostly good, the well-known congestion problem of JFK does not seem to be entirely weather-related. The total % of time does not sum to 100%, because there are occasional time intervals for which the weather is not reported.

**Table 3.2:** Reported weather conditions at JFK in 2007

Weather Conditions	Total hours in use	% of time in use	number of takeoffs
VMC	7549	86.18	180171
IMC	1179	14.46	24412

## VMC congestion analysis

The total number of runway configurations which were reported being used under VMC in 2007 is 41. The six most frequently runway configurations used at JFK in 2007 during visual meteorological conditions can be seen in Table 3.3, as well as the amount of time they were in use and the number of aircraft they served (the total number of aircraft that took off when each configuration was in use). We analyze the congestion for these six runway configurations, as the other ones are rarely used.

**Table 3.3:** Runway configurations use at JFK in 2007 under VMC

<i>RC</i>	Number	Total hours in use	% of time in use	takeoffs
31R   31L	1	1500.25	19.87	29633
31L, 31R   31L	2	1497.25	19.83	35833
13L, 22L   13R	3	1435.25	19.01	32409
22L   22R, 31L	4	772	10.02	24136
13L   13R	5	598.25	7.92	13726
4R   4L, 31L	6	426.5	5.65	13092
	[1-6]	6229.5	82.52	148829

Figures B-1 to B-6 of Appendix B display the takeoff rate  $\bar{T}_n(t + dt)$  as a function of  $N(t)$  for the six most frequently used runway configurations used in visual meteorological conditions. The results of the analysis are presented in Table 3.4.

**Table 3.4:** Congestion analysis for JFK in 2007 under VMC

RC	Optimal (n,dt)	Capacity (AC/hour)	$N^*$	# of hours in congestion	% of time in congestion	# of takeoffs in congestion	% of takeoffs in congestion
1	(15,15)	40.46	28	220.12	14.67%	8847	29.86%
2	(19,19)	41.35	25	313.5	20.94%	12397	34.60%
3	(15,15)	41.24	32	234.13	16.31%	9553	24.98%
4	(18,18)	46.09	29	127.05	16.46%	6016	24.93%
5	(15,15)	43.09	28	109.58	18.32%	4725	34.42%
6	(16,16)	43.71	26	107.63	25.24%	4827	36.87%
[1-6]		42	28	1112.02	17.85%	46365	31.15%

Table 3.4 reveals the magnitude of the congestion problem at JFK. The airport is congested 17.85% of the time when it operates in the six most frequently used runway configurations and 31.15% of the takeoffs take place while the airport is saturated. This means that 31.15% of the flights take off spending more time taxiing than needed to ensure that the airport operates at capacity. We note that the runway configurations 4 and 6, which utilize two runways for departures

“22R, 31L” and “4L, 31L” respectively) have the highest capacity, as one would expect. Finally, our estimates are reasonably close to the FAA benchmark report values: according to the report, configurations 1 and 2 have a benchmark capacity rate of 75 – 87 aircraft per hour [13]. Assuming a 50% mix of arrivals and departures, the benchmark rate corresponds to 37.5 – 43.5 AC/ hour departure service capacity. Our estimates are in this interval.

Figure 3-3 shows the congestion for different hours of the day. The solid bars depict the average values of  $N(t)$  during an hour of the day, as they were recorded each minute  $t$  of the particular hour under VMC at JFK throughout 2007. The error bars illustrate the standard deviation. This figure suggests that on average, the number of departing aircraft on the ground is greater than the average  $N^* = 28$  for three hours of the day. This shows that there is significant congestion expected at JFK on a daily basis even in good weather and indicates that the fundamental reason for congestion is the high demand for departures, which the airport cannot serve without experiencing congestion. This systematic mismatch of demand and capacity for a significant fraction of the day implies that an airport would benefit from some strategy to control excessive times and their environmental impact on a regular basis.

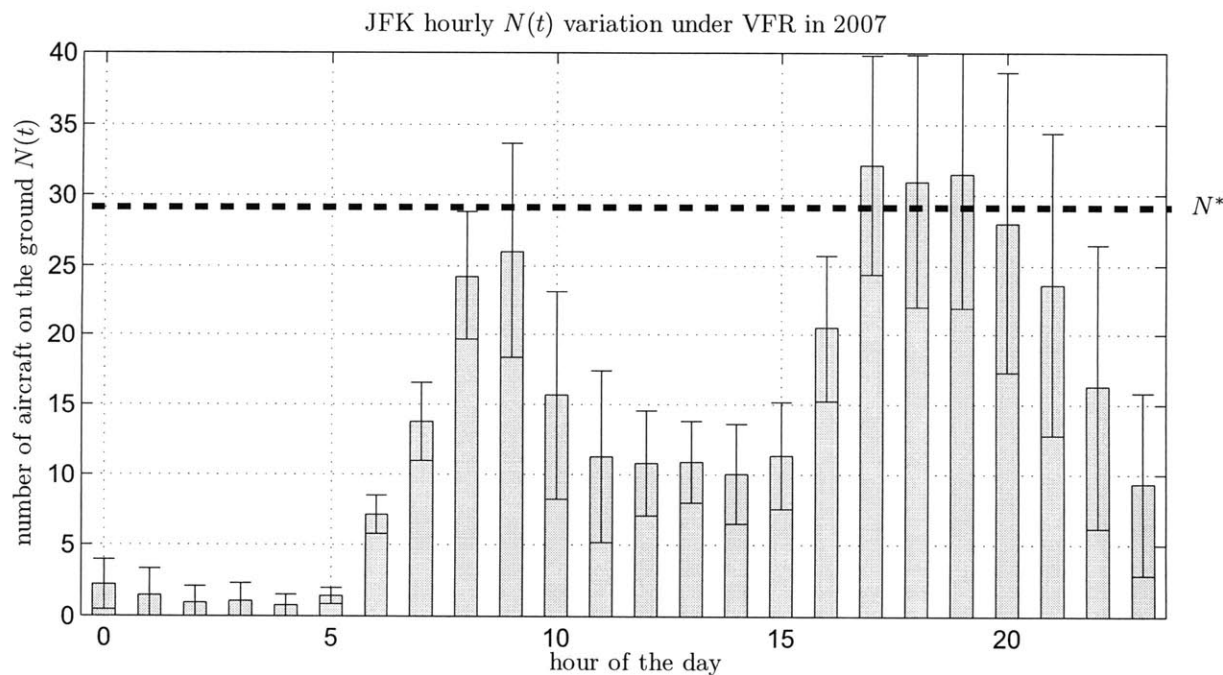


**Figure 3-3:** Congestion under VMC during different hours of the day

## IMC Congestion Analysis

As can be seen in Table 3.2, the weather conditions at JFK are relatively rarely classified as IMC. Even then, controllers tend to use a rich mix of runway configurations, so, in contrast to the VMC, there are no prevailing configurations, which are used most of the time. Therefore, in order to analyze the data, we take a different approach: We treat all runway configurations that are used under IMC as one segment. Figure B-7 of Appendix B displays the take-off rate  $\bar{T}_n(t + dt)$  as a function of  $N(t)$  for all the runway configurations used under instrumental meteorological conditions. The results of the analysis are presented in Table 3.5.

**Table 3.5:** Congestion analysis for JFK in 2007 under IMC

RC	Optimal (n,dt)	Capacity (AC/hour)	$N^*$	# of hours in congestion	% of time in congestion	# of takeoffs in congestion	% of takeoffs in congestion
all	(20,20)	35.65	27	283.92	24.09%	9926	40.94 %

This analysis is an approximation, since all runway configurations used under IMC are analyzed together. Nonetheless, it provides some useful information: the capacity under IMC is lower compared to the one under VMC as expected<sup>2</sup>, and 40.94% of the aircraft take off while the airport is saturated.

### 3.7.2 Newark Liberty International Airport (EWR)

#### Weather Conditions

Table 3.6 shows the reported meteorological conditions for EWR throughout 2007. The weather conditions are visual for EWR most of the time as well.

**Table 3.6:** Reported weather conditions at EWR at 2007

Weather Conditions	Total hours in use	% of time in use	number of takeoffs
VMC	6995.5	79.86	171280
IMC	1381.5	15.77	31181

## VMC Congestion Analysis

As can be seen in Figure A-2 of the Appendix A, EWR has fewer runways and a simpler layout than JFK. This is also reflected in the number of recorded runway configurations which were only 17 in

<sup>2</sup>According to the benchmark report the benchmark rate is 64-67 that corresponds to 32-33.5 departures/ hour. Our estimate is slightly higher than these numbers.



2007. The most frequently used runway configurations at EWR in 2007 under visual meteorological conditions are shown in Table 3.7. Configurations 1 to 6 were used 96.97% of the time when at VMC. We analyze the congestion for these six main runway configurations.

**Table 3.7:** Runway configurations use at EWR in 2007 under VMC

<i>RC</i>	Number	Total hours in use	% of time in use	takeoffs
22L   22R	1	2559.75	36.59	59324
4R   4L	2	1464.25	20.93	36690
11, 22L   22R	3	1355.5	19.38	33757
4R, 11   4L	4	757.5	10.83	18253
4R, 29   4L	5	406.25	5.81	9354
22L   22R, 29	6	240.25	3.43	7966
	[1-6]	6783.5	96.97	165344

Figures B-8 to B-13 of the Appendix B display the take-off rate  $\bar{T}_n(t + dt)$  as a function of  $N(t)$  for the six most frequently used runway configurations used in visual meteorological conditions. The results of the analysis are presented in Table 3.8.

**Table 3.8:** Congestion analysis for EWR in 2007 under VMC

RC	Optimal (n,dt)	Capacity (AC/hour)	$N^*$	# of hours in congestion	% of time in congestion	# of takeoffs in congestion	% of takeoffs in congestion
1	(11,11)	39.82	24	247.33	9.66%	9784	16.49%
2	(15,15)	41.06	28	174.25	11.90%	7139	19.46%
3	(12,12)	39.71	28	119.87	8.84%	4760	14.10%
4	(16,16)	36.23	23	156.02	20.60%	5635	30.87%
5	(12,12)	36.92	23	66.17	16.29%	2454	23.23%
6	(13,13)	45.89	22	86.25	35.90%	3944	49.51%
[1-6]		39.7	25	849.8	12.53%	33716	20.39%

As can be seen in Table 3.8, the departure capacity of the two most often used runway configurations “22L | 22R” and “4R | 4L” is around 40 aircraft/ hour. Adding an arrival runway reduces the departure capacity as can be seen by comparing the capacity of configurations 4 and 5 to the one of configuration 2. This occurs because the runway (11-29) intersects with the runway (4L-22R). Adding a runway for departures increases the departure capacity, as can be seen on the capacity of configuration 6 which is around 46 aircraft per hour. These results agree with the FAA benchmark report which gives an average optimum rate under VMC of 42 departures and 42 arrivals per hour [13].

Comparing Tables 3.8 and 3.4 we can see that EWR is less congested than JFK. Nonetheless, it suffers from severe congestion as well, since it is congested 12.53% of the time and 20.39% of the

flights take-off in the saturation area.

### IMC Congestion Analysis

Under IMC in EWR, the most frequently used configurations are “22L| 22R” and “4R|4L” ( used 82.12% of the time). We note that these are also the most frequently used runway configurations under VMC (Table 3.7). Figures B-14 and B-15 display the takeoff rate  $\bar{T}_n(t + dt)$  as a function of  $N(t)$  for the runway configurations 1 and 2. The results of the analysis are presented in Table 3.10.

**Table 3.9:** Most frequently runway configurations use in EWR in 2007 under IMC

<i>RC</i>	Number	Total hours in use	% of time in use	takeoffs
22L  22R	1	536	38.79%	11918
4R   4L	2	567.25	41.06%	13722
	[1-2]	1103.25	82.12%	25640

As can be seen in 3.8, configuration 2 has a higher capacity than configuration 1 under IMC, as was the case under VMC. Comparing Tables 3.10 and 3.8 one can observe that the capacity of both configurations 1 and 2 decrease under IMC compared to VMC, as expected.

There is a noticeable difference between the  $N^*$  values of the two configurations: 18 vs. 36. Figures B-14 and B-15 of the Appendix B illustrate the reason for this: the takeoff rate of configuration 1 saturates at around 0.6 aircraft/min=36 aircraft/hour when  $N = 18$ . In contrast, configuration 1 appears to stabilize around 0.58 aircraft/min=34.8 aircraft/hour for  $N$  taking values between 19 and 26 and then increases again to stabilize at 0.64 aircraft/min=38.4 aircraft/hour for  $N \geq 32$ . A possible reason for this behavior may be that controllers give priority to arrivals for low values of  $N$  and when the congestion of departing aircraft exacerbates, attempt to increase the departure service rate. The high value of  $N^*$  is also responsible for the apparently small congestion problem of configuration 2: all the operations which take place for  $N < 32$  are classified as non-congested. The congestion data for configuration 1, on the other hand, clearly show the effect of weather on the airport’s congestion: the airport is congested 23.23% of the time and 37.27% of the departing flights take off in the saturation area. These numbers are twice as much as the ones of configuration 1 under VMC (Table 3.8).

**Table 3.10:** Congestion analysis for EWR in 2007 under IMC

RC	Optimal (n,dt)	Capacity (AC/hour)	$N^*$	# of hours in congestion	% of time in congestion	# of takeoffs in congestion	% of takeoffs in congestion
1	(17,17)	35.92	18	124.52	23.23%	4442	37.27%
2	(19,19)	38.36	36	42.9	7.56%	1604	11.69%
[1-2]		37		267.42	15.17%	6046	23.58%

### 3.7.3 Philadelphia International Airport (PHL)

#### Weather Conditions

Table 3.6 shows the reported meteorological conditions at PHL for 2007. At PHL, as in the case of JFK and EWR, the weather conditions are mostly visual.

**Table 3.11:** Reported weather conditions at PHL in 2007

Weather Conditions	Total hours in use	% of time in use	number of takeoffs
VMC	7559	86.29	204002
IMC	1200.75	13.71	25976

#### VMC Congestion Analysis

The most frequently runway configuration use at PHL in 2007 during visual meteorological conditions can be seen in Table 3.12. The total number of the runway configurations which reported being used under VMC in 2007 is 38. However, configuration “26, 27R, 35 | 27L, 35” was used 77.75% of the times when the airport was under VMC, as can be seen in Table 3.11. We analyze the congestion for this and the other three runway configurations that were most frequently used at PHL.

**Table 3.12:** Runway configurations use at PHL in 2007 under VMC

RC	Number	Total hours in use	% of time in use	takeoffs
26, 27R, 35   27L, 35	1	5877	77.75	160357
9R, 17   8, 9L, 17	2	377	4.99	9652
9R, 35   8, 9L, 35	3	368.5	4.87	10818
26, 27R   27L	4	356.75	4.72	8419
	[1-4]	6979.25	92.33	189045

Figures B-16 to B-19 of Appendix B display the take-off rate  $\bar{T}_n(t+dt)$  as a function of  $N(t)$  for the four most frequently used runway configurations used during VMC. The results of the analysis

are presented in Table 3.13.

**Table 3.13:** Congestion analysis for PHL in 2007 under VMC

RC	Optimal (n,dt)	Capacity (AC/hour)	$N^*$	# of hours in congestion	% of time in congestion	# of takeoffs in congestion	% of takeoffs in congestion
1	(9,9)	46.97	20	836.47	14.23%	39390	24.57%
2	(9,9)	38.20	19	142.43	37.78%	5379	56.08%
3	(10,10)	42.71	23	80.77	21.92%	3492	32.35%
4	(8,8)	41.85	17	78.28	21.94%	3194	38.39%
[1 4]		46.01	20	1137.95	16.30%	51455	27.22%

As can be seen in Table 3.11, PHL is a very congested airport as well. On average, it is congested 16.30% of the time and 27.22% of the departing flights take off in the saturation area. Comparing these numbers with the corresponding ones for JFK and EWR in Tables 3.4 and 3.8, we observe that PHL is more congested than EWR and almost as congested as JFK. This result manifests the necessity for a congestion metric. Table 1.2 shows that EWR has higher average taxi-out times than PHL. However, this does not necessarily mean that EWR is more congested: taxi times may be higher simply because the aircraft may naturally need more time to reach the runway threshold. Configuration 1 which is much more frequently used than any others is the one with the highest capacity. Furthermore, configuration 4 which utilizes only a subset of the runways of configuration 1 has a lower capacity as expected.

### IMC Congestion Analysis

As can be seen in Table 3.11, the weather conditions at PHL are relatively rarely classified as IMC. Even then, controllers tend to use a rich mix of runway configurations, so, in contrast to VMC, there are no predominantly used configurations. Therefore, in order to analyze the data, we have to confine the analysis to the two configurations which are used almost 50% of the time: configurations 2 and 5.

**Table 3.14:** Most frequently runway configurations use at PHL in 2007 under IMC

RC	Number	Total hours in use	% of time in use	takeoffs
9R, 17   8, 9L, 17	2	282	23.49%	7243
9R   8, 9L	5	302.75	25.21%	7219
	[1-2]	584.75	48.70%	14228

Figures B-20 and B-21 of the Appendix display the recorded take-off rate  $\bar{T}_n(t+dt)$  as a function of  $N(t)$  for these two runway configurations under IMC. The results of the analysis are presented

in Table 3.15.

**Table 3.15:** Congestion analysis for PHL in 2007 under IMC

RC	Optimal (n,dt)	Capacity (AC/hour)	$N^*$	# of hours in congestion	% of time in congestion	# of takeoffs in congestion	% of takeoffs in congestion
2	(10,10)	38.61	18	83.97	29.77%	3245	45.70%
5	(10,10)	35.48	14	102.53	33.87%	3666	51.43%
[2-5]		37		186.5	31.9%	6911	48.75%

Table 3.15 reveals that PHL suffers the greatest congestion when it operates in configurations 2 and 5 under IMC. However, the weather seems to be only indirectly responsible for this exacerbation: By comparing Tables 3.13 and 3.15, one can observe that the departure capacity of the runway configuration 2 does not decrease due to the weather, nor does the saturation point shift significantly. This is in direct contrast to EWR where the characteristics of the runway configurations change significantly when the weather conditions change from VMC to IMC. To conclude, Configuration 2 appears to have similar service characteristics for departing flights under VMC and IMC. This suggests that instrumental weather conditions lead to a worse congestion problem at PHL, not because the capacity of the runway configurations drop, but because the airport cannot use the most efficient runway configuration (1) as much as it can under visual weather conditions.

### 3.7.4 Boston Logan International Airport (BOS)

#### Weather Conditions

Table 3.16 shows the reported meteorological conditions at BOS for 2007. The weather conditions are visual for BOS most of the time as well.

**Table 3.16:** Reported weather conditions at BOS in 2007

Weather Conditions	Total hours in use	% of time in use	number of takeoffs
VMC	7305.5	83.40	155060
IMC	1417.75	16.18	24893

#### VMC Congestion Analysis

As can be seen in Figure A-4 of Appendix A, BOS has a complicated runway complex consisting of five runways, four of which intersect with at least one other runway. This creates opportunities for numerous runway combinations: In 2007, 61 different runway configurations were reported

being used at BOS. The most frequently runway configuration use at BOS in 2007 under visual meteorological conditions are the first four of Table 3.17: “22L, 27 | 22L, 22R”, “4L, 4R | 4L, 4R, 9”, “27, 32 | 33L” and “33L, 33R | 27, 33L”. However, these four account for less than 70% of the VMC times. Therefore we analyze the congestion for the mix of 16 other configurations (denoted as 5, 6, ..., 20) which was used between 60 and 250 hours at BOS in 2007. In total they were used 26.28% of the time in 2007. The analysis for these runways is essentially an approximation similar to the one done for JFK under IMC.

**Table 3.17:** Runway configurations use at BOS in 2007 under VMC

<i>RC</i>	Number	Total hours in use	% of time in use	takeoffs
22L, 27   22L, 22R	1	2261	30.95	45783
4L, 4R   4L, 4R, 9	2	1280.5	17.53	30437
27, 32   33L	3	1026.5	14.05	23490
33L, 33R   27, 33L	4	398.75	5.46	9157
other	[5,6,...,20]	1920	26.28	36550
all	[1-20]	6886.5	94.26	145417

Figures B-22 to B-26 display the take-off rate  $\bar{T}_n(t + dt)$  as a function of  $N(t)$  for the four most frequently used runway configurations and the combination of configurations [5, 6, ..., 20] used in visual meteorological conditions. The results of the analysis are presented in Table 3.18.

**Table 3.18:** Congestion analysis for BOS in 2007 under VMC

RC	Optimal (n,dt)	Capacity (AC/hour)	$N^*$	# of hours in congestion	% of time in congestion	# of takeoffs in congestion	% of takeoffs in congestion
1	(9,9)	41.53	16	255.31	11.29%	10582	23.11%
2	(9,9)	43.89	17	81.38	6.36%	3609	11.86%
3	(9,9)	43.36	21	35.92	3.50%	1567	6.67%
4	(9,9)	49	21	6.70	1.68%	323	3.35%
[5-20]	(8,8)	40.61	18	88.95	4.63%	3555	9.73%
[1-20]		42.42	18	468.27	6.80%	19636	13.50%

It can be observed in Table 3.18 that configurations 1, 2 and 3 have similar capacities. This may seem counter-intuitive, since they appear to use two, three and one runway(s) for departures respectively. However, at BOS, controllers tend to primarily use one runway for departures regardless of what they can theoretically use in a particular configuration<sup>3</sup>. BOS has been studied extensively in the past and previous studies mention that configuration “4L, 4R | 4L, 4R, 9” has higher capacity than “22L, 27 | 22L, 22R”, consistent with our findings. The main reason is that arriving traffic

<sup>3</sup>Personal communication with MASSPORT personnel

on runway 27 interferes with the departures from runways 22L, 22R when configuration 2 is in use [11].

The differences between these three runway configurations manifest themselves more when looking at the values of the saturation point  $N^*$ . Runway configurations 1 and 2 use runways whose thresholds are located close to the terminals (Figure A-4 of Appendix A). In contrast, configuration 3 uses runway 33L for departures, which is more remotely located. It saturates at a higher value of  $N^*$ , because the aircraft can be spread more in the ramps and the taxiway system. Thus, more aircraft are needed compared to configurations 1 and 2 to achieve constant pressure to the runway in the subsequent time period.

Finally, configuration 4 appears to have a much higher capacity than the other configurations, but it is rarely used (and is also congested very rarely<sup>4</sup>), so the observed value may not have statistical significance.

It is observed that BOS suffers from less congestion than the other three airports examined. Nonetheless, configuration 1, which is the one most frequently used suffers from significant congestion: it is congested 11.39% of the time and 23.11% of the flights take off when the airport is saturated.

### IMC Congestion Analysis

As can be seen in Table 3.16, the weather conditions at BOS are relatively rarely classified as IMC. Even then, controllers tend to use a rich mix of runway configurations: the recorded runway configurations under IMC in 2007 were 42. Some of them were very rarely used. In contrast to JFK, different runway configurations have different capacity and saturation values, so we cannot group all of them. However, we can analyze the congestion for a set of three configurations which are used 50% of the time when the conditions are instrumental, as can be seen in Table 3.19. These configurations are the equivalent of “4L, 4R | 4L, 4R, 9” under VMC.

**Table 3.19:** Most frequently runway configurations use at BOS in 2007 under IMC

<i>RC</i>	Number	Total hours in use	% of time in use	takeoffs
4R   4L, 4R, 9	10			
4R   9	12	709.75	50.06%	15152
4R   4R, 9	13			

Figure B-27 display the take-off rate  $\bar{T}_n(t + dt)$  as a function of  $N(t)$  for all the runway configu-

<sup>4</sup>This is important because the capacity is inferred as the takeoff rate of the congested periods.

rations used under instrumental meteorological conditions. The results of the analysis are presented in Table 3.20.

**Table 3.20:** Congestion analysis for BOS in 2007 under IMC

RC	Optimal (n,dt)	Capacity (AC/hour)	$N^*$	# of hours in congestion	% of time in congestion	# of takeoffs in congestion	% of takeoffs in congestion
[10,12,13]	(10,10)	35.84	15	97.67	13.76%	3424	22.60%

As can be seen in Table 3.20, the instrumental meteorological conditions result in decreasing capacity compared to the one under visual meteorological conditions. The time the airport experiences congestion under IMC is twice as much as the time it experiences congestion under VMC and 22.60% of the departing flights take off when the airport is saturated. This is a significant increase from the VMC case, where only 13.50% of the takeoffs take place when the airport is saturated. We conclude that although BOS is a relatively non-congested airport, instrumental weather conditions decrease its capacity and result in a significant increase of congestion.

### 3.8 Summary

In this chapter we performed a preliminary assessment of the congestion at major US airports. We introduced metrics for the measurement of the capacity and the congestion and applied them to four major airports, showing that congestion impacts them to different extents. We also showed that the performance of airports depends on runway configuration changes and weather conditions. The main conclusions are that JFK, EWR and PHL suffer from severe congestion even when they are able to use their most efficient runway configurations. Thus, the congestion problem is primarily related to the very high demand for departures, which the airport cannot serve without incurring congestion and unacceptable delays. This motivates the investigation of how the long taxi times and the corresponding emissions can be mitigated in a systematic manner.



## Chapter 4

# The effect of surface congestion on taxi times

### 4.1 Introduction

In Chapter 3, we discussed two significant factors used to analyze airport performance, namely, the sustained departure capacity and the surface congestion. In this chapter, we propose metrics to evaluate the effects of congestion on taxi times by introducing two baselines for comparison. Sections 4.2 and 4.3 describe the baselines and methods for their estimation, while Section 4.4 describes how they can be used to calculate the impact of surface congestion on taxi-out times.

### 4.2 The unimpeded taxi-out time metric

#### 4.2.1 Definition of unimpeded taxi-out times

The unimpeded taxi-out time is the nominal, free flow taxi out time. As the name reveals, it is the taxi-out time of an aircraft if it taxis and takes off in the absence of any obstacles. The FAA defines the unimpeded taxi-out time as *the taxi-out time under optimal operating conditions, when neither congestion, weather nor other factors delay the aircraft during its movement from gate to takeoff* [27]. For instance, in Figure 3-1, the unimpeded taxi-out time is the time that a departing aircraft spends on the surface if it spends no time in the queues of the departure process. We note that as per this definition, the unimpeded taxi-out time is not the minimum time that an aircraft would need to taxi-out and take off, but rather, it is the average time an aircraft needs to complete

the departure process when the aircraft spends no time waiting in queues. The service time for each of the steps of the departure process may vary among flights for several reasons:

- Differences during the dispatch stage
- Routing through different taxiways
- Different taxi speeds
- Different runway assignments
- Variability in the duration of pushback and engine-start
- Differences in pilot-controller communications

Factors such as communication delays cannot readily be observed in the recorded data and contribute to the stochasticity of the unimpeded taxi time, as considered by earlier models [5].

The unimpeded taxi time cannot be directly observed, and needs to be estimated. In the following section we describe the FAA estimation procedure and present an alternative estimation method, which is used throughout this study.

#### 4.2.2 Estimation of unimpeded taxi-out times

The following technique is used to estimate the unimpeded taxi-out time in the ASPM database: First, the unimpeded taxi-out time is redefined in terms of available data as *the taxi-out time when the departure queue is equal to one<sup>1</sup> AND the arrival queue is equal to zero*. Second, a linear regression of the observed taxi-out times as a function of observed departure and arrival queues is computed. The unimpeded taxi-out time is then estimated using this linear estimator, by setting the departure queue to 1 and arrival queue to 0 [26].

In the present work, we use the observations of Idris *et al.* that (1) there is poor correlation of the taxi-out times with arriving traffic, and (2) the taxi-out time of a flight  $\tau(i)$  is more strongly correlated with its takeoff queue than the number of departing aircraft on the ground ( $N(t)$ ) [18]. We therefore redefine the unimpeded taxi-out time as the taxi-out time when the takeoff queue  $N_Q(i)$  is equal to 0 (that is, when the number of takeoffs which take place between the pushback time of an aircraft and its takeoff time is equal to 0).

---

<sup>1</sup>ASPM defines the departure queue as the number of aircraft on the ground, so it is equivalent to  $N(t)$ , as defined in Section 5.3

In Figure 4-1, we show the scatter (bubble) plot of  $\tau(i)$  vs.  $N_Q(i)$  in BOS for all runway configurations under all meteorological conditions, as well as the linear regression fit. The size of each bubble is proportional to the frequency with which that point is observed.

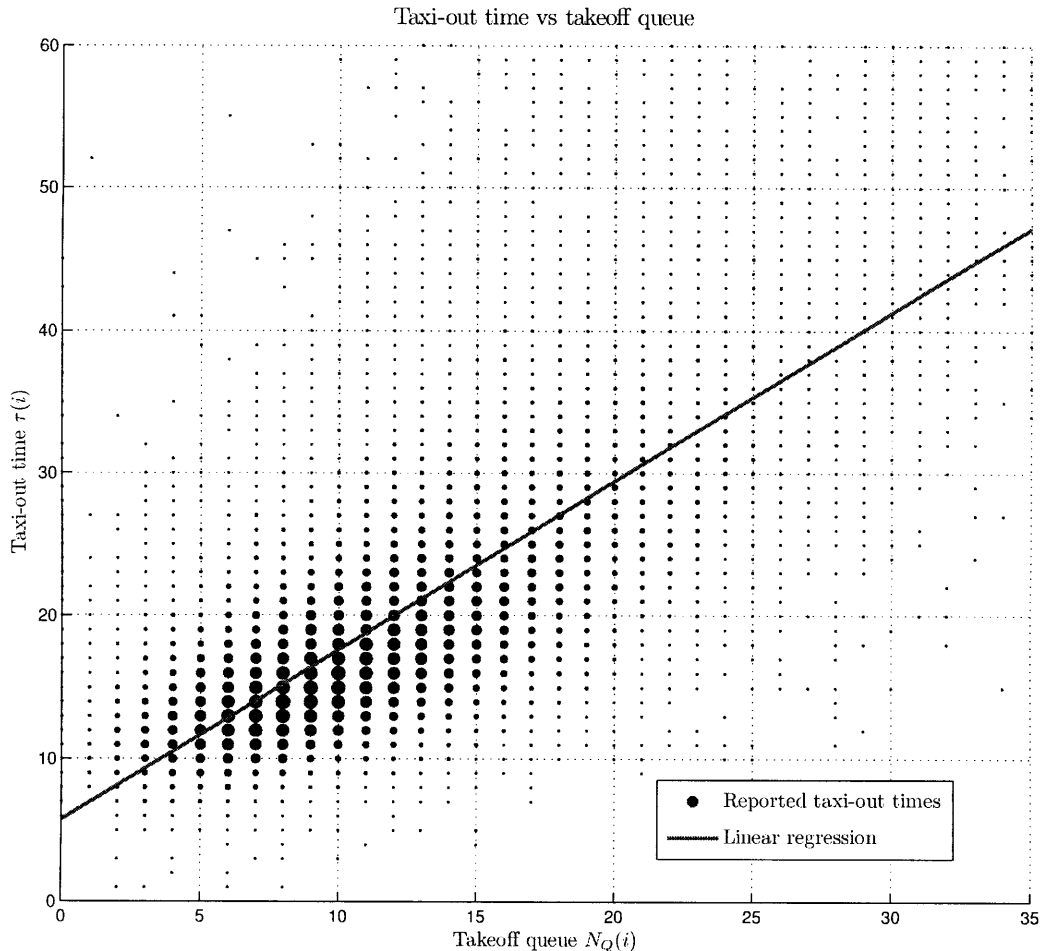


**Figure 4-1:**  $\tau(i)$  vs.  $N_Q(i)$  scatter

The bubble plot indicates that the linear regression may not be appropriate for getting a good estimate of the unimpeded taxi-out time, since the line is significantly below the majority of the observations for low values of  $N_Q(i)$ . While the linear regression gives a fairly good fit for much of the data ( $R^2 = 0.538$ ), it is not a good approximation for the regime that we are interested in, namely, for low values of takeoff queue length. The ASPM database corrects for this effect by excluding the highest 25 percent of the values of actual taxi-out time from the regression while estimating the unimpeded taxi-out times. This step is taken to “remove the influence of extremely large taxi-out times from the estimation of expected taxi time under optimal operating conditions” [26]. This is, however, an empirical metric, and does not explain why the 75<sup>th</sup> is an appropriate

percentile of flights to use (in order to exclude congestion effects), or why the bias that the flights under medium-traffic conditions introduce in the estimation is not important. Figure 4-1 suggests that a piecewise linear regression might be more appropriate. In that case, the first line-segment could be used to estimate the unimpeded taxi time. However, there is no clear choice of the number of the segments in a piecewise regression.

We know that by definition, unimpeded taxi times are observed when neither congestion nor other extraneous factors delay the aircraft during its movement from gate to takeoff. Therefore, we need to restrict our analysis to small values of  $N_Q(i)$ . Unfortunately, this renders the population size of our sample small, and we cannot ensure that the statistical significance of the other factors is negligible. We also need to address the practical problem of choosing the critical value of  $N_Q(i)$  below which it is regarded as “small”. In the following discussion, we propose a new method for systematically inferring the unimpeded taxi-out times.

Let us assume that the taxi-out time is of the form

$$\tau(i) = p_o + p_1 N_Q(i) + W(i), \tag{4.1}$$

where  $W_1, \dots, W_n$  are independent identically distributed (i.i.d.) normal random variables with mean zero and variance  $\sigma^2$ . Then, given  $N_Q(i)$  and the realized values of  $\tau(i)$ , the Maximum Likelihood estimates of the parameters  $p_0$  and  $p_1$  can be calculated using standard linear regression formulas.

We begin the linear regression  $\tau(i)$  vs.  $N_Q(i)$  by keeping  $N_Q(i) \leq 4$ . We use Student’s t-test to evaluate whether the estimates of  $p_1$  thus obtained have statistical significance. If not, we increment the limit of  $N_Q(i)$  (below which flights are included in the regression analysis) by 1 until we obtain a significantly positive estimate of  $p_1$ , and a significantly positive estimate of  $p_0$ . We denote this limit  $N_U$ . The unimpeded taxi time is then given by

$$\tau_{unimped} = p_o \tag{4.2}$$

and its variance is given by its unbiased estimator [3]:

$$\hat{S}_n^2 = \frac{1}{(n-2)} \sum (\tau(i) - p_o + p_1 N_Q(i))^2. \tag{4.3}$$

This regression analysis is conducted for each segment ( $RC, MC$ ) in the airports analyzed and

for each airline, with the operating airline of a flight serving as a surrogate for the “gate location”, the starting point of the aircraft. This works well in BOS, where because there is no dominant airline and each major airline uses a spatially proximate and small (less than 20) set of gates, as will be illustrated in the next subsection. We note that this approach may not extend to an airport such as EWR, where Continental Airlines (COA) uses more than 50 gates that are separated by as much as 1 km. In such a scenario, the airline assignment alone does not offer enough information on the starting point of a departing flight. In such scenarios, terminal and gate information from either the airport, or a travel website, such as [www.flightstats.com](http://www.flightstats.com) [9] could be used to supplement the data. For the sake of simplicity, we use the airline as a proxy for the starting point of each flight.

We also note that the available data does not differentiate between different runways for configurations that utilize more than one departure runway. In theory, the unimpeded taxi time reflects the nominal travel time from start point A to end point B. Major airlines use different gates, so they have different start points, while different departure runways represent different end points. However, since this data is not available, we calculate a single unimpeded taxi time distribution for each airline in every segment analyzed.

We illustrate this process in the next section with an example in BOS.

### 4.2.3 Example of unimpeded taxi-out time calculation

Figure 4-2 shows the bubble plot of the taxi-out times  $\tau(i)$  of Comair (COM) vs.  $N_Q(i)$  when configuration 4L, 4R | 4L, 4R, 9 is in use at BOS under VMC. We also depict the linear regression across all data, which lies below the majority of the observed taxi-times for low values of  $N_Q(i)$ , as was the case when we considered all flights (Figure 4-1).

If we apply the above described methodology to estimate the unimpeded taxi-out time of Comair when configuration 4L, 4R | 4L, 4R, 9 under VMC is in use, we find that the smallest  $N_Q(i)$  which provides estimates that have statistical significance is  $N_U = 7$ . When we apply linear regression for  $\tau(i)$  vs.  $N_Q(i)$  while keeping  $N_Q(i) \leq 7$ , we have a total of 491 observations, and applying Equations 4.2 and 4.3 we estimate the unimpeded taxi-out time of Comair to be given by a normal random variable  $\mathcal{N}(12.45, 3.03)$ . Had we applied the linear regression to the whole dataset, we would have gotten as an estimate of the unimpeded taxi-out time the value of 7.34 minutes. If, on the other hand, we had inferred the unimpeded taxi time as the average observed taxi time of Comair when a Comair aircraft was the sole aircraft on the ground ( $N_Q(i) = 0$ ), we would have estimated the unimpeded taxi time to be 15.27 minutes. This large deviation occurs because there

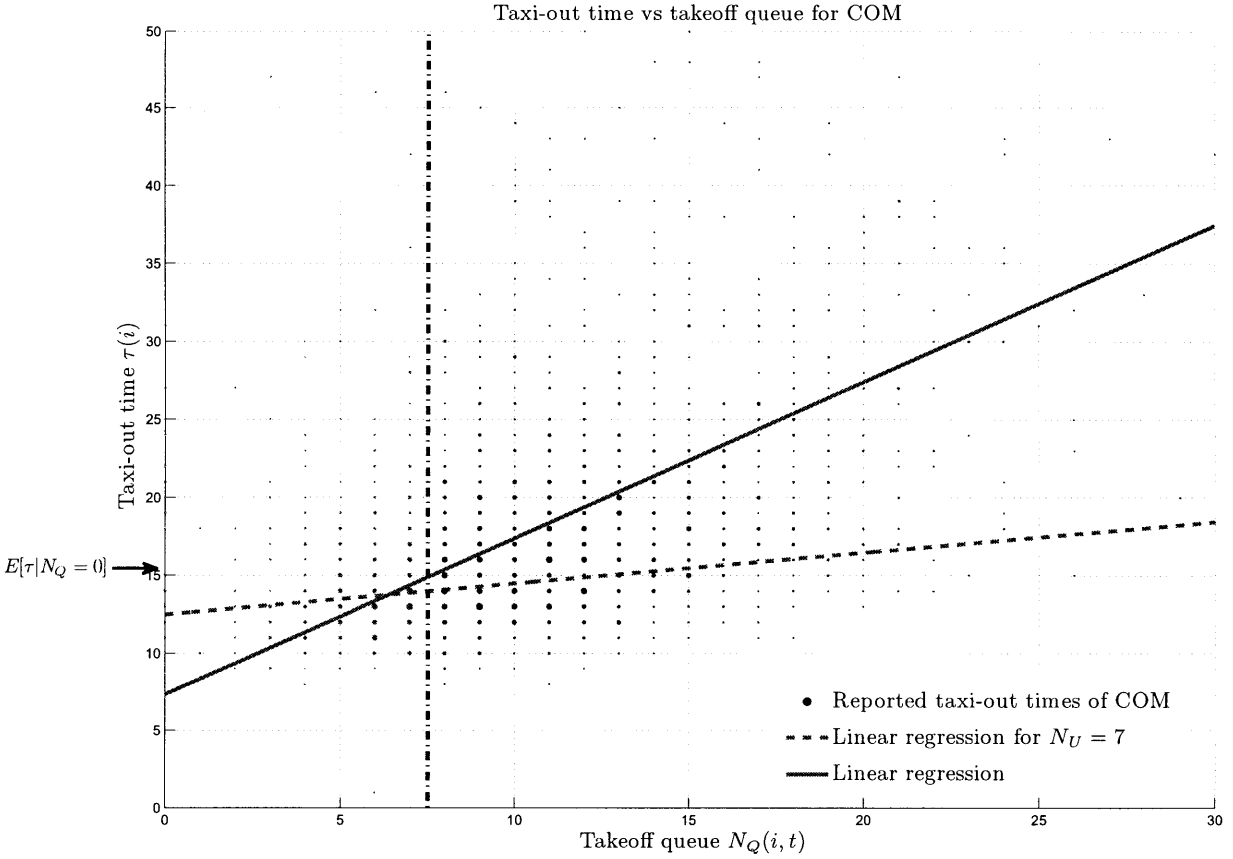


**Figure 4-2:**  $\tau(i)$  vs.  $N_Q(i)$  scatter for Comair

are only 11 observations for  $N_Q(i) = 0$ , and an estimate based solely on them is likely to be prone to error. The choice of  $N_U$  is essentially a compromise between the need for having a sufficient number of observations to obtain a statistically significant estimate, and the need to not include observations corresponding to high values of  $N_Q(i)$  will bias the estimate. A final observation that can be made by comparing the two regression fits in Figure 4-2 is that the red line (corresponding to the linear regression on all observations) has a steeper slope than the (almost flat) blue line (corresponding to observations with  $N_Q(i) \leq 7$ ). This is to be expected since in the low congestion regime (low values of  $N_Q(i)$ ), the marginal delay cost of adding one more aircraft in the takeoff queue is smaller than the average value over all congestion levels.

ASPM provides four seasonal estimates for the unimpeded taxi-out times of Comair in Boston, the average of which is 16.85 min. However, ASPM does not differentiate between different runway configurations, or weather conditions. Several authors [28, 19] have already noted the dependence of the unimpeded taxi time on the runway configuration and we have also verified this observation

in our analysis. This observation can be explained intuitively since the unimpeded time is the nominal time an aircraft needs to travel from point A (its gate) to point B (the runway), and will depend on the location of point B (the runway assignment). A possible approach to adapt the ASPM analysis method on a particular runway configuration is the following:

- Obtain the scatter plot of the taxi time  $\tau(i)$  vs. the number of aircraft on the ground  $N(t)$  for a given runway configuration
- Apply the truncated linear regression to the above data omitting the highest 25 percent of the observed taxi times (that is, using 75 percentile of the data)
- The unimpeded taxi time can then be determined by the intercept of the linear regression fit with the y-axis<sup>2</sup>.

In figure 4-3, we illustrate this process. We also show the highest 25% of the taxi times and the linear regression fit using all taxi times vs.  $N(t)$ .

The following observations can be made regarding Figures 4-2 and 4-3:

- The data in Figure 4-2 exhibit a more narrow scatter than the data in Figure 4-3. In addition, the  $R^2$  value in the latter case is only 0.10 compared to 0.51 in the former. This is consistent with the conclusion of Idris *et al.* that the taxi-out time  $\tau(i)$  of a flight is more strongly correlated with its takeoff queue than with the number of departing aircraft on the ground [18].
- Excluding the highest 25% of the reported taxi times partially corrects for the bias that is introduced by including observations corresponding to large values of  $N(t)$ . However, there is no clear justification for choosing the highest 25% of the reported taxi times, and in addition, we find that the number of aircraft on the ground,  $N(t)$ , is a poor predictor the expected taxi-out time, especially when compared to the length of the takeoff queue,  $N_Q(i)$ .
- The line of the linear regression using all data in Figure 4-2 has a steeper slope than the corresponding one in Figure 4-3 (a value of 1.1 compared to 0.7). This implies that the incremental delay cost incurred by a flight  $i$  from adding one more flight in its takeoff queue, that is, to  $N_Q(i)$ , is higher than that from adding one more departing flight on the surface (i.e., to  $N(t)$ ). This is due to the fact that there is a non-zero probability that the additional

---

<sup>2</sup>According to the definitions we gave in Section 5.3,  $N(t) = 0$  when an aircraft pushes back and is the sole departing aircraft on the surface of the airport

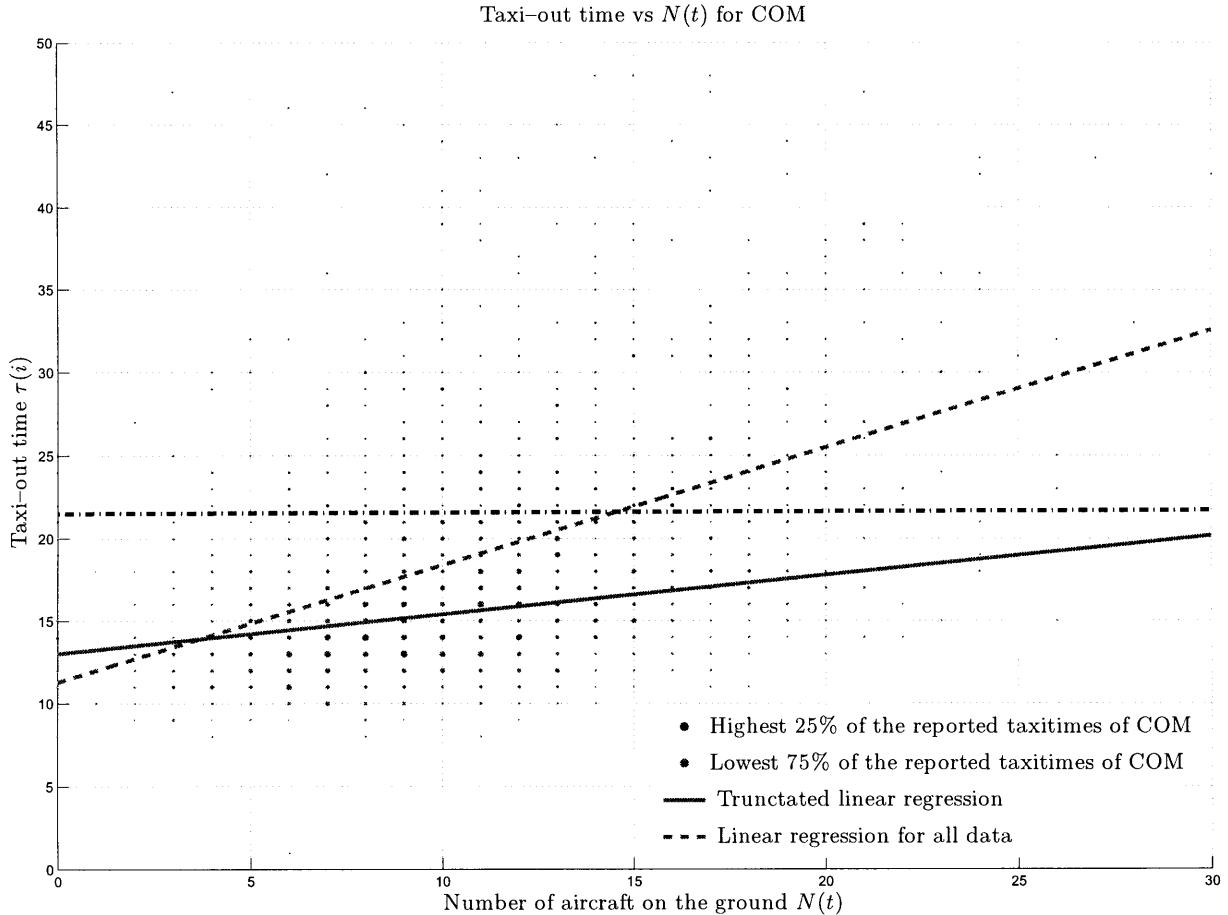


**Figure 4-3:**  $\tau(i)$  vs.  $N(t)$  scatter for Comair

aircraft on the surface will be behind the aircraft  $i$  or will be overtaken by it in the taxiing process [18], and that it will not be in the takeoff queue of flight  $i$ .

#### 4.2.4 Unimpeded taxi-out times estimation for a segment in BOS

We now illustrate the calculation of the unimpeded taxi times for a particular segment (4L, 4R | 4L, 4R, 9; VMC) at BOS. For each airline, we give the estimated normal distribution  $\mathcal{N}(\hat{\mu}, \hat{\sigma})$ , of their unimpeded taxi time. We also give the  $N_U$  that yields statistically significant results for each airline. The results, shown in Table 4.1, are arranged in increasing order of the unimpeded taxi time.

In the calculations, only OOOI flights are included. Although the ASPM data contains flights from 210 distinct airlines in BOS in 2007, some airlines have very few or no OOOI flights. Non-OOOI flights of a carrier are not included in the calculations since their taxi time estimates are based on the average taxi times and do not contain any information about specific airlines.



For BOS in 2007, the proposed method yields results (for finite values of  $N_U$ ) for 15 airlines. All other airlines are treated as one airline, named “Other”. For these airlines, we calculate an approximate unimpeded taxi time estimate by employing the proposed method over all flights (both OOOI and non-OOOI).

**Table 4.1:** Unimpeded taxi time estimation in BOS segment (4L, 4R | 4L, 4R, 9; VMC)

Airline	$\hat{\mu}$	$\hat{\sigma}$	$N_U$
American Eagle Airlines	8.52	2.94	4
America West Airlines	9.57	2.30	6
Pinnacle Airlines	9.66	3.45	6
US Airways	9.87	3.13	6
Air Canada	10.06	2.86	5
Federal Express	10.28	2.83	4
Mesa Airlines	10.91	3.61	9
Delta Air Lines	11.01	3.11	4
United Airlines	11.03	2.61	4
American Airlines	11.21	2.78	5
AirTran Airways	11.73	2.16	5
Comair	12.45	3.03	7
Other	12.87	2.96	5
Jet Blue Airways	12.97	3.11	6
Continental Airlines	13.44	3.14	5
Northwest Airlines	16.42	3.66	9

The results can be analyzed with the help of Figure A-5 (which depicts the allocation of gates to different airlines at BOS in May 2008) and Figure A-4. To the best of our knowledge, the gate assignment to airlines did not change significantly between 2007 and 2008. Figure A-5 shows that the airline of a departing aircraft can be used as a surrogate for the “gate location” at BOS. We see that all major airlines operating out of BOS use their own gates, which are organized in groups of neighboring gates at a specific terminal of the airport. Figure A-4 shows the runway thresholds for this configuration, which are all close to each other.

Results of the unimpeded taxi time estimation follow the intuitive pattern that taxi time increases with the distance between the gate location and the runway. For example, American Eagle and America West are the closest to the runway thresholds, and correspondingly have the smallest unimpeded taxi times. US Airways, which uses the same terminal as America West, has slightly higher taxi times because its gates are a little further from the entrance to the taxiways. The gates of Air Canada are deep within terminal B, and it therefore has marginally a higher unimpeded

taxi time. Mesa Airlines, which operates for United Airlines, and uses the same gates as United Airlines in BOS, comes next. It operates from terminal C, which is further than terminal B from the runways 4L, 4R, 9. As expected, United has approximately the same unimpeded taxi time as Mesa since they use the same gates. Delta Airlines has an unimpeded taxi time that is similar to United and Mesa. Delta operates from terminal A which is approximately at the same distance as terminal C from the runways 4L, 4R, 9. Federal Express operates from South Cargo Terminal, which is to the west of terminal A. This explains the fact that Federal Express has a smaller unimpeded taxi time than Delta. Finally, Northwest Airlines, which operates from terminal E and is the furthest terminal from the runways in use, has the longest unimpeded taxi time.

However, there are airlines for which the results are not intuitive: For example, Jet Blue and AirTran operate from Terminal C and have higher unimpeded taxi times than United despite the fact that their gates are closer to the runways than those of United. American Airlines has a much higher taxi time than American Eagle although they use neighboring gates. Similarly, Pinnacle Airlines, which operates regional flights for Northwest Airlines, has much smaller unimpeded taxi times than Northwest. These results suggest that the unimpeded taxi time may not be only a function of the gate (the starting point), but also of the airline. As we mentioned in Section 4.2.1, the unimpeded taxi time also depends on the control and communication processes, and not only the travel time from the gate to the runway threshold. It may therefore be the case that some airlines complete these processes faster than others. The trend in the Table 4.1 suggests that regional carriers tend to be faster than the airlines they serve. A possible reason for this could be the runway assignment: this particular runway configuration has three departure runways, with one primary runway<sup>3</sup>. However, it is possible that smaller airplanes use the secondary runways. Another reason for the anomaly may be that the regional carriers sometimes do not use a contact stand, so they can pushback quicker. The results reinforce the fact that the unimpeded taxi time incorporates events other than the travel time from the gate to the runway and may be airline dependent. If so, the airline variable is more than a surrogate for just the gate location, and reflects the expected time it takes an aircraft to complete the departure process in the absence of any delays. This hypothesis could be investigated with field measurements.

---

<sup>3</sup>Personal communication with MASSPORT

### 4.2.5 Unimpeded taxi-out time as a baseline

The unimpeded taxi-out time provides us with a metric for what the taxi-out time of an aircraft could be, if it spent no time in the queues of the departure process. Although we do not know how much time each aircraft spent in the different queues of the departure process we can estimate its taxi time had it spent no time in each of these queues. This unimpeded taxi-out time is used as a baseline in this work to evaluate the problem of surface congestion: by comparing the observed taxi-out times to the unimpeded taxi-out time, we can obtain a metric for the time that aircraft spend queuing at an airport.

### 4.2.6 Method description

For each segment at an airport, we calculate the unimpeded taxi time of each airline,  $\tau_{unimped}$ . We then identify flights that have a taxi time higher than the unimpeded taxi time of their airline. We define these flights as “impeded flights”, because they do not take off within their unimpeded taxi time. Their taxi time,  $\tau$ , can be decomposed in two terms:

$$\tau = \tau_{unimped} + \tau_{impeded} \quad (4.4)$$

The sum of  $\tau_{unimped}$  over all impeded flights will be defined as the total excessive taxi time for a segment. Finally, for each segment, we calculate the mean unimpeded taxi time,  $\bar{\tau}_{unimped}$  as the weighted average of the unimpeded taxi times of the different airlines. The weight of each airline is the ratio of the number of flights it serves at a particular airport to the total number of flights out of the airport. This measure is an estimate of the mean unimpeded taxi time of a segment.

## 4.3 Saturation taxi time

### 4.3.1 Definition of saturation taxi time

While the comparison of the taxi times to the unimpeded ones is a good metric for the impact of queuing on taxi time, the ability to achieve unimpeded taxi-out times in practice is questionable. With the current level of coordination and operations planning at airports, the unimpeded taxi times are achievable only when the demand for resources (ATC communications, gates, ramp area, taxiways and runways) is close to zero. This can usually be achieved only when the number of aircraft taxiing is very small. Otherwise, some queuing delay is expected. If there were more

planning, coordination, control and certainty in the system, one could possibly plan operations in such a way that the airport achieves both high throughput and small queuing delays. In such a scenario, a controller would make use of some decision support system and plan aircraft pushback times, dispatch, routing, speed profile and sequencing. With accurate information and control of the system, it could be possible for the airport to achieve its sustained departure capacity with little queuing, small taxi delays and minimal emissions. Such a future scenario is the subject of ongoing research and development by NASA [25].

However, with the current level of coordination and planning, the saturation point  $N^*$  denotes the operational condition at which the airport reaches its sustained departure capacity. An airport needs to have, on average, at least  $N^*$  aircraft active on the surface so as to reach its capacity. If there are fewer than  $(N^* + 1)$  active aircraft on the surface, the level of traffic and the corresponding taxi times and emissions may be characterized as acceptable. This motivates us to define a second baseline of acceptable taxi time: It is the mean taxi time all the aircraft having  $(N^* - 1)$  aircraft in their takeoff queue. This time is denoted the “saturation taxi time”. The taxi time of an aircraft  $i$  having  $N^*$  or more aircraft in its takeoff queue,  $N_Q(i)$ , can be characterized as excessive.

At this point it is important to emphasize the distinction between the number of aircraft on the ground  $N$  and the takeoff queue,  $N_Q(i)$ , of an aircraft  $i$ . In Chapter 3, we defined the saturation point,  $N^*$ , as the expected number of aircraft on the ground necessary for an airport to reach its “sustained departure capacity”. In this chapter, we define flights in congestion to be flights where the number of aircraft in their takeoff queue  $\geq N^*$ . These flights will have to wait for more than  $N^*$  aircraft to be served before they takeoff. Since however  $N^*$  aircraft are necessary for the airport to operate efficiently, *flights in congestion* may as well wait at the gate and pushback when their takeoff queue reaches  $(N^* - 1)$ . This would neither cause delay to the aircraft nor lower the throughput of the airport.

If we were to define flights in congestion as those flights that pushback when there are  $N^*$  aircraft on the ground, we would get different results. Referring to the results of the unimpeded taxi time calculation for a BOS segment in Subsection 4.2.4, an American Eagle flight may pushback when there are  $N^*$  aircraft on the ground. As per this alternative definition, this is a flight in congestion. However, it may be the case that several of the flights on the ground are of airlines with unimpeded taxi times larger than that of the American Eagle flight. For instance, let us say that Delta, Continental, AirTran or Northwest flights have just pushed back. Then, suppose that some of them are overtaken by the American Eagle flight on their way to the runway. Let us also assume

for the sake of simplicity that there are no other pushbacks until all these flights takeoff. In this case, after the American Eagle flight has pushed back, there are  $(N^* + 1)$  aircraft on the ground. From this moment on, the flight that will be the last to takeoff, will spend the longest time on the ground, and is the flight facing the longest takeoff queue. This is not the American Eagle flight, which is the last to pushback, but manages to overtake other flights. This is the reason that the flight we would prefer to keep at the gate is the flight with a takeoff queue of length  $N^*$ , rather than the American Eagle flight.

In practice, keeping flights with takeoff queues of length  $\geq N^*$  may be challenging: the takeoff queue of a flight is not known at the moment of pushback. Therefore, in order to keep aircraft with takeoff queue  $\geq N^*$  at the gate, we must accurately estimate the re-sequencing of aircraft on their way from the gate to the runway. A simpler control strategy may be to control the number of the ground  $N \leq N^*$ . This strategy is significantly easier to implement, but comes at a cost. Referring to the previous example, this strategy would delay at the gate the American Eagle flight. That would have two consequences:

1. The flight that gets held at the gate does not have the longest taxi time. The taxi time, fuel burn and emissions reduction will therefore be smaller.
2. There may be a loss in efficiency:  $N^*$  is the minimum expected number of aircraft for the airport to reach its departure capacity. As the throughput plots in Appendix B show, there is a significant variance in the distribution of the throughput. By holding back the flight that pushes back last, but does not necessarily take off last, we may not be fully utilizing the capacity. Several of the remaining aircraft may be far from the runway and there may be some capacity loss. On the other hand, allowing American Eagle to pushback while holding back the flight with a takeoff queue of length  $N^*$  would make this event less likely.

### 4.3.2 Estimation of the saturation taxi time

For each segment at an airport, the saturation taxi time,  $\tau_{sat}$  is calculated as the mean taxi time of all the aircraft having  $(N^* - 1)$  aircraft in their takeoff queue. There is no need to differentiate between different gates or airlines in this case, because when an aircraft has  $(N^* - 1)$  aircraft in its departure queue, it is expected to spend a fair amount of time in the different queues of the system. Its starting point will mainly affect where this time is spent.

## Method description

All the aircraft which have  $N^*$  or more aircraft in their takeoff queue are characterized as “flights in congestion”. A flight in congestion does not contribute to the throughput of the airport, but contributions to the surface congestion. Such flights could be delayed without incurring insurmountable delays or compromising airport efficiency.

The taxi time of a flight in congestion is called the “taxi time in congestion”. We calculate the mean taxi time of all flights in congestion,  $\bar{\tau}$  *in congestion* as the arithmetic mean of all *flights in congestion*. As we have shown in the subsection 4.2.2 the taxi time of an aircraft scales with its takeoff queue. Thus, the difference between the  $\bar{\tau}$  *in congestion* and the  $\tau_{sat}$  provides a quick and practical estimate of how deep in the congestion area the airport tends to operate. This metric complements the *flights in congestion* metric, as the latter does not provide information about how deep in the congestion these operations take place and how much longer the taxi time is than  $\tau_{sat}$ . For example, two different airports could have 10,000 flights in congestion. However, if in the first case the difference between the  $\bar{\tau}$  *in congestion* and the  $\tau_{sat}$  is 30 minutes whereas in the second it is only 2 minutes, the first airport faces a more severe congestion problem; whereas the second tends to operate quite often at a point marginally higher than its saturation point.

## 4.4 Taxi times analysis

In the following sections we give the excessive taxi time baselines and metrics for the most frequently used segments of the four airports for which the congestion was analyzed in Chapter 3. More specifically, for each segment we give the following metrics:

- The mean taxi time,  $\bar{\tau}$
- The mean unimpeded taxi time,  $\bar{\tau}_{unimped}$
- The number and mean taxi time of the impeded flights,  $\bar{\tau}_{unimped}$
- The saturation taxi time of the segment,  $\tau_{sat}$
- The number of flights in congestion, and their taxi time  $\bar{\tau}$  *in congestion*

#### 4.4.1 JFK taxi times

##### VMC taxi times analysis

The results from JFK reinforce the observation of Chapter 3 that the airport is very congested: 139,713 flights out of the 148,829 served in the segments [1-6] had taxi times longer than their unimpeded times. It is also worth noting the extent to which flights end up getting delayed: the mean taxi time in congestion can be as much as 18 minutes larger than the saturation taxi time. This indicates that JFK suffers from significant surface inefficiencies: 33,743 flights operate in congestion and taxi on average 15 minutes longer than the saturation taxi time contributing to congestion, fuel burn and emissions of the airport. This suggests that there is a great opportunity for improvement in JFK. The results also show that the runway configurations (4 and 6) with two departure runways have lower unimpeded taxi times.

**Table 4.2:** Congestion analysis for JFK in 2007 under VMC

<i>RC</i>	$\bar{\tau}$	$\bar{\tau}_{unimped}$	# of impeded flights	$\bar{\tau}$ of impeded flights	$\bar{\tau}_{impeded}$	$\tau_{sat}$	# of flights in cong.	$\bar{\tau}$ in cong.
1	36.08	16.49	27517	39.25	22.92	42.66	6891	60.02
2	34.54	16.28	33923	37.04	21.22	40.05	8114	56.38
3	37.46	17.00	30717	40.23	23.43	47.60	7194	61.59
4	31.16	15.15	22871	34.55	19.48	38.18	4239	48.85
5	36.32	17.14	12301	39.09	21.89	39.54	3794	54.97
6	33.27	15.27	12384	36.67	21.87	34.36	3511	49.32
[1-6]	34.99	16.37	139713	37.92	21.87	41.31	33743	56.40

##### IMC taxi times analysis

The IMC analysis shows that the congestion problem worsens under instrumental meteorological conditions: 7,866 out of the 24,412 flights pushback under congestion and spend on average 69 minutes taxiing, 20 minutes more than the saturation taxi time. From comparing Tables 4.2 and 4.3, it can be seen that the unimpeded taxi times are higher under IMC than under VMC. This will be the case for all airports we analyze and is expected, because aircraft need longer time to complete the stages of the departure process under instrumental weather conditions.

Table 4.3: Congestion analysis for JFK in 2007 under IMC

<i>RC</i>	$\bar{\tau}$	$\bar{\tau}_{unimped}$	# of impeded flights	$\bar{\tau}$ of impeded flights	$\bar{\tau}_{impeded}$	$\tau_{sat}$	# of flights in cong.	$\bar{\tau}$ in cong.
all	45.23	19.00	23273	51.81	32.95	47.46	7866	68.83

#### 4.4.2 EWR taxi times

##### VMC taxi times analysis

Table 4.4 shows the taxi time analysis for the most frequently used VMC segments in EWR in 2007. It can be seen that the taxi times tend to be lower than the ones in JFK. Nonetheless, 157,153 out of the 165,344 flights record taxi times higher than their unimpeded ones. In every segment, a large number of flights encounter a congested takeoff queue, but the total number of flights in congestion is smaller than at JFK. However, the taxi times in congestion at EWR can be as much as 18 minutes longer taxiing than the saturation taxi time. This indicates significant inefficiencies on the surface and that surface management strategies would have great impact in this airport as well. On average, aircraft in congestion spend almost 14 minutes longer than the saturation taxi time. Comparing Tables 4.2 and 4.4, it can also be observed that unimpeded taxi times tend to be higher in JFK than EWR. Possible reasons for this are the more complicated layout of JFK and the longer distances between the terminals and the runways. Therefore, although the mean taxi-time in JFK for the major VMC configurations is 7 minutes higher than the one in EWR, the mean impeded taxi time in JFK is only about 5 minutes higher than the one in EWR.

Table 4.4: Congestion analysis for EWR in 2007 under VMC

<i>RC</i>	$\bar{\tau}$	$\bar{\tau}_{unimped}$	# of impeded flights	$\bar{\tau}$ of impeded flights	$\bar{\tau}_{impeded}$	$\tau_{sat}$	# of flights in cong.	$\bar{\tau}$ in cong.
1	25.55	13.25	56089	29.28	16.08	36.19	8177	50.09
2	29.55	13.77	35890	32.42	18.69	41.23	6476	54.23
3	27.81	13.48	31494	29.31	15.85	43.35	3707	54.46
4	32.7	14.37	16737	34.61	20.18	38.32	4591	56.08
5	30.43	14.32	8697	31.8	17.49	37.73	2111	52.19
6	28.95	11.97	8246	31.49	19.66	28.39	2719	41.05
[1-6]	28.13	13.54	157153	30.83	17.33	38.02	27781	51.90



## IMC taxi times analysis

The results from the two most frequently used runway configurations at EWR under IMC are shown in Table 4.5. Runway configurations 1 and 2 yield very different results although they tend to show similar behavior under VMC. This discrepancy is explained by the very high value of  $N^*$  of configuration 2, as explained earlier in Section 3.7.2. Therefore, in this case, a comparison between the statistics of the two configurations in congestion is not very helpful. We note that the weather seems to affect the taxi times only marginally. The mean impeded taxi time increases only by 3 minutes, whereas at JFK the difference in the impeded taxi time between VMC and IMC is 11 minutes.

Table 4.5: Congestion analysis for EWR in 2007 under IMC

<i>RC</i>	$\bar{\tau}$	$\bar{\tau}_{unimped}$	# of impeded flights	$\bar{\tau}$ of impeded flights	$\bar{\tau}_{impeded}$	$\tau_{sat}$	# of flights in cong.	$\bar{\tau}$ in cong.
1	29.01	14.03	11813	32.87	18.83	29.58	3587	45.26
2	32.7	13.68	13544	34.96	21.27	57.16	914	70.19
[1-2]	30.99	13.84	25357	33.99	20.14	35.18	4501	50.32

### 4.4.3 PHL taxi times

#### VMC taxi times analysis

The results for the most frequently used runway configurations at PHL under VMC are presented in Table 4.6. It can be seen that PHL is a very congested airport as well: 48,137 flights out of the 189,045 flights (25.5%) face a congested takeoff queue, as opposed to 33,743 out of 148,829 (22.7%) flights in JFK. However, the net effect of congestion appears to be similar: The average impeded taxi times is less than 14 minutes, and the taxi time of the congested flights is only 11 minutes longer than the saturation taxi time. Therefore, although many flights face congestion, they are affected in a more moderate way, and the mean taxi time is much smaller than at JFK or EWR. The mean taxi time comparison alone does not show the full picture: the unimpeded taxi time at PHL is almost 5 minutes shorter than the unimpeded taxi time at JFK.

A comparison of the taxi times analysis of the VMC segments at PHL and at EWR is also informative. We can see that both the total and the impeded taxi times are higher at EWR than at PHL. On the other hand, the product of the total number of congested flights and their taxi times

(48,137 \* 37.1) is higher at PHL than at EWR (27,781 \* 52.33). A strategy aimed at reducing the taxi times during congested periods would be more effective at PHL than at EWR.

**Table 4.6:** Congestion analysis for PHL in 2007 under VMC

<i>RC</i>	$\bar{\tau}$	$\bar{\tau}_{unimpeded}$	# of impeded flights	$\bar{\tau}$ of impeded flights	$\bar{\tau}_{impeded}$	$\tau_{sat}$	# of flights in cong.	$\bar{\tau}$ in cong.
1	21.45	11.39	140992	23.63	12.28	25.47	39098	35.78
2	33.91	12.72	9354	39.27	26.61	28.7	3925	48.65
3	27.59	11.37	10127	29.43	18.08	32.35	2930	46.16
4	23.11	12.24	7278	30.35	18.36	25.13	2184	37.39
[1-4]	22.51	11.50	167751	25.15	13.70	26.13	48137	37.53

### IMC taxi times analysis

Table 4.7 shows the analysis results for the most frequently used IMC segments at PHL. A comparison between VMC and IMC performance for runway configuration 2 supports the analysis of Section 3.7.3. Runway configuration 2 has very similar performance characteristics under VMC and IMC (unimpeded taxi time and saturation taxi time), and it is more congested under VMC (higher impeded taxi time, higher taxi-time in congestion, and more flights in congestion). Configuration 5 has the shortest saturation taxi time. A large proportion of its flights face a congested takeoff queue (2,976 out of the 7,219), their taxi times are however in the same range as those of the congested flights in other segments. To summarize, instrumental weather conditions do not seem to affect congestion and the resulting taxi times at PHL.

**Table 4.7:** Congestion analysis for PHL in 2007 under IMC

<i>RC</i>	$\bar{\tau}$	$\bar{\tau}_{unimpeded}$	# of impeded flights	$\bar{\tau}$ of impeded flights	$\bar{\tau}_{impeded}$	$\tau_{sat}$	# of flights in cong.	$\bar{\tau}$ in cong.
2	27.81	12.4	6769	33.08	20.77	27.45	2458	41.52
5	26.66	12.32	6606	29.93	17.67	23.17	2976	38.83
[2,5]	27.22	12.36	13375	31.52	19.24	25.10	5434	40.05

#### 4.4.4 BOS taxi times

##### VMC taxi times analysis

Table 4.8 shows the analysis results for the most frequently used VMC segments at BOS. It is noted that BOS is the least congested airport among the four major airports considered in this analysis. The impeded taxi times are shorter than 10 minutes, and shorter than the unimpeded ones for all the configurations. Taxi times in congestion are less than 10 minutes larger than the saturation taxi times. The number of flights in congestion at BOS is much smaller than at PHL.

**Table 4.8:** Congestion analysis for BOS in 2007 under VMC

<i>RC</i>	$\bar{\tau}$	$\bar{\tau}_{unimped}$	# of impeded flights	$\bar{\tau}$ of impeded flights	$\bar{\tau}_{impeded}$	$\tau_{sat}$	# of flights in cong.	$\bar{\tau}$ in cong.
1	20.25	12.84	40016	21.81	8.96	23.58	8540	32.10
2	18.59	11.52	27469	19.75	8.24	23.83	3250	34.16
3	21.40	13.15	21561	22.59	9.51	30.27	1594	39.77
4	19.60	13.23	8111	20.60	7.59	28.63	329	36.16
[5-20]	19.50	12.65	31536	21.63	9.04	27.04	2904	38.56
[1-20]	19.87	12.59	128693	21.38	8.83	24.98	16617	34.45

##### IMC taxi times analysis

Table 4.9 shows the analysis results for the most frequently used IMC segments at BOS. Configurations [10,12,13] are more congested in relative terms than the corresponding segment (VMC;2): 2,876 out of the 15,152 flights are congested, whereas only 3,250 out of 30,437 flights are congested in segment (VMC;2). The taxi time in congestion is almost 12 minutes higher than the saturation taxi time, and the impeded flights have higher taxi times than the impeded ones under VMC. These results suggest that BOS congestion and its effects on taxi times are larger under IMC and a strategy to mitigate congestion would be more effective under IMC.

**Table 4.9:** Congestion analysis for BOS in 2007 under IMC

<i>RC</i>	$\bar{\tau}$	$\bar{\tau}_{unimped}$	# of impeded flights	$\bar{\tau}$ of impeded flights	$\bar{\tau}_{impeded}$	$\tau_{sat}$	# of flights in cong.	$\bar{\tau}$ in cong.
[10,12,13]	21.61	12.58	12923	24.03	11.57	25.54	2876	37.22

## 4.5 Emissions analysis

Table 4.10 shows the fuel burn and emissions for the departing flights taking off from the configurations analyzed in the four airports we consider. It also shows the fuel burn and emissions if the flights departed with their unimpeded taxi times. It is striking that in JFK, EWR and PHL, the actual fuel burn and emissions are more than double than the ones resulting from the unimpeded operations. These results suggest that the environmental footprint of the airports and the fuel costs could be significantly reduced if the aircraft could depart within their unimpeded taxi times.

The fuel burn and emissions calculations were performed in cooperation with Indira Deonandan according the methodology outlined in [12], assuming that each flight taxis at 7% throttle setting, and using fuel burn and emissions indices from ICAO [22]. In practice, some taxiing aircraft, especially those delayed because of downstream restrictions, are diverted to holding pads where they typically have their engines off. Qualitative data on this is not available. In order to keep our estimates realistic, the fuel burn and emissions from flights having a taxi time longer than 90 minutes are truncated to the ones with a 90 minute taxi time. In other words, we assume that a flight does not taxi with engines on for longer than 90 minutes.

**Table 4.10:** Fuel burn and emissions in JFK, EWR, PHL and BOS

Airport	Reported taxi times				Unimpeded taxi times			
	Fuel (10 <sup>3</sup> gal)	HC (kg)	CO (kg)	NOx (kg)	Fuel (10 <sup>3</sup> gal)	HC (kg)	CO (kg)	NOx (kg)
JFK	27,665	157,773	1,798,774	360,341	12,483	71,917	808,654	162,514
EWR	20,778	124,752	1,550,600	268,279	10,213	59,192	749,569	131,918
PHL	21,521	163,736	1,593,594	275,793	9,914	75,820	732,084	126,725
BOS	13,656	89,007	945,291	172,563	8,444	54,781	584,203	106,901

As mentioned earlier in this chapter, it does not seem realistic to currently achieve unimpeded taxi times for all flights. For this reason, we perform the following additional calculation: We calculate the fuel burn and the emissions of all congested flights and we compare them to the fuel burn and the emissions that would result if their taxi time were the saturation taxi time of their segment. We compare the fuel burn and emissions of the congested flights to the expected values if their takeoff queue had the saturation value of their segment. The results are shown in Table 4.11.

From Table 4.11 it can be observed that significant fuel burn and emissions reductions could be achieved if the congested flights had the saturation taxi time of their segment. It is worth noting that PHL appears to be able to achieve the highest reductions in fuel burn and emissions despite

**Table 4.11:** Fuel burn and emissions in JFK, EWR, PHL and BOS

Airport	Reported taxi times				Unimpeded taxi times			
	Fuel (10 <sup>3</sup> gal)	HC (kg)	CO (kg)	NOx (kg)	Fuel (10 <sup>3</sup> gal)	HC (kg)	CO (kg)	NOx (kg)
JFK	10,804	59,032	687,460	141,388	8,327	45,508	530,845	108,998
EWR	5,648	35,915	434,560	73,139	4,291	27,185	329,536	55,538
PHL	9,144	69,418	673,457	117,323	6,232	47,573	460,954	79,946
BOS	3,079	20,750	217,956	38,765	2,188	14,554	154,162	27,572

having a lower average taxi time than JFK and EWR. The reductions which seem to be possible by controlling the pushback of aircraft so as to avoid unnecessary accumulation of active aircraft on the surface are quite substantial, and motivate us to investigate this issue further. In Chapter 5, we develop a model of the departure process. In Chapter 6, the model is used to simulate the departure process and evaluate the impact of a strategy aimed at controlling the number of active aircraft on the surface to within the saturation point  $N^*$ .



## Chapter 5

# A queuing model of the departure process

### 5.1 Introduction

In this chapter we develop a queuing model of the departure process. We calibrate and validate this model in terms of its ability to predict taxi-out times and the flow of aircraft at Boston Logan International Airport (BOS).

### 5.2 Related work

Prior work on the modeling of the departure process at airports can be broadly classified into two groups. The first group focuses on computing runway-related delays under dynamic and stochastic conditions [23, 24]. This runway-centric approach is justified by the observation that the main throughput bottleneck at an airport is the runway system [20]. This approach views the runway complex of an airport as a queuing system whose customers are aircraft that need to land or takeoff. The models are then used to predict the expected system behavior, and their results are typically most useful for long-term planning (for example, estimating the expected reduction in delays from the construction of a new runway), but are less useful for predicting taxi-out times for individual flights.

The second category of prior research focused on predicting taxi-out times. Shumsky developed a model to predict taxi times using a variety of explanatory variables such as the airline, the departure runway and departure demand [30]. He also developed a queuing model for the runway

service process. However, the queuing model was based on cumulative behavior and did not reflect the stochastic nature of the process [30]. Idris *et al.* analyzed the main causal factors that affect taxi times and based on this analysis, they developed a statistical regression model to predict taxi times [18]. This work, however, did not explicitly model the runway service process, and required knowledge of the number of aircraft on the ground in order to predict taxi times. It could therefore not be used for strategic flow management applications such as the one considered in this thesis, where we like to consider gate-to-runway traffic states, and determine how surface queues can be managed in order to reduce taxi-out times.

While the above papers identified several key factors that influence taxi-out times, they did not develop a model that was capable of predicting taxi-out times. In contrast, Pujet *et al.* extended some these notions to predict taxi times using a simple queuing model [28]. They assumed that an aircraft will need a certain (fixed) amount of time, defined to be the *travel time*, to reach the departure runways. In their model, upon reaching the departure runways, aircraft line up in the *runway queue*, where they get served by the runway server according to a probabilistic service process. Pujet *et al.* estimated the travel time for each flight based on several casual factors and also modeled the probabilistic service process. Given a pushback schedule, their model estimated taxi-out time as the sum of travel time and the wait time for service (takeoff) at the runway queue.

Section 4.2.2 provided a better method for estimating the travel times of aircraft to the departure runways and Section 5.6.3 provides a better model of the service process at the runways. A key objective of this chapter is to develop a good predictive model of airport operations that will also reflect a fact that several researchers have observed, but that as yet remains unmodeled, namely that, although the runway is the main flow constraint in departure processes, *the airport is a complex system of interacting queues* [19].

### 5.3 Model inputs and outputs

The primary objective of this Chapter is to develop a model that adequately describes the departure process, given operations data from an airport. The desired outputs of such a model include:

- The level of congestion on the airport surface in the immediate future.
- The predicted loading of the different surface queues.
- The predicted taxi-out time of each departing flight.



The inputs to the model are based on the explanatory variables identified in previous studies [18, 30, 7, 2]. Idris *et al.* [18] identified the runway configuration, weather conditions and downstream restrictions, the gate location, and the length of the takeoff queue that a flight experiences as the critical variables determining the taxi time of a departing flight. The length of the takeoff queue experienced by a flight is defined as *the number of takeoffs which take place between the pushback time of an aircraft and its takeoff time*.

The present study is an attempt to construct a predictive model of surface congestion, so the takeoff queue size is not available as an input. Instead, we use the pushback schedule, which is the schedule of aircraft pushing back from their gates. We note that we do not predict the pushback schedule based on the published departure schedule; such models that predict pushback schedules based on the departure schedule may be found in Shumsky’s thesis [30]. Furthermore, the general weather conditions (denoted either Visual Meteorological Conditions, or Instrumental Meteorological Conditions) are used as surrogates for weather and downstream airspace conditions. Andersson *et al.* introduced the concept of the *segment*, which they defined as a particular combination of runway configuration and weather conditions [2]. The runway configuration is characterized by both the runways used for arrivals as well as those used for departures. Each segment is defined as a combination of the runway configuration and the general weather conditions (VMC or IMC). Therefore, we denote a segment as (Weather Conditions; Arrival Runways | Departure Runways). For example, a segment denoted ‘(R1,R2 | R3,R4; VMC)’ would correspond to runways R1 and R2 being used for arrivals, and R3 and R4 being used for departures under Visual Meteorological Conditions.

To summarize, the inputs to the model are

- The pushback schedule,  $PS$ .
- The gate location of the departing flight,  $GL$ .
- The segment in use,  $(RC; MC)$ , expressed as the combination of the runway configuration,  $RC$ , and the general weather conditions,  $MC$ .

We define

- $P(t)$  = the number of aircraft pushing back during time period  $t$ .  $P(t)$  is an input to the model.

- $N(t)$  = the number of departing aircraft on the surface at the beginning of period  $t$ .  $N(t)$  is the first output of the model, indicating the congestion of departing aircraft on the ground.
- $Q(t)$  = the number of aircraft waiting in the departure queue at the beginning of period  $t$ . The departure queue is defined as the queue which is formed at the threshold(s) of the departure runway(s), where the aircraft queue for takeoff.  $Q(t)$  is the second output of the model, and gives the loading of the departure queues.
- $R(t)$  = the number of departing aircraft taxiing in the ramp and the taxiways at the beginning of period  $t$  (*i.e.*, the number of departures on the surface that have not reached the departure queue).
- $C(t)$  = the (departure) capacity of the departure runways during period  $t$ .
- $T(t)$  = the number of takeoffs during period  $t$ .
- $N_Q(i)$  = the number of aircraft taking off between the pushback and takeoff time of aircraft  $i$  (the length of the takeoff queue experienced by aircraft  $i$  queue [18]).
- $\tau(i)$  = the taxi time of each departing aircraft. This is the third output of the model.

Using the above notation, the following relations are satisfied:

$$N(t) = Q(t) + R(t) \tag{5.1}$$

$$N(t) = \min(C(t), Q(t)) \tag{5.2}$$

$$N(t) = N(t-1) + P(t-1) - T(t-1) \tag{5.3}$$

Combining Equations (5.1) and (5.3), we get

$$Q(t) = Q(t-1) - T(t-1) + R(t-1) - R(t) + P(t-1), \tag{5.4}$$

which is the update equation of the departure queue.

## 5.4 Model structure

The three outputs of the model,  $N(t)$ ,  $Q(t)$  and  $\tau(i)$ , are related through the departure process. The departure process can be conceptually described in the following manner:

Aircraft pushback from their gates according to the pushback schedule. They enter the ramp and then the taxiway system, and taxi to the departure queue which is formed at the threshold of the departure runway(s). During this traveling phase, aircraft interact with each other. For example, aircraft queue to get access to a confined part of the ramp, to cross an active runway, to enter a taxiway segment in which another aircraft is taxiing, or they get redirected through longer routes to minimize interference with built up congestion. We cumulatively denote these spatially distributed queues and delays which occur while aircraft traverse the airport surface from their gates towards the departure queue as *ramp and taxiway interactions*. After the aircraft reach the departure queue, they line up to await takeoff. We model the departure process as a server, with the departure runways “serving” the departing aircraft in a First-Come-First-Serve (FCFS) manner. This conceptual model of the departure process is depicted in Figure 5-1.

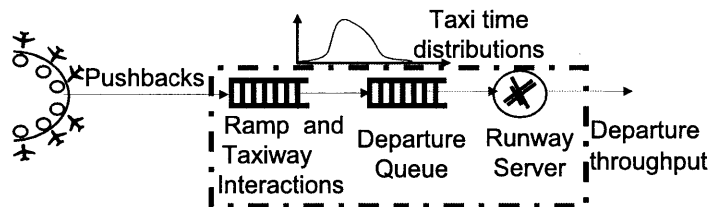


Figure 5-1: Integrated model of the departure process

By modeling the departure process in this manner, the taxi-out time  $\tau$  of each departing aircraft can be expressed as

$$\tau = \tau_{unimped} + \tau_{taxiway} + \tau_{dep.queue} \quad (5.5)$$

The first term of Equation (5.5),  $\tau_{unimped}$ , reflects the nominal or *unimpeded taxi-out time* of the flight. This is the time that the aircraft would spend in the departure process if it were the only aircraft on the ground. The second term,  $\tau_{taxiway}$ , reflects the delay due to aircraft interactions on the ramp and the taxiways. In other words,  $\tau_{taxiway}$  reflects the delay incurred due to other aircraft that are on their way to the departure queue. The number of such aircraft is given by  $R(t) = N(t) - Q(t)$ . The magnitude of this delay will depend on the exact interactions among the taxiing aircraft, or in other words, the level of congestion in the taxiways. The third term,  $\tau_{dep.queue}$ , is the time the aircraft spends in the departure queue. The duration of this time depends on the number of aircraft at the departure queue ( $Q(t)$ ) and the runway service characteristics.

We observe that the taxi time of each departing aircraft depends on the model inputs and the two other model outputs ( $N(t) - Q(t)$  and  $Q(t)$ ). In contrast, the number of aircraft on the ground

and in the departure queue,  $N(t)$  and  $Q(t)$  respectively, may be updated using Equations (5.3) and (5.4), as aircraft takeoff and pushback. Therefore, assuming that Equation 5.5 is an appropriate way to describe the departure process, the model may be built using the following steps:

1. Model  $\tau_{unimped}$  as a function of the explanatory variables  $GL$ ,  $RC$  and  $MC$ .
2. Model the dependence of  $\tau_{taxiway}$  on  $R(t)$ , given  $RC$  and  $MC$ .
3. Model the statistical characteristics of the runway service process given  $RC$  and  $MC$ .

Then, given a pushback schedule and gate locations, we can use Equations (5.3-5.5) to get the outputs of the models.

In order to extract the dependencies mentioned above, we analyze a data set of observations from aircraft taxiing out at an airport. Combining the observed data with the explanatory variables, we can analytically describe  $\tau_{unimped}$ ,  $\tau_{taxiway}$  and  $\tau_{dep.queue}$  and construct the required model.

## 5.5 Data requirements

Ideally, we would like a dataset which consists of  $\tau_{unimped}$ ,  $\tau_{taxiway}$  and  $\tau_{dep.queue}$ , in order to study how these variables change with the model inputs. However, this information is not recorded. The recorded data that is publicly available for flights departing from an airport of study during a time period consists of:

1. Actual pushback time times
2. Actual takeoff times

In addition to these, we can obtain the following information about the explanatory variables at each time-period:

3. Pushback schedules
4. Runway configuration
5. Reported meteorological conditions, and
6. Gate location for each departing flight

Fields (1-??) are obtained from the ASPM database following the method outlined in Chapter 2. Fields 4 and 5 are also obtained from the ASPM database [14], where runway configurations and weather conditions are reported in 15-minute intervals. As in Chapter 4, the the operating airline of a flight serving as a surrogate for the “gate location”, the starting point of the aircraft.

## 5.6 Model development for BOS

In this section, we analyze how we can get estimates of the three terms of Equation (5.5), given a set of the explanatory variables ( $RC, MC, GL, PS$ ) for Boston Logan International Airport (BOS). An inherent difficulty in the model calibration is the poor resolution of the available data: we do not have observations of  $\tau_{unimped}$ ,  $\tau_{taxiway}$  and  $\tau_{dep.queue}$ , but instead only the actual pushback and takeoff times of flights. As a result, the calibration of the model makes several assumptions which are addressed in the next few sections. We also illustrate how these assumptions can be used for the calibration of the model for a particular runway configuration under VMC in BOS. The same procedure has also been utilized to calibrate the model for two other frequently used runway configurations under VMC in BOS.

### 5.6.1 Unimpeded taxi time calculation

The unimpeded taxi time calculation is performed following the steps outlined in Chapter 4.

### 5.6.2 Identification of throughput saturation points

In order to determine the amount of time that each aircraft will spend waiting in the departure queue, we need to first determine the statistical characteristics of the runway departure process. This can be done through the observation of runway performance under heavy loading. Under such conditions runways operate at their capacity, and by observing the output of the process the statistical properties of the server (the runways) may be inferred [28]. However, the regimes in which the runway process is saturated and the runway operates at capacity need to first be identified.

Following the approach proposed by Pujet [28], we use the number of departing aircraft on the ground as an indicator of the loading of the departure runway. We define  $\bar{T}_n(t + dt)$  as the takeoff rate over the time periods  $(t + dt - n, t + dt - n + 1, \dots, t + dt, \dots, t + dt + n)$ . The maximum correlation between  $N(t)$  and  $\bar{T}_n(t + dt)$  is obtained for  $n = 10$  and  $dt = 10$  for BOS, for the high-throughput configurations used under VMC conditions. This means that the number of departures on the surface at time  $t$ , namely  $N(t)$ , is a good predictor of the number of takeoffs during the time interval  $(t, t + 1, t + 2, \dots, t + 20)$ <sup>1</sup>.

---

<sup>1</sup>In a prior study, Pujet estimated that  $(n, dt) = (5, 6)$  [28]. This difference can be explained by the observation that his data included only 65% of flights and because both traffic and reporting rates at BOS have risen significantly over the past 10 years.

As  $N(t)$  increases, the takeoff rate initially increases, but saturates at a critical value  $N^*$ . The existence of  $N^*$  can be explained as follows: initially, as the number of aircraft on the surface increases, so does the number of departing aircraft. Beyond this threshold value of  $N$ , the runway becomes the defining capacity constraint, and increasing the number of aircraft further does not increase the throughput of the airport. This is consistent with the findings of prior studies [30, 28]. Applying similar techniques to BOS data for the year 2007, we determine the following *saturation points* for the most frequently used runway configurations in BOS under VMC conditions (Table 5.1).

**Table 5.1:** Runway saturation points for most frequent configurations used in BOS

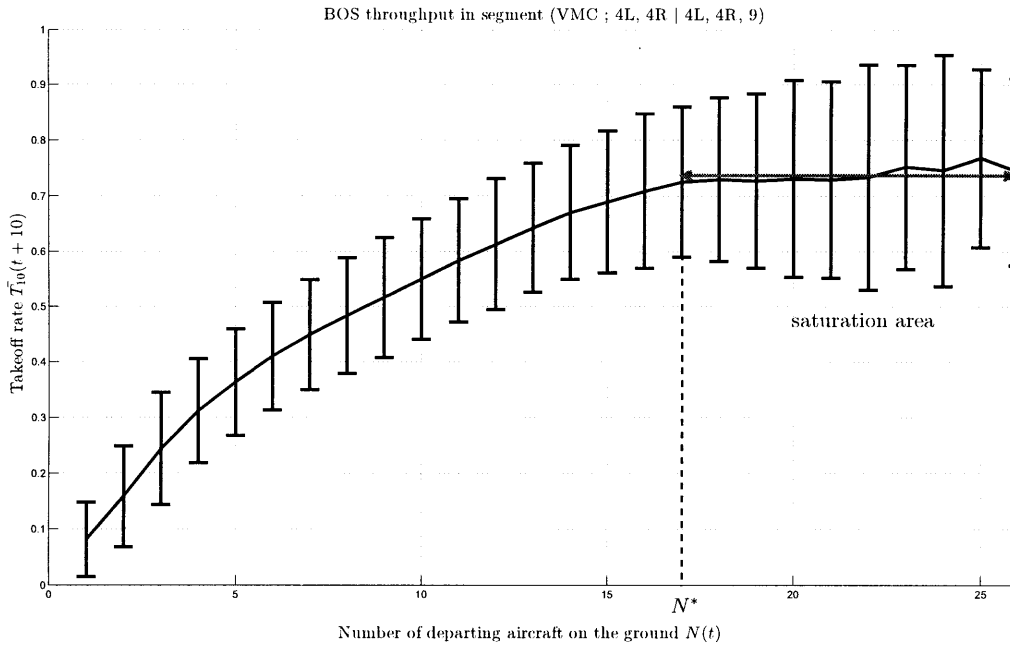
Configuration	$N^*$
22L, 27   22L, 22R	16
4L, 4R   4L, 4R, 9	17
27, 32   33L	21

Figure 5-2 shows the average takeoff rate as a function of  $N(t)$  for the segment (4L, 4R | 4L, 4R, 9; VMC) in BOS. The saturation point is also denoted. We note that the takeoff rate initially increases as  $N(t)$  increases, but subsequently saturates at about 0.73 aircraft/min or 44 aircraft/hour. This number can be viewed as the sustained departure capacity of BOS for the segment.

### 5.6.3 Modeling the runway service process

Having identified the regime of operations when the runway loading is high, it is possible to model the runway departure process itself. One possible approach (adopted by Pujet [28]) is to observe the takeoff rate  $\bar{T}_n(t + dt)$  when  $N(t)$  is larger than  $N^*$ , and to then model the runway capacity as a binomial random variable with the same mean and variance as the observed  $\bar{T}_n(t + dt)$ . While this is convenient for mesoscopic modeling, this approach does not try to reflect the characteristics of the runway, but instead reproduces the first and second order moments of the training data (a year of operations). Some of the inherent problems of the above modeling approach (pertaining to runway performance in particular) were noted by Carr [7].

In this study, we propose an alternate approach to modeling the runway service process. Let us examine the inter-departure times of the aircraft configurations: 4L, 4R | 4L, 4R, 9 at BOS during high loads ( $N(t) > 17$ ). We use this data to construct a histogram of inter-departure times, as



**Figure 5-2:** Takeoff rate as function of  $N(t)$

shown in Figure 5-3 (left). From this histogram, we find the mean inter-departure time to be 1.3 minutes with a standard deviation of 0.9 minutes. Another noteworthy observation is that 75% of the departures are separated by two minutes or less.

The distribution (during congested operations) reflects a combination of endogenous factors such as the departure process (availability of more than one departure runway; ATC wake vortex separation), and exogenous factors such as communication delays or interactions with arriving traffic. Ideally, one would like to factor in all these parameters in the model. However, for the sake of simplicity, we model the departure process probabilistically in the following manner:

We assume that the service time of each aircraft is random variable of the event “departure” that has three possible outcomes. The first two possible outcomes are one and two minutes. This is consistent with the fact that the typical runway occupancy time for commercial air carriers is approximately a minute. In addition, looking at all of the airports we have considered including this particular segment of BOS, the vast majority of the inter-departure times are within two minutes. Lastly, the third outcome is the next minute increment that satisfies the conditions:

- All three outcomes have positive probabilities
- The sum of the probabilities is 1
- the resulting probability mass function (PMF) has equal first two moments to the observed

one

In this particular segment, this event is the 5-min service time. The original histogram and the resulting PMF used in the model can be seen in figure 5-3.

In this way we account for the probabilistic nature of the runway service process, but model it in a simple way. Given an estimate of the times at which departing aircraft reach the runway, we can use this model of runway operations to predict the amount of time that each flight will spend waiting in the runway queue (denoted  $\tau_{dep.queue}$ ).

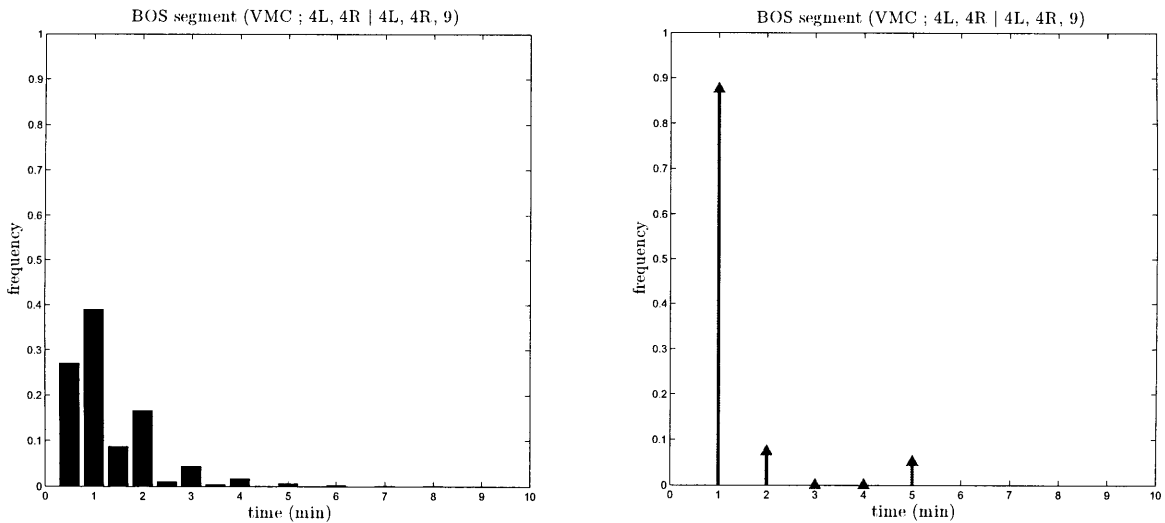


**Figure 5-3:** [Left] Histogram of inter-departure times; [Right] Simplified histogram of inter-departure times.

#### 5.6.4 Modeling ramp and taxiway interactions

The remaining unmodeled term in Equation (5.5), namely  $\tau_{taxiway}$ , represents the effect of queuing in the ramp area and the taxiways. This term is the most difficult to estimate, since there are no distinct operating conditions in which it is the dominant term. As a first step, we neglect this term. In other words, we assume that aircraft travel for their unimpeded taxi-out times and then reach the runway queue where they are processed according to the probabilistic process described in the previous section.

We test this model on the departure schedule from BOS in 2007 for the time intervals when the runway configuration 4L, 4R | 4L, 4R, 9 was used under VMC conditions. We only consider time intervals that the segment was in use consecutively for longer than four hours so as to immune the performance of the model from transitional effects that are out of the scope of this model. Figure 5-4 compares the performance of the model with the observed data.



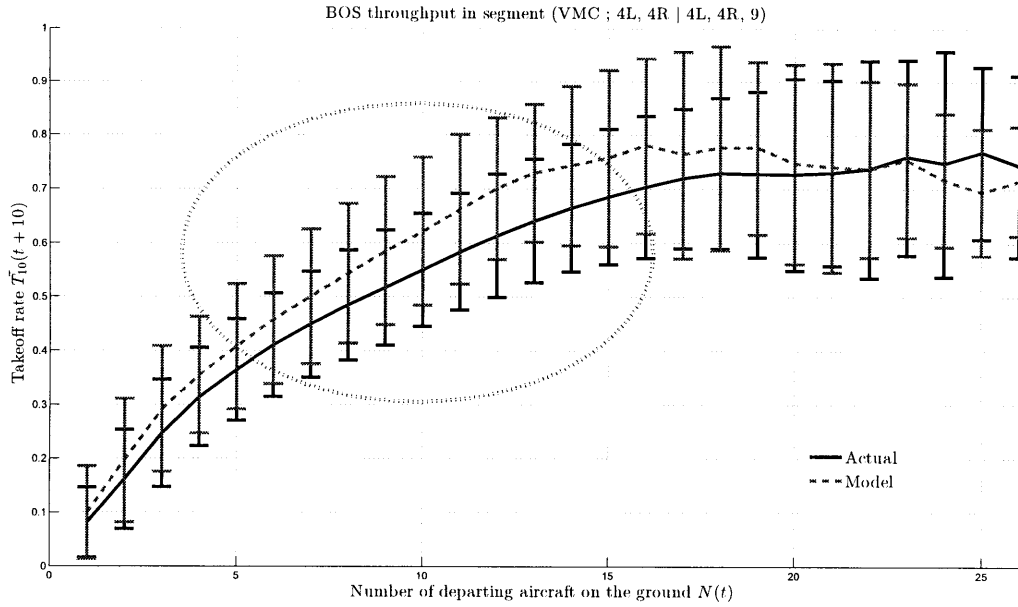


**Figure 5-4:** Actual and modeled takeoff rate as a function of  $N(t)$ , when taxiway interactions are neglected.

We observe that the performance of the model deteriorates at medium traffic conditions. This behavior may be explained through a closer look at the model: aircraft are assumed to reach the runway queue within their unimpeded taxi-out times, which are realized in light traffic conditions. Therefore, neglecting taxiway interactions is a reasonable approximation in low traffic. In heavy traffic conditions, the runway is saturated and the takeoff queue is expected to be long, so the runway queue time is the dominant factor in predicting the total taxi time. However, at medium traffic conditions, the assumption that aircraft always travel their nominal taxi time leads to predictions that are more optimistic than in real operations, as seen in Figure 5-4. This is because the model predicts that aircraft reach the runways at a higher rate than in reality (since the model assumes that they only taxi for their unimpeded times), and do not wait at the runway (since the runway queues are not saturated). This issue can also be seen in Figure 5-5, which depicts the frequency that different congestion states are observed in reality and in the model: The model predicts the airport being at low congestion levels much more often than observed. This happens because the predicted takeoff rates tend to be greater than the observed rates. We hypothesize that this happens because of neglecting  $\tau_{taxiway}$  and that the performance of the model can be improved by including this term.

In addition, accounting for taxiway congestion effects allows us to obtain better estimates of the number of aircraft in the taxiway system ( $R(t)$ ) and in the runway queue ( $Q(t)$ ). In particular,

a good estimate of  $Q(t)$  will also help in the departure planning process.

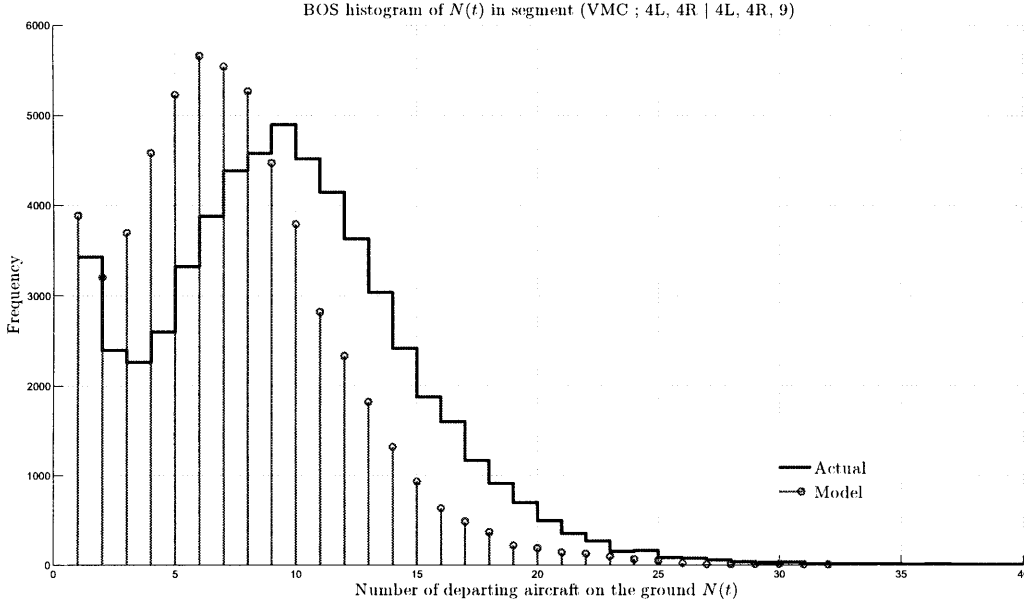


**Figure 5-5:** Actual and modeled  $N(t)$  histogram, when taxiway interactions are neglected.

We now refine our model by relaxing the assumption that the aircraft take just their unimpeded taxi-out time to reach the runway. Equation (5.5) is modified so that the travel time of an aircraft from its gate to the runway queue depends on its unimpeded taxi-out time and on the amount of traffic on the ramps and the taxiway at the time. The modified equation becomes

$$\tau = \tau_{travel} + \alpha R(t) + \tau_{dep.queue} \quad (5.6)$$

The term  $\alpha R(t)$  is a linear term used to model the interactions among departing aircraft on the ramps and taxiways.  $\alpha$  is a parameter that depends on the airport and the runway configuration. Its value can be chosen so as to yield the optimal fit between the actual and the modeled distributions. There are four quantities that are critical to the performance of the model, namely, the plot of  $\bar{T}_n(t + dt)$  vs.  $N(t)$ , the histogram of  $N$ , the distribution of  $\tau$  vs.  $N$ , and the histogram of  $\tau$ .

Since  $\alpha$  is the only parameter in our control, we would like to choose  $\alpha$  so as to get optimal fit between the modeled and the actual statistics for the above quantities. We decide to choose  $\alpha$  so as to get the optimal fit between the distributions of observed and modeled  $N(t)$ . This is based on the following argument:

For all different values of  $\alpha$  we try, we obtain different distributions of  $N(t)$ . The one that has the optimal fit to the observed  $N(t)$  will also predict optimally the take-off rate. As we have shown

**Table 5.2:** Parameter  $\alpha$  for different BOS runway configurations

Segment	$\alpha$
(VMC; 22L, 27   22L, 22R)	0.44
(VMC; 4L, 4R   4L, 4R, 9)	0.54
(VMC; 7, 32   33L)	0.56

in equation (3),  $N(t)$  is updated in the following manner:  $N(t) = N(t - 1) + P(t - 1) - T(t - 1)$ . The pushback schedule is fixed and the same for all different values of  $\alpha$  that we try. The only way to make a transition from  $N = 0$  to  $N = 1$  is through a pushback. So, this transition is the same for all values of  $\alpha$ . All other transitions are a function of pushbacks, which are fixed, and takeoffs, which are predicted by the model. Thus, the optimal fit between the observed and modeled  $N(t)$  will ensure the optimal prediction of the take-off rate across the different states of surface traffic.

A good estimate of the histogram of  $N$  also has the added benefit of yielding good estimates of taxi time metrics. If this were not the case, taxi times would tend to be lower or higher in the model than they are in reality. That would, in turn, lead to a bad fit between the actual and the observed histogram of  $N$ : If the estimated taxi times were smaller, then modeled  $N$  frequencies would be higher than the actual and the high values of  $N$  would be under-represented. If the estimated taxi times were larger, then modeled  $N$  frequencies would be lower than the actual and the high values of  $N$  would be over-represented.

To summarize, choosing  $\alpha$  to find the best fit between the distributions of observed and modeled  $N$  will optimize the overall performance of the model. We choose the Pearson's  $\chi^2$ -test statistic to measure the fit:

$$\chi^2 = \sum_{i=1}^n \frac{(O_i - E_i)^2}{E_i} \quad (5.7)$$

where  $\chi^2$  = the test statistic;  $O_i$  = the modeled frequency of the congestion state  $i$ ;  $E_i$  = the actual frequency of the congestion state  $i$ ;  $n$  = the number of different congestion states observed.

For the most frequently used segments in BOS, the optimal values of  $\alpha$  are given in Table 5.2. We run the model again using Equation 5.6 for configuration 4L, 4R | 4L, 4R, 9 under VMC conditions. A comparison of Figures 5-4 and 5-6, and Figures 5-5 and 5-7, illustrate the benefits of including the taxiway interaction term in the expression for taxi-out time.

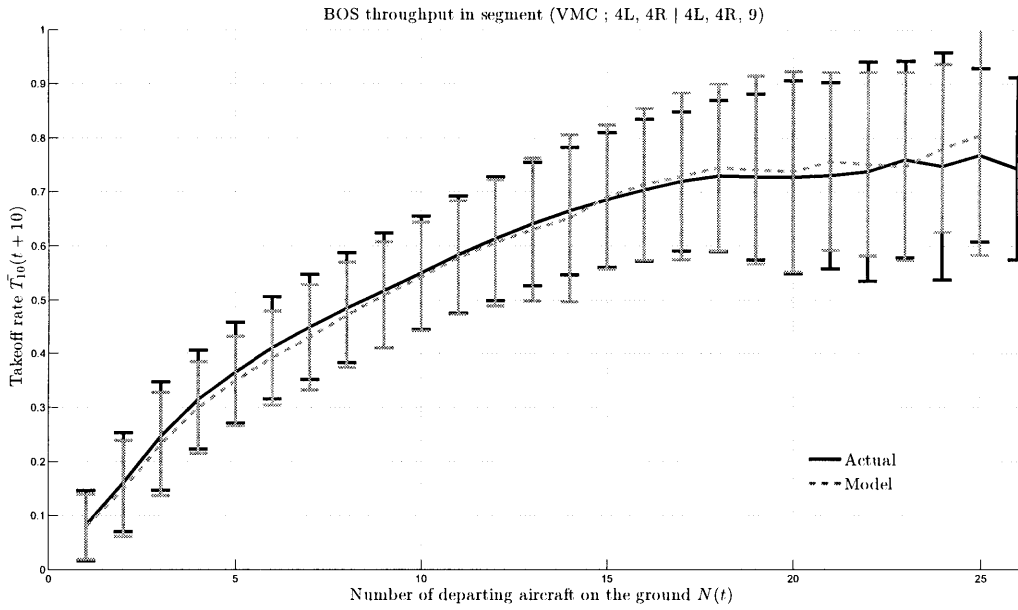


**Figure 5-6:** Actual and modeled takeoff rate as a function of  $N(t)$ , when taxiway interactions are included.

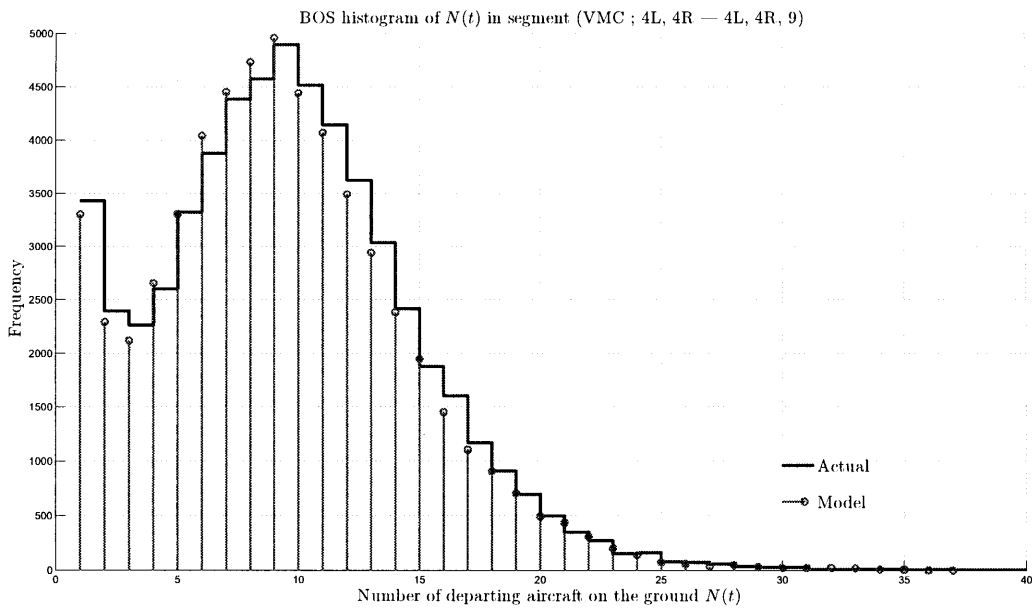


**Figure 5-7:** Distributions of observed and modeled  $N(t)$

## 5.7 Model results

### 5.7.1 Taxi times prediction

Table 5.3 lists the three most frequently used segments in BOS and the number of flights that were observed to both pushback and take-off in each segment when the segments were consecutively used for four hours or longer. The reason we test the model for periods of use to that are not shorter than four hours and only for flights that pushed back and took off in a particular segment is for minimizing the effects of configuration or weather change events when measuring the performance of the model. Table 5.3 also lists the actual and the modeled mean taxi time for each segment, and Tables 5.4-5.6 contain more detailed statistics about the number of aircraft and the taxi times in different congestion levels. These statistics were obtained from the average values of running the model 10 times. In addition, the typical taxi time distributions predicted and observed over

**Table 5.3:** Actual and modeled taxi times for different BOS segments

Segment	Hours in use	Flights	Actual avg. taxi time	Modeled avg. taxi time
(VMC; 22L, 27   22L, 22R)	2,077	40,009	20.25	20.29
(VMC; 4L, 4R   4L, 4R, 9)	1,190.5	27,306	18.63	18.59
(VMC; 7, 32   33L)	954	20401	21.36	21.51

**Table 5.4:** Model predictions for segment (VMC; 22L, 27 | 22L, 22R)

Congestion level	Act. # of flights	Act. avg. taxi time	Modeled # of flights	Modeled avg. taxi time
$(N \leq 8)$	14,253	16.43	13,792	16.42
$(9 < N \leq 16)$	19,856	20.62	20,703	20.48
$(N \geq 17)$	5,900	28.24	5,514	29.03

**Table 5.5:** Model predictions for segment (VMC; 4L, 4R | 4L, 4R, 9)

Congestion level	Act. # of flights	Act. avg. taxi time	Modeled # of flights	Modeled avg. taxi time
$(N \leq 8)$	10,884	15.88	10,948	15.60
$(9 < N \leq 16)$	13,841	19.46	13,805	19.50
$(N \geq 17)$	2,481	25.96	2,553	26.74

**Table 5.6:** Model predictions for segment (VMC; 7, 32 | 33L)

Congestion level	Act. # of flights	Act. avg. taxi time	Modeled # of flights	Modeled avg. taxi time
$(N \leq 8)$	6,298	17.43	5,732	17.79
$(9 < N \leq 16)$	10,728	21.58	11,707	21.66
$(N \geq 17)$	3,375	27.94	2,962	28.40

different ranges of  $N(t)$  can also be analyzed. The actual taxi time distributions and an instance of the ones provided by a random model run are shown in Figures 5-8, 5-9 and 5-10 for the three most frequently used segments.

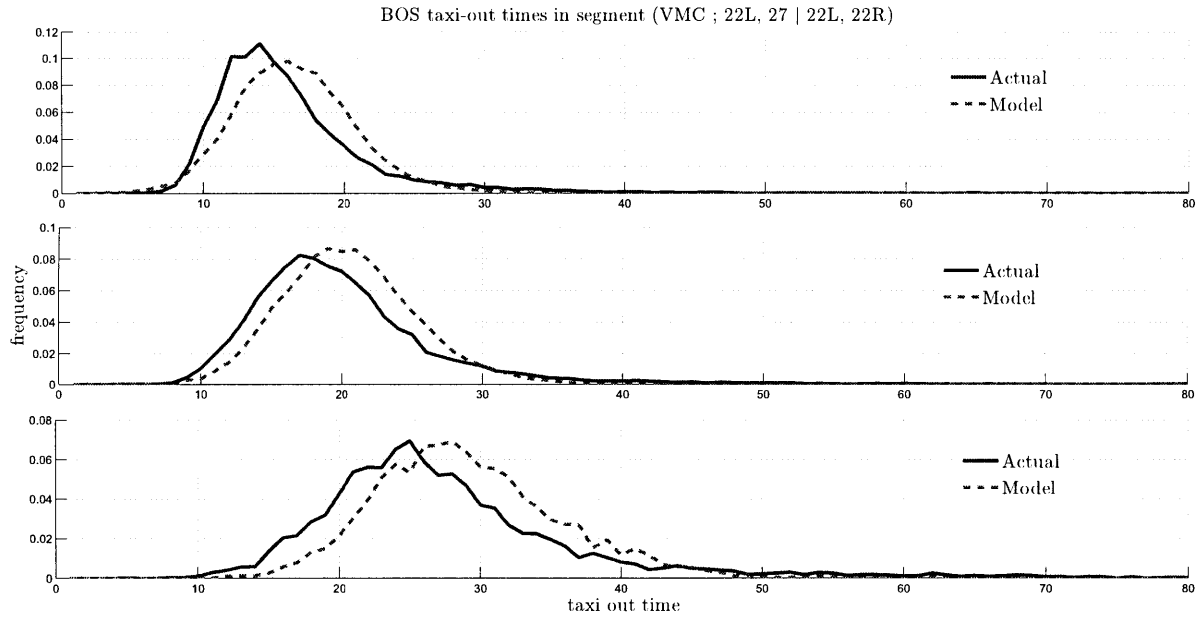


**Figure 5-8:** Taxi-out time distributions under low ( $N \leq 8$ ), medium ( $9 < N \leq 16$ ) and heavy ( $N > 17$ ) departure traffic on the surface for configuration 27, 32 | 33L.

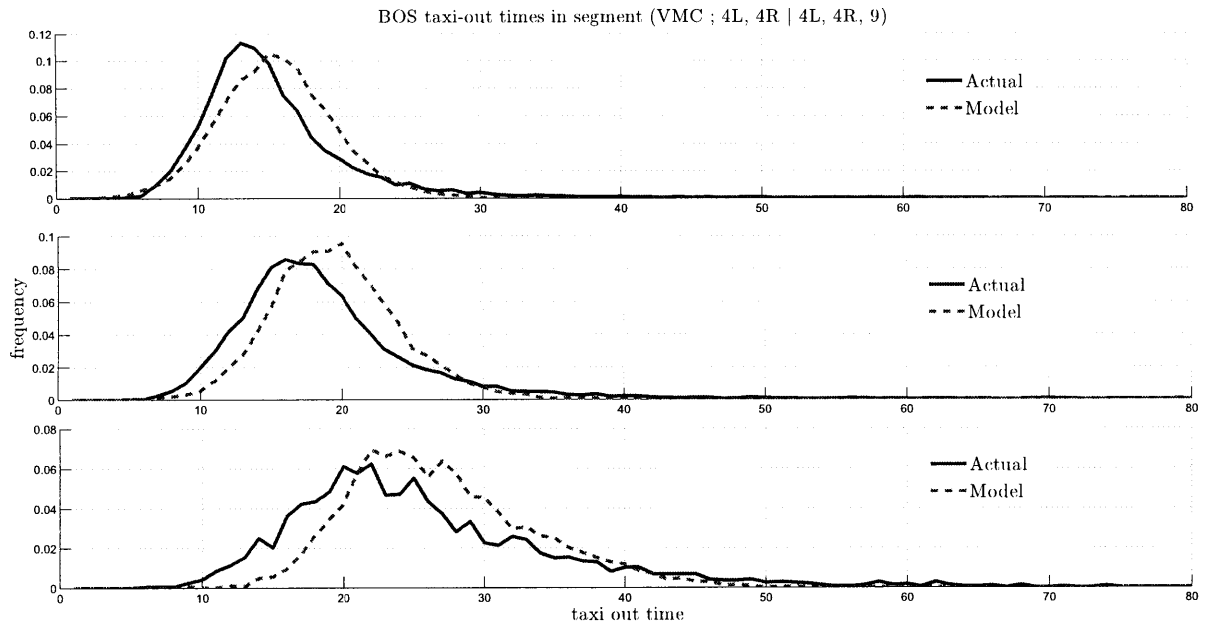


**Figure 5-9:** Taxi-out time distributions under low ( $N \leq 8$ ), medium ( $9 < N \leq 16$ ) and heavy ( $N > 17$ ) departure traffic on the surface for configuration 4L, 4R | 4L, 4R, 9.

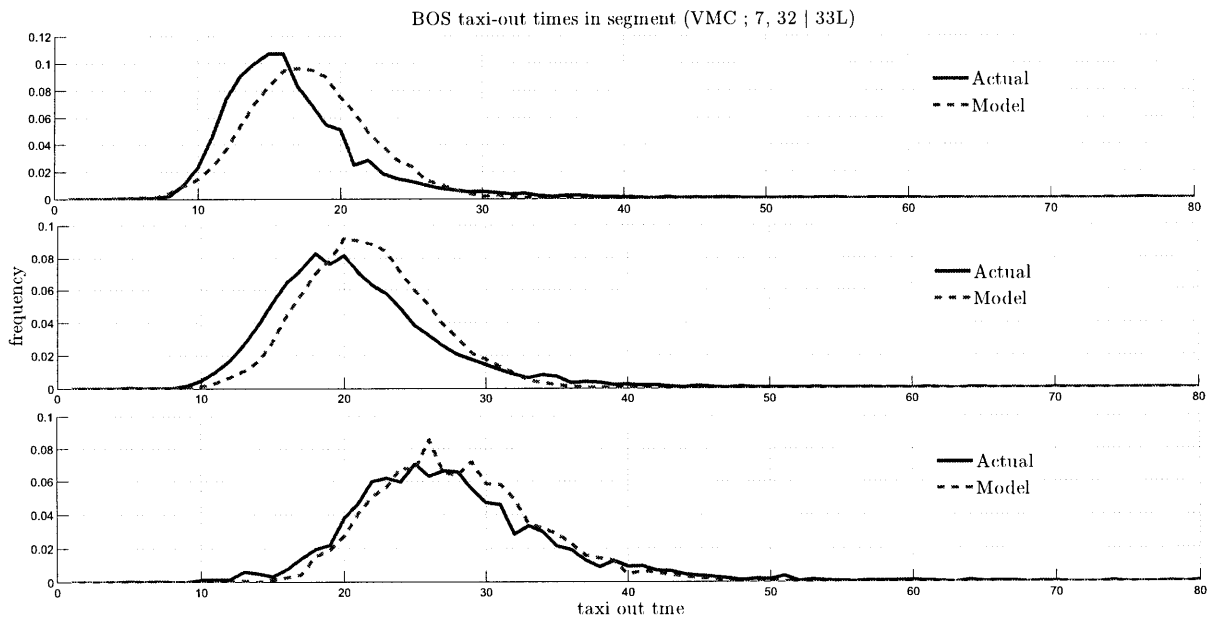


**Figure 5-10:** Taxi-out time distributions under low ( $N \leq 8$ ), medium ( $9 < N \leq 16$ ) and heavy ( $N > 17$ ) departure traffic on the surface for configuration 22L, 27 | 22L, 22R.

### 5.7.2 Predicting runway queues and taxiway congestion

It is possible to use Equation (5.6) with the identified parameters to predict the amount of time an aircraft will spend taxiing on the taxiway and the amount of time in the runway queue. An example is shown for a particular configuration at BOS, in Figure 5-11. We note that as congestion increases, an aircraft can spend more than half of its total taxi time in the runway queue. This demonstrates the potential for reducing emissions by controlling the length of the runway queue.

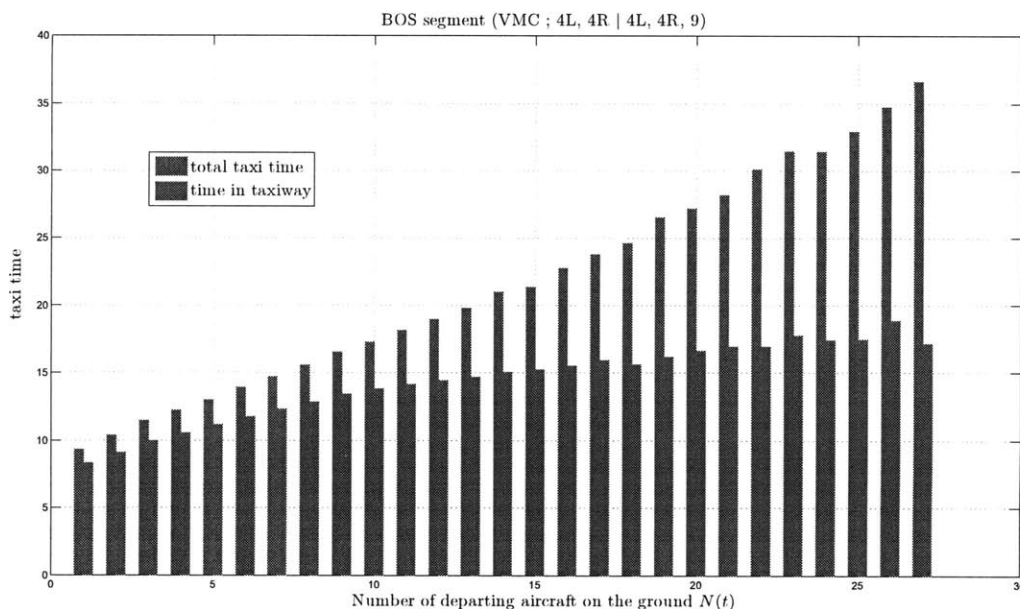


**Figure 5-11:** Estimated time spent by an aircraft transiting the taxiways and waiting in the runway queue for different levels of surface traffic.

### 5.7.3 Emissions and fuel burn prediction

In addition to testing the model in terms of predicting taxi times, and congestion, we can validate its performance in terms of predicting fuel burn and emissions correctly. Tables 5.7, 5.8 and 5.9 show the fuel burn and emissions for the flights of the three modeled configurations in BOS. The fuel burn and the emissions correspond to the taxi times of Table 5.3. The calculations were performed in cooperation with Indira Deonandan according to the methodology outlined in [12]. Similarly to 4.5, the mapping of taxi times to emissions truncated taxi times to values less or equal to 90 minutes.

The comparison between the actual fuel burn and emissions and the ones predicted by the model demonstrate that the model can predict fuel burn and emissions very accurately.



**Table 5.7:** Actual and modeled emissions for BOS segment (VMC; 22L, 27 — 22L, 22R) in 2007

	Fuel burn (gallons)	HC (kg)	CO (kg)	NOx (kg)
Actual	3,340,022	22,093	233,541	42,121
Model	3,339,920	22,089	232,769	42,182

**Table 5.8:** Actual and modeled emissions for BOS segment (VMC; 4L, 4R — 4L, 4R, 9) in 2007

	Fuel burn (gallons)	HC (kg)	CO (kg)	NOx (kg)
Actual	2,156,310	14,131	150,363	27,242
Model	2,133,344	14,008	148,163	26,989

**Table 5.9:** Actual and modeled emissions for BOS segment (VMC; 7, 32 — 33L) in 2007

	Fuel burn (gallons)	HC (kg)	CO (kg)	NOx (kg)
Actual	1,802,491	12,214	127,491	22,647
Model	1,793,627	12,072	126,258	22,590

## 5.8 Model Validation

The model parameters in the previous sections were identified using BOS operations data from 2007. We validate this model using data from 2008. We evaluate the performance of the model in terms of throughput predictions, the frequencies of the predicted and observed values of  $N(t)$ , and the distributions of actual and observed taxi times. The validation process consists of:

1. Using the model with the parameters calculated in Section 5.6 for different configurations and weather conditions (runway capacity model,  $\alpha$  and  $\tau_{travel}$  identified using 2007 data) to simulate operations with the reported pushback times during 2008.
2. Comparing the simulation results with the reported departure throughput and taxi-out times for 2008.

Similar to Table 5.3, Table 5.10 lists the three most frequently used segments in BOS and the number of flight that were observed to both pushback and take-off in each segment when the segments were consecutively used for four hours or longer. Table 5.10 also lists the actual and the modeled mean taxi time for each segment. Tables 5.11 to 5.13 contain more detailed statistics about the number of aircraft and the taxi times in different congestion levels. The statistics of the model predictions in Table 5.10 and in Tables 5.11 to 5.13 were obtained from the average values of running the model 10 times.

**Table 5.10:** Actual and modeled taxi times for different BOS segments in 2008

Segment	Hours in use	Flights	Actual avg. taxi time	Modeled avg. taxi time
(VMC; 22L, 27   22L, 22R)	1,805	32,895	19.79	19.63
(VMC; 4L, 4R   4L, 4R, 9)	1,136.5	23,978	17.30	18.45
(VMC; 7, 32   33L)	894.25	20401	21.51	21.19

**Table 5.11:** Model predictions for segment (VMC; 22L, 27 | 22L, 22R) for 2008

Congestion level	Act. # of flights	Act. avg. of flights	Modeled # taxi time	Modeled avg. taxi time
( $N \leq 8$ )	13,362	16.81	13,436	16.51
( $9 < N \leq 16$ )	16,008	20.68	16,271	20.49
( $N \geq 17$ )	3,525	28.24	3,188	28.44

**Table 5.12:** Model predictions for segment (VMC; 4L, 4R | 4L, 4R, 9) for 2008

Congestion level	Act. # of flights	Act. avg. of flights	Modeled # taxi time	Modeled avg. taxi time
( $N \leq 8$ )	11,271	15.45	10,235	15.52
( $9 < N \leq 16$ )	11,447	18.39	11,715	19.70
( $N \geq 17$ )	1,230	23.96	2,028	26.00

**Table 5.13:** Model predictions for segment (VMC; 7, 32 | 33L) for 2008

Congestion level	Act. # of flights	Act. avg. of flights	Modeled # taxi time	Modeled avg. taxi time
( $N \leq 8$ )	6,199	17.58	6,187	17.81
( $9 < N \leq 16$ )	8,960	21.94	9,512	21.78
( $N \geq 17$ )	2,766	28.91	2,224	28.02

We observe that, with the exception of the segment (VMC; 4L, 4R | 4L, 4R, 9), the model predicts 2008 taxi times very accurately and there is no apparent difference in the performance of the model against the training (2007) and the test data set (2008). Comparing Figures 5-8 and 5-12 further shows that the model predicts 2008 taxi times as well as it fits the 2007 data. Figure 5-13 shows the observed and predicted takeoff rate for this segment in 2008.

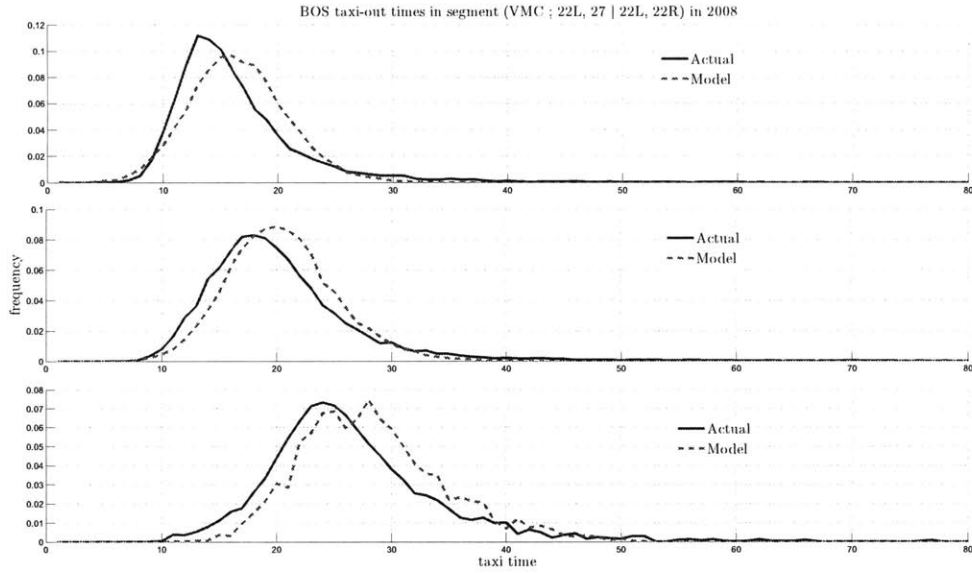


**Figure 5-12:** Taxi-out time distributions under low ( $N \leq 8$ ), medium ( $9 < N \leq 16$ ) and heavy ( $N \geq 17$ ) surface traffic for configuration 22L, 27 | 22L, 22R in BOS in 2008.

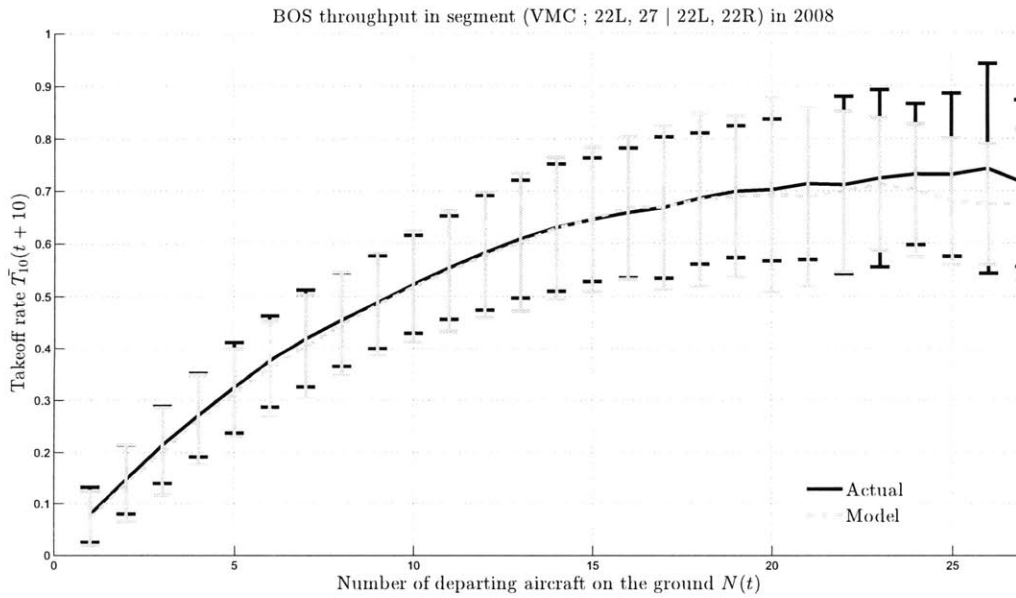


**Figure 5-13:** Takeoff rate  $\bar{T}_9(t+9)$  as a function of  $N(t)$  for configuration 22L, 27 | 22L, 22R in BOS in 2008. The model was derived from a training set of data from 2007.

## 5.9 A predictive model of departure operations

Two key advantages of the proposed model are that (1) it offers a novel method that estimates, at any time, both the number of aircraft in the taxiway system and in the runway queue, and (2) it allows us to estimate, for each flight, the time of arrival at the departure queue as well as the wheels-off time.

The data available from ASPM does not allow us to validate all these estimates, since we only know the pushback and wheels-off times of each flight. However, we believe that the validation that we have presented using these available quantities suggests that the other estimates, namely, the states of the runway queue and the time of arrival at the runway queue are accurate as well. In the future, we would like to validate our estimates of these quantities using a combination of operational observations and surface surveillance data.

### 5.9.1 Estimating the states of surface queues and taxi-out times

Given the times at which flights call for pushbacks clearance, we would like to estimate the amount of time it will take them to taxi to the runway, the amount of time that they will spend in the runway queue, the overall state of the airport surface (for example, the number of departures on the ground), and the length of the departure queue. In order to achieve the above, we consider two approaches to predicting the desired variables, using Equation 5.6:

- Model 1 generates  $\tau_{unimped}$  for each flight using a normal random variable with mean and standard deviation (corresponding to the particular airline) as given by Equations 4.2 and 4.3.
- Model 2 assumes the  $\tau_{unimped}$  of each airline to be the mean of the random variable, given by Equation 4.2.

Figure 5-14 shows the results of making predictions using the pushback schedule from a 10-hour period on July 22, 2007, along with observed data. The estimates are obtained through 100-trial Monte Carlo simulations, and the average and standard deviation of these trials are presented. The first subplot shows the observed and predicted number of departures in a 15-minute interval, the second subplot contains the average taxi-out times of the flights that depart in the corresponding 15-minute interval, and the third subplot shows the average predicted departure queue size for each 15-minute interval.

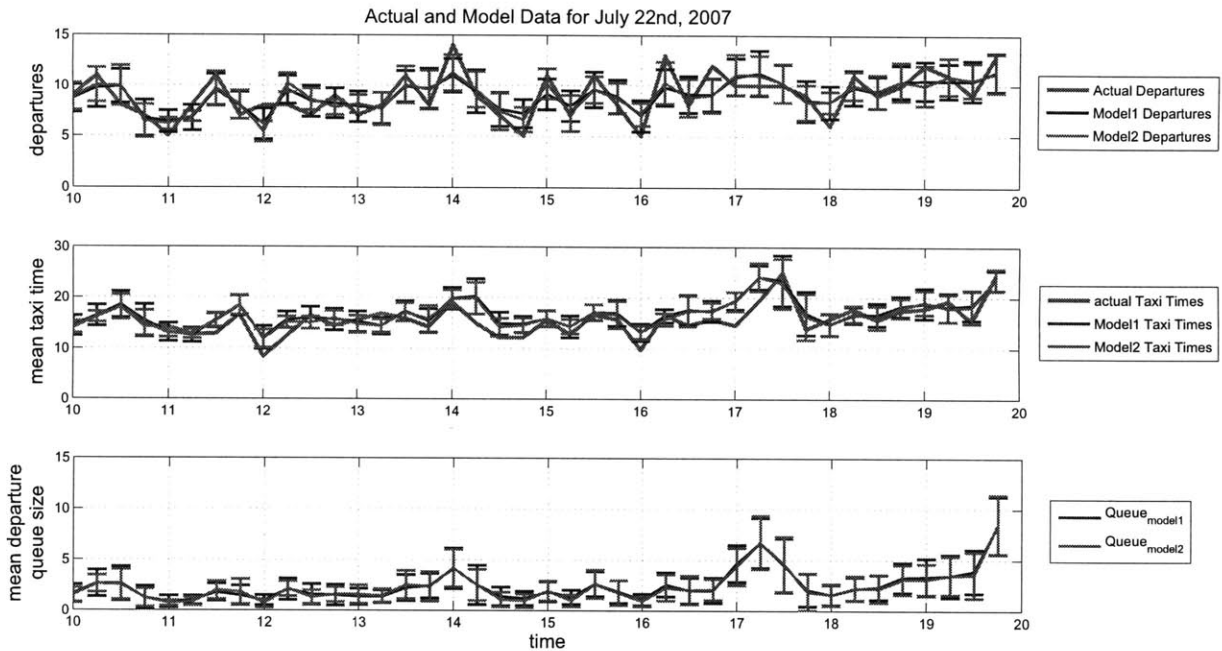


**Figure 5-14:** Prediction of departure throughput, average taxi-out times and departure queue lengths in each 15-min interval over a 10-hour period on July 22, 2007. The error bars denote the standard deviations of the estimates.

We note that the model predictions match the observations reasonably well. We also compute the root mean square error (RMSE), the root mean square percentage error (RMSPE), the mean error (ME), and the mean percentage error (MPE) between the observed measurements and the average of the results of the 100 trials.

**Table 5.14:** Evaluation of model predictions using Monte Carlo simulations.

	RMS Error	RMS % Error	Mean Error	Mean % Error
Model 1 (# of departures)	1.477	0.200	1.171	0.142
Model 2 (# of departures)	1.423	0.186	1.103	0.133
Model 1 (Taxi-out time)	2.222	0.157	1.725	0.119
Model 2 (Taxi-out time)	2.111	0.151	1.627	0.112

Figure 5-14 shows that both models have comparable performance. The difference between the two models is in the way the unimpeded taxi time is generated, and we would expect that as the number of trials increases, the average of the unimpeded taxi times generated in Model 1 tends to the deterministic value (average unimpeded taxi time) assumed by Model 2. Table 5.14 shows that the errors are also comparable. However, we note that because Model 2 uses a deterministic

unimpeded taxi-out time, estimates from Model 2 will have a smaller variance than those from Model 1.

## **5.10 Summary**

In this chapter, we presented a new queuing network model of the departure processes at airports. In Chapter 6, the model is used to simulate the departure process and evaluate the impact of a strategy aimed at controlling the number of active aircraft on the surface to within a specified number for the three segments of BOS which were modeled in this chapter.

## Chapter 6

# Management of the pushback queue

### 6.1 Introduction

In this chapter, we apply the model developed in Chapter 5 to simulate the impact of a strategy aimed at controlling the number of active aircraft on the surface within a certain limit. This strategy is called *N-Control*, and is described in Section 6.2. In Section 6.3, the benefits and costs of such a strategy are illustrated by simulating its impact on taxi times, fuel burn, emissions and delays. The simulation is applied to the three BOS segments for which the departure process model of Chapter 5 was calibrated.

The motivation for simulating the *N-Control* strategy is twofold: on one hand, we desire to investigate its impact on taxi times, fuel burn, emissions and delays; on the other hand, we seek to evaluate if this is a sufficient manner of controlling the takeoff queue of each aircraft.

### 6.2 The N-Control strategy

The data analysis confirms prior observations [28, 30] that there is a strong correlation between the number of the aircraft on the ground and the departure throughput, and that there is a critical number of aircraft on the ground  $N^*$  at which the departure process gets saturated. In other words, increasing the number of the aircraft on the ground any further does not increase the departure throughput. The estimated values of  $N^*$  for different runway configurations at BOS are listed in Table 5.1.

We would like to use  $N^*$  as listed in table 5.1 for taxiing operations control. This approach had been considered previously in the Departure Planner [17] and variants of it have been extensively

studied [29, 8, 4]. We use the models developed in this paper to evaluate in detail the potential benefits of the strategy initially studied by Pujet *et al.* [28]. The proposed algorithm can be thought of as *virtual departure queuing* and is often referred to as *N-Control* [8, 6]. It can be summarized as follows: At each time period  $t$ ,

- If  $N(t) \leq N^*$ ,
  - If the *virtual departure queue* (set of aircraft that have requested clearance to pushback) is not empty, clear aircraft in the queue for pushback in FCFS order
- If  $N(t) > N^*$ , for any aircraft that requests pushback,
  - If there is another aircraft waiting to use the gate, clear departure for pushback, in FCFS order
  - Else add the aircraft to the *virtual departure queue*.

In other words, when  $N(t) > N^*$ , we regulate the pushback time of an aircraft unless it may delay an arrival that is waiting to use the gate. In order to maintain fairness, aircraft which request pushback clearance and are not cleared immediately form a FCFS-*virtual departure queue*. When the congestion decreases and  $N(t) \leq N^*$ , we allow the aircraft in the virtual departure queue to pushback in the order they requested pushback clearance. This approach enables reductions in fuel burn and emissions, without decreasing the departure throughput. A schematic of the controlled departure process is shown in Figure 6-1.

Finally, it may be the case that the initial estimate of  $N^*$  leads to gate holds or delays longer than airlines are willing to accept, or that the airport operator wishes to exercise more aggressive emissions control. We therefore allow the critical number of aircraft at which the aircraft are held in the *virtual departure queue* to take different values in the simulations. We denote this value as  $N_{ctrl}$ .

## 6.3 Potential benefits of N-Control

### 6.3.1 Taxi times reduction

The models of departure operations developed so far allow us to estimate the potential benefits of the proposed queue management strategy. In the following discussion, we present the results for the configurations for which the model was calibrated in Chapter 5: “22L, 27 | 22L, 22R”, “4L, 4R



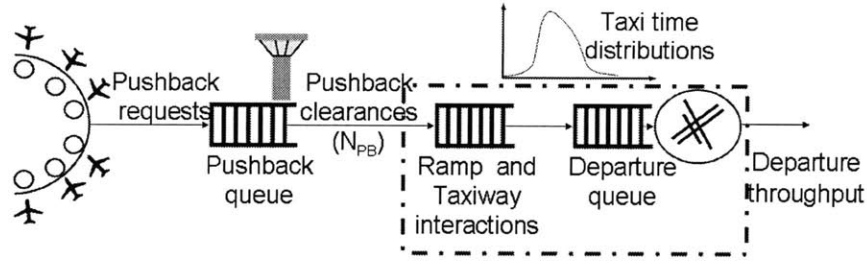


Figure 6-1: Integrated model of the *controlled* departure process

| 4L, 4R, 9” and “7, 32 | 33L”. We simulate the strategy only for time intervals the segment was in use for at least four hours continuously. We exclude flights that have pushbacked or taken off in different configurations from the analysis. The number of flights analyzed for each configuration is given in Table 5.3. We also present the tradeoffs involved in selecting  $N_{ctrl}$  at values different from the  $N^*$  in Table 5.1.

Table 6.1 shows the results of the model in terms of taxi-out times, delays and annual taxi-out time reductions for the segment (VMC; 22L, 27 | 22L, 22R) if the queue management strategy were to be implemented over all occurrences of this segment in a year that lasted four hours or longer. We present the expected taxi times for a range of values of  $N_{ctrl}$ , namely: 10, 15, 16, 17, 18, 19, 20, 21 and 22. The surface saturation point was estimated to be  $N^* = 16$  (Table 5.1), but we also evaluate the strategies of controlling surface traffic to smaller and larger values of  $N^*$  to compare expected benefits and costs. The taxi time savings are calculated by comparing the expected taxi-out times with and without control (Tables 5.3 and 6.1). In Table 6.1, the mean delay/flight is defined as the sum of mean taxi time and the mean gate holding time minus the mean taxi time in the base case (without control).

In Table 6.1, we also list more detailed information for the flights that would be held in the *virtual departure queue* for different values of  $N_{ctrl}$ :

- The total number of gate-held flights: the total number of flights that would be held in the *virtual departure queue*
- The mean gate-holding time: The mean time spent in the *virtual departure queue* (computed over all flights that are held in the *virtual departure queue*)
- The mean delay of held flights: the sum of mean taxi time and the mean gate holding time minus the mean taxi time of the base case (without control) (computed over all flights held

in the *virtual departure queue*)

- The mean taxi-out time of held flights (without control): The mean taxi time of flights which get held in the *virtual departure queue*, in the base case (without control)
- Total duration of the policy: Total time for which the policy would be activated (measured as the sum of all instances that a flight is held in the *virtual departure queue*)

**Table 6.1:** Taxi-out time reduction for different values of  $N_{ctrl}$  in segment (22L, 27 | 22L, 22R; VMC)

Ncontrol	10	15	16	17	18	19	20	21	22
Mean taxi time (min)	17.70	19.12	19.33	19.51	19.68	19.82	19.94	20.03	20.10
Mean delay/flight (min)	23.38	0.72	0.34	0.15	0.06	0.02	0.01	0.00	0.00
Total number of gate-held flights	33374	11109	8406	6440	4933	3747	2828	2103	1536
Mean gate-holding time (min)	30.75	6.91	6.33	5.93	5.65	5.46	5.31	5.22	5.19
Mean delay/held flight (min)	27.52	2.24	1.25	0.65	0.32	0.17	0.13	0.12	0.10
Mean taxi time of held flights, no control (min)	21.25	26.08	27.40	28.66	29.89	31.13	32.36	33.61	34.98
Total duration of the policy (hours)	1022	279	207	156	119	90	68	50	37
Annual taxi time reduction (hours)	1729	781	646	523	413	317	237	175	128

We note that the taxi time savings increase by decreasing the value of  $N_{ctrl}$ . These savings are however at the cost of increasing the total departure delay. We also observe that choosing  $N_{ctrl}$  at a value estimated to be marginally higher than the surface saturation point (16, in this case) decreases the expected taxi times without increasing the expected departure delays. If we choose a smaller value of  $N_{ctrl}$ , we operate the airport at a smaller throughput than the maximum achievable, and the expected departure delay increases. A significant portion of the increased delay is incurred at the gate, and the total taxi-out times and emissions decrease. We also include the extreme case of  $N_{ctrl} = 10$ . The results show that while the taxi-out times decrease significantly, the average delay increases to 23.38 min per flight as a consequence of a considerable under-utilization of resources. The calculations are repeated for the next two most frequently used configurations (Tables 6.2 and

6.3).

**Table 6.2:** Reduction in taxi-out time for different values of  $N_{ctrl}$  in segment (4L, 4R | 4L, 4R, 9; VMC)

Ncontrol	10	15	16	17	18	19	20	21	22
Mean taxi time (min)	16.88	17.99	18.11	18.21	18.29	18.36	18.41	18.46	18.49
Mean delay/flight (min)	16.27	0.74	0.41	0.22	0.12	0.06	0.03	0.01	0.01
Total number of gate-held flights	20635	5858	4312	3168	2289	1633	1169	832	592
Mean gate-holding time (min)	23.52	6.27	5.70	5.29	5.02	4.89	4.81	4.77	4.78
Mean delay/held flight (min)	21.10	2.94	2.07	1.45	0.95	0.60	0.38	0.24	0.16
Mean taxi time of held flights, no control (min)	19.73	23.83	24.88	25.95	27.06	28.20	29.33	30.46	31.58
Total duration of the policy (hours)	602	142	102	74	52	37	26	19	13
Annual taxi time reduction (hours)	775	270	218	172	135	103	79	59	43

**Table 6.3:** Reduction in taxi-out time for different values of  $N_{ctrl}$  in segment (7, 32 | 33L; VMC)

Ncontrol	10	15	16	17	18	19	20	21	22
Mean taxi time (min)	19.17	20.75	20.90	21.01	21.12	21.20	21.27	21.33	21.37
Mean delay/flight (min)	31.89	1.78	1.02	0.57	0.31	0.16	0.09	0.04	0.02
Total number of gate-held flights	17938	6943	5115	3734	2675	1881	1336	958	688
Mean gate-holding time (min)	37.76	7.53	6.55	5.88	5.44	5.19	5.05	4.91	4.79
Mean delay/held flight (min)	34.97	4.79	3.50	2.52	1.75	1.15	0.77	0.47	0.28
Mean taxi time of held flights, no control (min)	22.17	25.26	26.30	27.37	28.51	29.69	30.92	32.17	33.40
Total Duration of the policy (hours)	574	180	130	93	65	45	32	22	16
Annual taxi time reduction (hours)	798	260	210	170	135	106	82	64	48

### 6.3.2 Fuel burn and emissions reduction

In addition to the anticipated reduction in taxi times, we can calculate the expected reduction in fuel burn and emissions. Tables 6.4, 6.5 and 6.6 show the fuel burn and emissions reduction for the flights of the three modeled configurations in BOS. The fuel burn and the emissions correspond to the taxi times of Table 5.3. The calculations were performed in cooperation with Indira Deonandan according the methodology outlined in [12]: assuming that each flight taxis at 7% throttle setting, and using fuel burn and emissions indices from ICAO [22]. Similarly to Table 4.5, the mapping of taxi times to emissions truncated taxi time lengths to values less or equal to 90 minutes.

**Table 6.4:** Fuel burn and emissions reduction for different values of  $N_{ctrl}$  in segment (22L, 27 | 22L, 22R; VMC)

$N_{ctrl}$	10	15	16	17	18	19	20	21	22
Fuel burn (gallons)	421,308	178,066	146,445	117,811	93,148	71,880	53,933	39,817	29,317
HC (kg)	2,766	1,193	988	801	637	496	376	280	208
CO (kg)	29,412	12,563	10,385	8,397	6,667	5,172	3,907	2,897	2,143
NOx (kg)	5,347	2,258	1,856	1,492	1,179	908	682	503	371

**Table 6.5:** Fuel burn and emissions reduction for different values of  $N_{control}$  in segment (VMC; 4L, 4R | 4L, 4R, 9)

$N_{ctrl}$	10	15	16	17	18	19	20	21	22
Fuel burn (gallons)	183,276	57,725	45,468	35,583	27,633	21,526	16,388	12,333	8,986
HC (kg)	1,234	388	310	244	189	149	114	87	64
CO (kg)	12,870	4,150	3,291	2,595	2,020	1,581	1,214	919	680
NOx (kg)	2,319	730	575	450	349	272	207	155	113

**Table 6.6:** Fuel burn and emissions reduction for different values of  $N_{control}$  in segment (VMC; 7, 32 | 33L)

$N_{ctrl}$	10	15	16	17	18	19	20	21	22
Fuel burn (gallons)	206,954	65,557	52,927	43,575	34,949	27,780	21,899	17,150	13,164
HC (kg)	1,374	443	359	301	245	196	156	123	95
CO (kg)	14,416	4,663	3,786	3,142	2,540	2,027	1,618	1,270	981
NOx (kg)	2,615	830	670	551	441	351	276	216	166

### 6.3.3 Strategy assessment

The results of Tables 6.4, 6.5 and 6.6 demonstrate that a simple N-Control strategy can reduce emissions and fuel burn even in a relatively non-congested airport such as BOS. As described in Section 6.2, a first choice for  $N_{ctrl}$  would be  $N^*$ . This is because by choosing the number of active aircraft on the surface to be within  $N^*$ , the airport can reach its capacity but does not get unnecessarily congested.

For  $N_{ctrl} = N^*$ , we present the expected reductions in taxi time, fuel burn and emissions in Table 6.7. It reveals that for  $N_{ctrl} = N^*$ , the reductions in taxi time, fuel burn and emissions are significant. Nonetheless, the total delay is also significant. As a reminder, the delay of a flight, in the context of this chapter, is defined as the sum of the time that it is held in the virtual departure queue and its taxi time in the *N-control* scenario minus its taxi time in the base case (without control). In theory, one would expect the delay/flight to be close to zero for  $N_{ctrl} = N^*$ . However, as can be seen in Tables 6.1 and 6.2, the mean delay/flight approaches zero for values of  $N_{ctrl}$  higher than  $N^*$ . When  $N_{ctrl} = N^*$ , the mean delay/flight is around 20 sec. More specifically, the flights that are held back are delayed for longer than one minute.

We also give the percentages in reductions in Table 6.8. It is remarkable that at an airport that suffers moderate congestion, such a simple strategy can yield savings up to 5% of total fuel burn and emissions, depending on the configuration. Finally, in Table 6.8, the effect of truncating taxi times to 90 minutes for the fuel burn and emissions mapping is illustrated: in most of the cases, the relative taxi time reduction is larger than the fuel burn or emissions reduction.

## 6.4 Comparison to the saturation taxi time metric

In Section 4.3, we introduced and defined the saturation taxi time metric. It is clear that the *N-control* strategy attempts to operate within the *saturation point*, thereby minimizing the number of flights at congestion and the excessive taxi times. However, there is a significant difference between the congestion as defined by the *saturation taxi time* metric and the congestion that *N-Control* abates: The saturation taxi time metric characterizes as congested all flights that face a takeoff queue  $\geq N^*$  whereas *N-control* keeps at the gate flights requesting for pushback when the number of aircraft on the ground is  $\geq N^*$ . As emphasized in Section 4.3, keeping the number of active aircraft on the surface within a certain value is different from keeping the takeoff queue of each aircraft within the same value. Using the terminology of Chapter 4, a strategy abating congestion,

**Table 6.7:** Estimated taxi time, fuel burn and emissions reduction from controlling  $N(t)$  to the saturation value.

<i>Reduction in:</i>	Taxi time (hours)	Total delay (hours)	Fuel burn (gallons)	HC (kg)	CO (kg)	NOx (kg)
22L, 27   22L, 22R	646	-226	146,445	988	10,385	1,856
4L, 4R   4L, 4R, 9	172	-103	35,583	244	2,595	450
27, 32   33L	64	-14	17,150	123	1,270	216
[1-3]	882	-342	199,177	1,354	14,250	2,522

**Table 6.8:** Estimated taxi time, fuel burn and emissions percentage reduction from controlling  $N(t)$  to the saturation value.

<i>Percentage reduction in:</i>	Taxi time	Total delay	Fuel burn	HC	CO	NOx
22L, 27   22L, 22R	4.77%	-1.67%	4.38%	4.48%	4.46%	4.40%
4L, 4R   4L, 4R, 9	2.04%	-1.21%	1.67%	1.74%	1.75%	1.67%
27, 32   33L	0.87%	-0.19%	0.96%	1.02%	1.01%	0.96%
[1-3]	3.01%	-1.17%	2.74%	2.81%	2.81%	2.75%

as defined by the *saturation taxi time* metric, would control the *flights in congestion* and change their pushback time so as they face a takeoff queue shorter than  $N^*$ . In Table 6.9, the congestion statistics for the three segments of BOS, which are simulated in this chapter, are reproduced from Chapter 4.

**Table 6.9:** Congestion analysis for BOS in 2007 under VMC using the two different metrics

<i>RC</i>	$\tau_{sat}$	# of flights in congestion	$\bar{\tau}$ in congestion
22L, 27   22L, 22R	23.58	8540	32.10
4L, 4R   4L, 4R, 9	23.83	3250	34.16
27, 32   33L	30.27	1594	39.77
[1-3]	24.44	13384	33.51

In Table 6.10, the simulated benefits from *N-control* calibrated at  $N^*$  for the three BOS segments are compared to the benefits of a theoretical scenario where all flights experiencing a takeoff queue  $\geq N^*$  have the expected taxi time of the flights experiencing a takeoff queue  $(N^* - 1)$ . This is essentially the case where the *flights in congestion* of Table 6.9 have the saturation taxi time,  $\tau_{sat}$ , of their segment.

Table 6.10 shows that there is a big difference between the gains that seem achievable from controlling the takeoff queue and the simulated ones from controlling the number of active aircraft on the surface to within  $N^*$ . There are several reasons for this discrepancy:

**Table 6.10:** *N*-control strategy evaluation

<i>Reduction in</i>	Taxi time (hours)	Fuel burn (gallons)	CO (kg)	NOx (kg)	HC (kg)
scenario $\max(N_Q(i)) = N^*$	882	199,177	1,354	14,250	2,522
simulation $N_{ctrl} = N^*$	2,024	556,546	3,930	40,761	6,974

1. The first reason is that the results for  $N_{ctrl} = N^*$  are those that the simulation shows that would be achieved if the strategy was implemented. The results of the scenario  $\max(N_Q(i)) = N^*$  refer to a hypothetical situation where all *flights in congestion* have the saturation taxi time,  $\tau_{sat}$ , of their segment. It is not certain that simulations controlling for the takeoff queue would yield the reductions that the scenario  $\max(N_Q(i)) = N^*$ , as listed in Table 6.10, suggests are achievable.
2. For the scenario  $\max(N_Q(i)) = N^*$ , the impact is determined by subtracting  $\tau_{sat}$  from the taxi times of the *flights in congestion* whereas the simulation  $N_{ctrl} = N^*$  compares the taxi times of the model without control to the taxi times of the model with  $N_{ctrl} = N^*$ . So, in the first case we determine the results having real data as the baseline whereas in the latter, we measure having the model as the baseline.
3. For modeling purposes, in the model we take into account only periods of use of a segment that are not shorter than four hours and only flights that pushed back and took off in a particular segment. In the scenario  $\max(N_Q(i)) = N^*$ , all flight pushing back in a particular segment are included. Therefore, more flights are included in the analysis and the benefits are bound to appear larger.
4. A final reason is that the scenario  $\max(N_Q(i)) = N^*$  and the simulation  $N_{ctrl} = N^*$  refer to different strategies: The former is indicative of the results that are possible by controlling the takeoff queue, whereas the latter simulates the strategy of controlling the total number of departing aircraft on the ground. As explained in Section 4.3, the strategy controlling the takeoff queue to within a certain number may have different impact and implications from the strategy controlling the number of aircraft on the surface to within the same number.

We speculate that the Item 2 will play a small role since the model matches very well with the observations. We also speculate that Item 3 only marginally affects the results because the number of flights that ends up being excluded is very small. We therefore focus on understanding Items



1 and 4. For doing this, we re-calculate the congestion statistics at BOS, following the method of Section 4.3, but by modifying the saturation taxi time and congestion metrics as follows:

- $\tau'_{sat}$  is defined as the mean taxi time of the aircraft that pushback when there are  $(N^* - 1)$  aircraft on the ground.
- *pushbacks in congestion* are defined as the flights that pushback when there are at least  $N^*$  aircraft on the ground.

This enables us to calculate the theoretically achievable reductions by controlling the number of aircraft on the ground, compare them to the simulated reductions achieved by *N-Control*, and to also compare them to the theoretically achievable reductions by controlling the number of aircraft in the takeoff queues. In Table 6.11, the statistics derived from these congestion metrics are contrasted to the ones resulting from the congestion metrics defined in Chapter 4. We can see the stark difference between the two metrics. We can also note that the number of *pushbacks in congestion* is very similar to the number of flights that would be held at the gate if  $N_{ctrl} = N^*$  in the three runway configurations, as can be seen in Tables 6.1, 6.2 and 6.3. The mean taxi time,  $\tau_{sat}$  in saturation of the *pushbacks in congestion*, as seen in Table 6.11, is very close to the mean taxi time of the flights that would be held at the gate if  $N_{ctrl} = N^*$  in the three runway configurations, as can be seen in Tables 6.1, 6.2 and 6.3.

Finally, in Table 6.12, we compare the theoretically achievable reductions by controlling the number of aircraft on the ground (scenario  $\max(N(t)) = N^*$ ), the simulated reductions achieved by *N-Control* (simulation  $N_{ctrl} = N^*$ ) and the theoretically achievable reductions by controlling the number of aircraft in the takeoff queues (scenario  $\max(N_Q(i)) = N^*$ ). The scenario  $\max(N(t)) = N^*$  refers to the hypothetical situation where all *pushbacks in congestion* have the saturation taxi time,  $\tau'_{sat}$ , of their segment. This is the situation where all flights pushing back when there are  $N^*$  or more aircraft on the surface would push back when there were  $(N^* - 1)$  aircraft on the surface, and would therefore have  $\tau'_{sat}$  taxi time. The simulation  $N_{ctrl} = N^*$  attempts to emulate this scenario.

The similarity between the reductions that seem achievable from scenario  $\max(N(t)) = N^*$  and that the simulation  $N_{ctrl} = N^*$  achieves is striking. This similarity suggests that the proposed algorithm is a very good implementation of the queue management strategy attempting to keep the number of departing aircraft on the ground to within  $N^*$ . This is reinforced by the fact that the number of *pushbacks in congestion* is very similar to the number of flights that would be held at

the gate if  $N_{ctrl} = N^*$  in the three runway configurations, as can be seen in Tables 6.1, 6.2 and 6.3. The saturation taxi time,  $\tau'_{sat}$ , as seen in Table 6.11, is very close to the mean taxi time of the held flights under  $N_{ctrl} = N^*$  in the three runway configurations, as can be seen in Tables 6.1, 6.2 and 6.3. This shows that *N-Control* holds at the gate the flights that would theoretically be expected to be held at the gate, and when these flights pushback their taxi time is close to  $\tau'_{sat}$ . On the other hand, the stark contrast between the scenario  $\max(N(t)) = N^*$  and the scenario  $\max(N_Q(i)) = N^*$  reinforces the point that controlling the number of aircraft on the ground is substantially different from controlling the takeoff queue. To summarize, Table 6.11 shows that *N-Control* yields the expected theoretical benefits from controlling the number of aircraft on the ground, and suggests that a strategy controlling the takeoff queues of aircraft would lead to substantially higher benefits.

**Table 6.11:** Congestion analysis for BOS in 2007 under VMC using the two different metrics

<i>RC</i>	$\tau_{sat}$	# of flights in congestion	$\bar{\tau}$ in congestion	$\tau'_{sat}$	# of pushbacks in congestion	$\bar{\tau}'$ in congestion
1	23.58	8540	32.10	22.58	9039	26.98
2	23.83	3250	34.16	22.61	2895	25.63
3	30.27	1594	39.77	27.98	1260	30.71
[1-3]	24.44	13384	33.51	23.10	13194	27.04

**Table 6.12:** *N-control* strategy evaluation

<i>Strategy</i>	Taxi time (hours)	Fuel burn (gallons)	CO (kg)	NOx (kg)	HC (kg)
scenario $\max(N_Q(i)) = N^*$	2,024	556,546	3,930	40,761	6,974
scenario $\max(N(t)) = N^*$	865	172,739	1,038	12,129	2,172
simulation $N_{ctrl} = N^*$	882	199,177	1,354	14,250	2,522

## 6.5 Operational challenges

Queue management strategies require a greater level of coordination among traffic on the surface than is currently employed. For example, if gate-hold strategies are to be used to limit surface congestion, there need to be mechanisms that can manage pushback and departure queues depending on the congestion levels. In addition, ATC procedures need to also be addressed: for example, currently, departure queues are First-Come-First-Serve (FCFS), creating incentives for aircraft to

pushback as early as possible. If gate-hold strategies are to be applied, virtual queues of pushback priority will have to be maintained. We note that the Department of Transportation's airline on-time performance metrics are calculated by comparing the scheduled and actual pushback times. This creates incentives for pilots to pushback as soon as they are ready, rather than to hold at the gate to absorb delay. In addition, gate assignments also create constraints on gate-hold strategies; for example, an aircraft may have to pushback from its gate if there is an arriving aircraft that is assigned to the same gate. This phenomenon is a result of the manner in which gate use, lease and ownership agreements are conducted in the US. At most European airports, gate assignments appear to be centralized and do not impose the same kind of constraints on gate-hold strategies.



# Chapter 7

## Conclusions

### 7.1 Summary of results

In the first part of this this thesis, we analyzed congestion at four major airports (JFK, EWR, PHL and BOS). For this analysis, two metrics were used, one for determining the sustained departure capacity of an airport, and another for determining the congestion level. This analysis showed that the departure processes at JFK, EWR and PHL suffered from surface congestion 10% to 20% of the time in 2007. The congestion was seen to be equally significant at different airport configurations and weather conditions. This suggested that the major reason for the observed levels of congestion is the very high departures demand that the airports cannot serve without incurring significant congestion. The analysis also showed that BOS suffers from congestion only moderately compared to the other three airports. However, at BOS, instrumental weather conditions decrease its capacity and double the time that the airport spends in congestion.

The next step was to estimate the effect of congestion to taxi times. For this, it was necessary to calculate the difference between the observed taxi time of a flight and the unimpeded one. The difference between the observed taxi time and the unimpeded one was estimated as the total queuing delay. The analysis showed that taxi times tend to be 2-3 times the unimpeded ones in JFK, EWR and PHL, and that fuel burn and emissions could be reduced to nearly half of their current values if the taxi times were reduced to their unimpeded values. The analysis also showed that the unimpeded taxi times differ from airport to airport, and that taxi times alone do not completely reflect the time that aircraft spend queuing on the surface. For this reason, a new metric for measuring the effect of congestion on taxi-out times was introduced. This method classified as congested all flights that faced a takeoff queue larger than the one necessary to achieve

the airport's capacity. Based on this metric, PHL was shown to be more congested than EWR and as congested as JFK.

In order to further analyze how congestion builds up on the surface and to evaluate queue management strategies aimed at decreasing fuel burn and emissions, we presented a new queuing network model of departure processes. A predictive model that is capable of estimating taxi-out times and the state of surface queues was also developed. This model has the potential to provide some of the information that is required to improve coordination of departure processes, and thereby increase surface efficiency. The model was calibrated for the major runway configurations at BOS using ASPM data from 2007, and was validated using data from 2008.

Using the proposed model, we calculated the effect on taxi time, delays, fuel burn and emissions that would result if a queue management strategy, *N-Control*, was implemented at BOS. The strategy was simulated for the major runway configurations of BOS. The results showed that even at a moderately congested airport, such as BOS, *N-Control* can yield reductions in taxi times, fuel burn and emissions between 1% and 5% depending on the runway configuration, over the entire fleet operating at BOS. These reductions are predominantly experienced during the most congested periods of operation: analysis showed that the reductions in taxi times, fuel burn and emissions for flights pushing back during such periods are about 20%. The analysis also showed that the benefits could be doubled by modifying *N-Control* as to control the takeoff queue of an aircraft and not just the number of active aircraft on the surface.

## 7.2 Contributions of the thesis

The major contributions of this thesis are

- It was shown that the ASPM pushback and taxi-out time estimates for non-OOOI flights are not reliable and should be recalculated before being used in any study assessing, measuring, or modeling taxi times. It was shown that a method based on the mean taxi time of the OOOI flights taking off in the same time interval and from the same runway configuration is a good estimator of the taxi time of a non-OOOI flight, and removes the bias experienced by the ASPM estimates.
- A novel method for calculating the unimpeded taxi times was developed and demonstrated. This method addresses many of the problems of previous methods.

- A new queuing model for the departure process was proposed. This model is the first to quantitatively model ramp- and taxiway-related queues and delays. The model is *mesoscopic* in nature, is portable, and easy to parametrize. As a result, it can be used for a variety of other purposes, including predictive congestion control and the cost-benefit analysis of operational tow-outs.
- The queue management strategy (*N-Control*) was extensively evaluated for the three major runway configurations at BOS making use of the proposed queuing model.
- It was shown that the benefits of *N-Control* could be increased if it was modified to control the takeoff queue of each aircraft and not the number of aircraft on the ground.





## Appendix A

# Airport diagrams

A.1 John F. Kennedy International Airport(JFK)

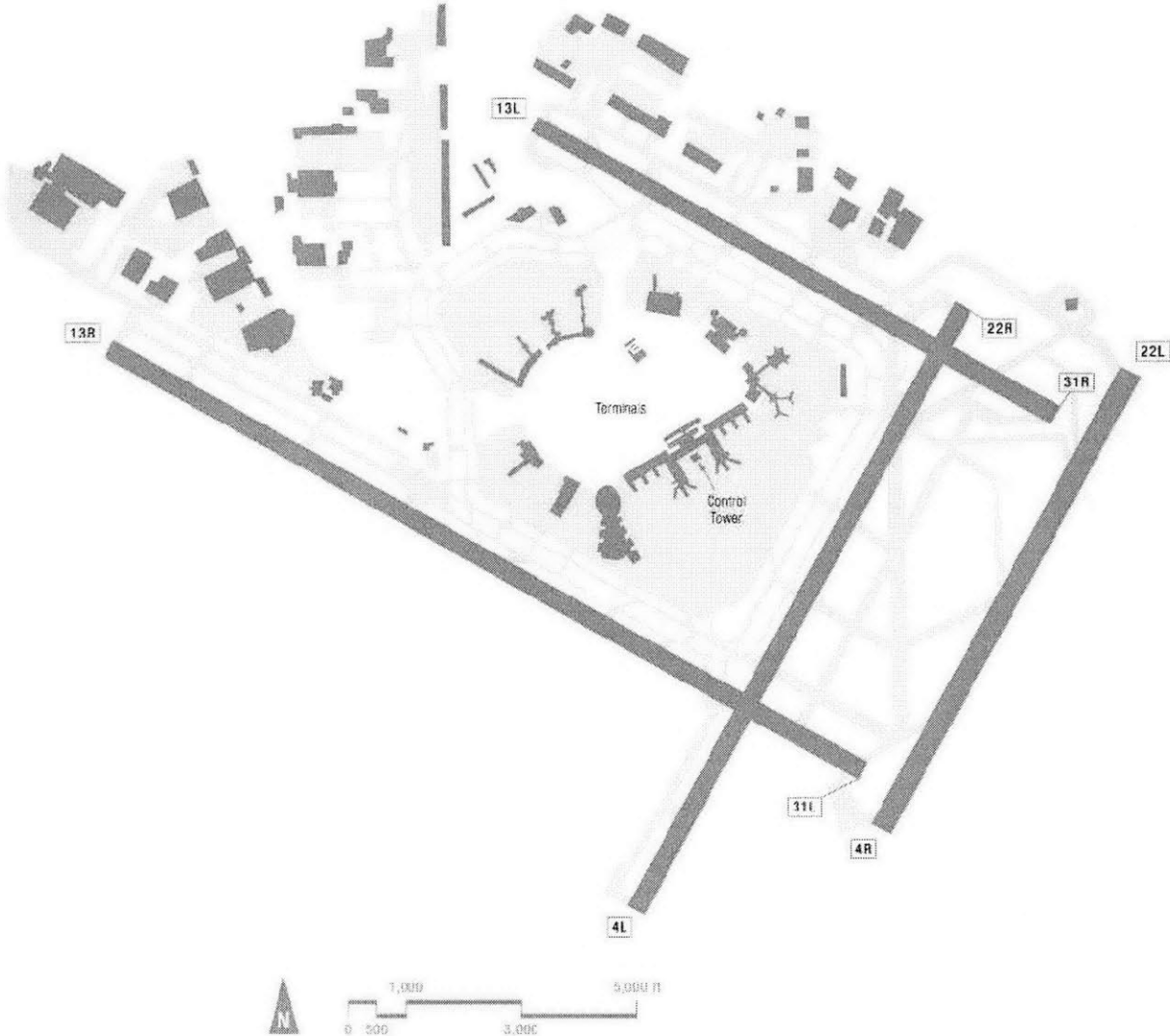


Figure A-1: JFK airport diagram[13]

## A.2 Newark Liberty International Airport (EWR)

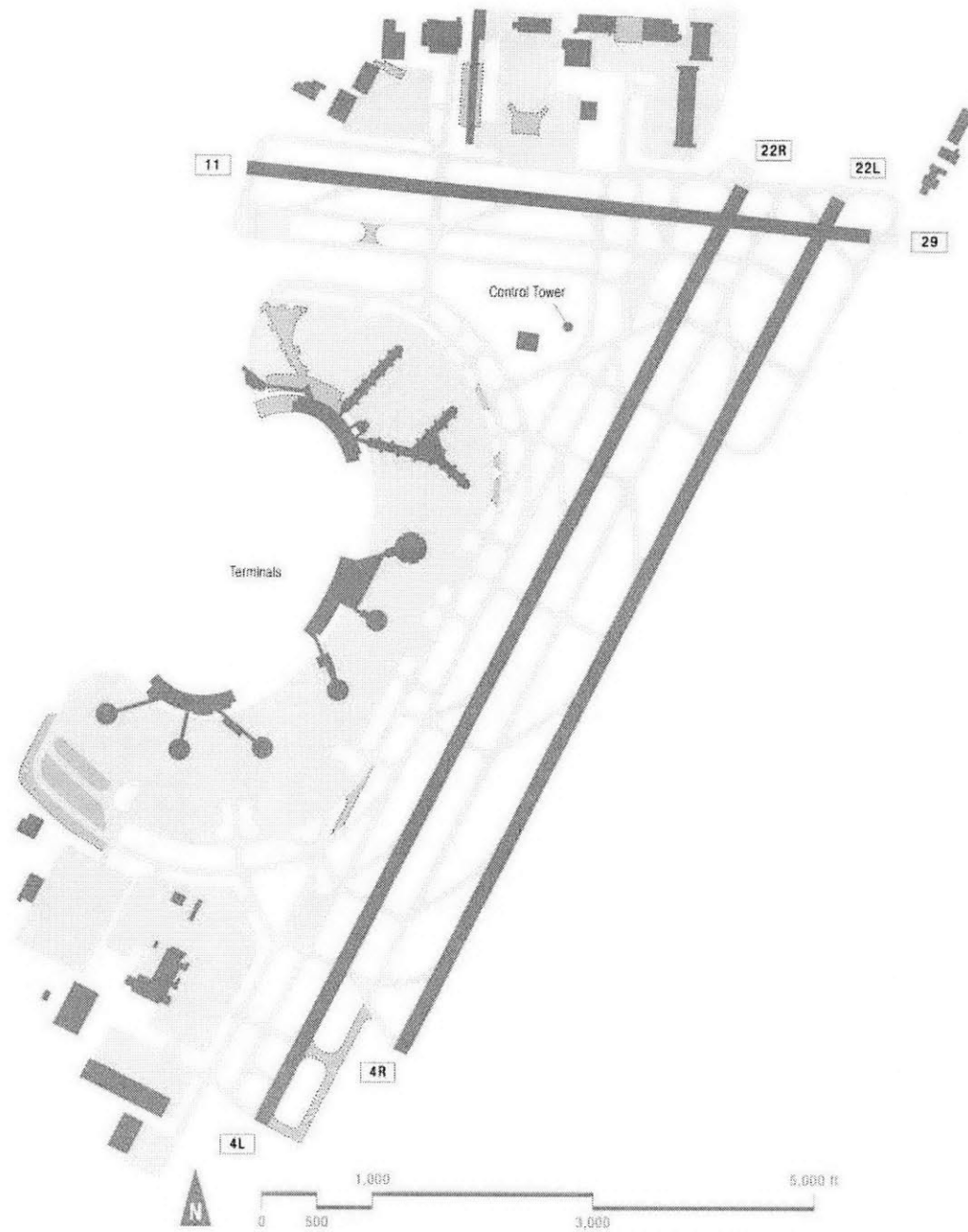


Figure A-2: EWR airport diagram[13]

A.3 Philadelphia International Airport (PHL)

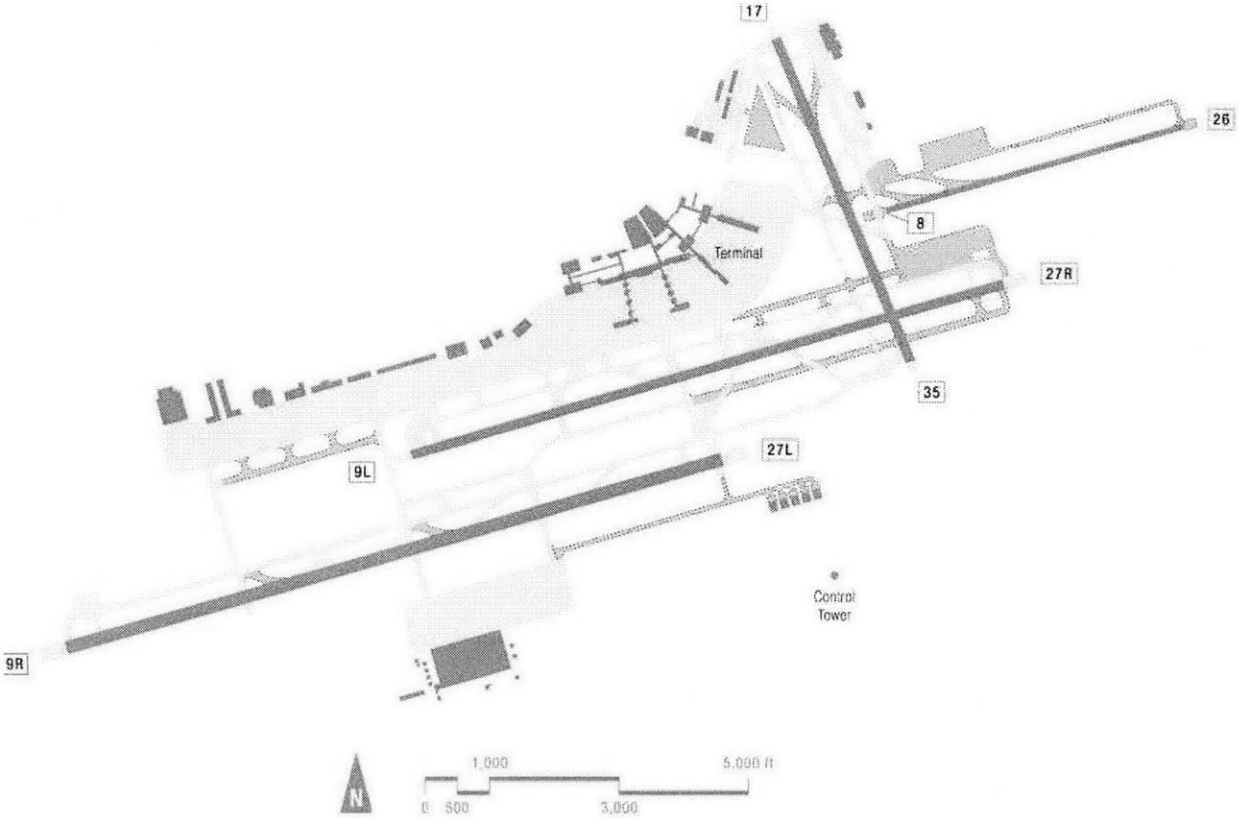


Figure A-3: PHL airport diagram[13]

A.4 Boston Logan International Airport(BOS)

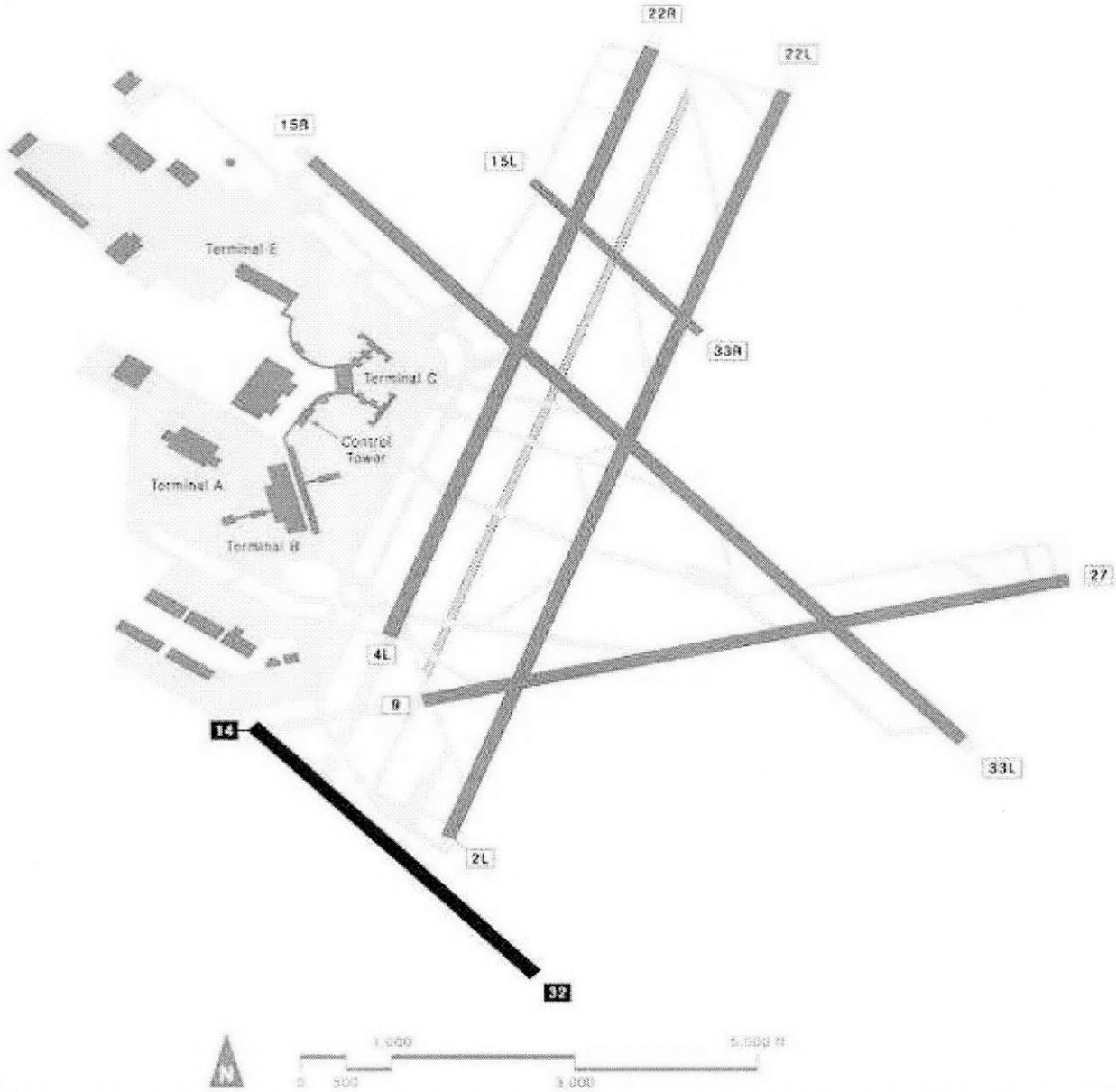


Figure A-4: BOS airport diagram[13]

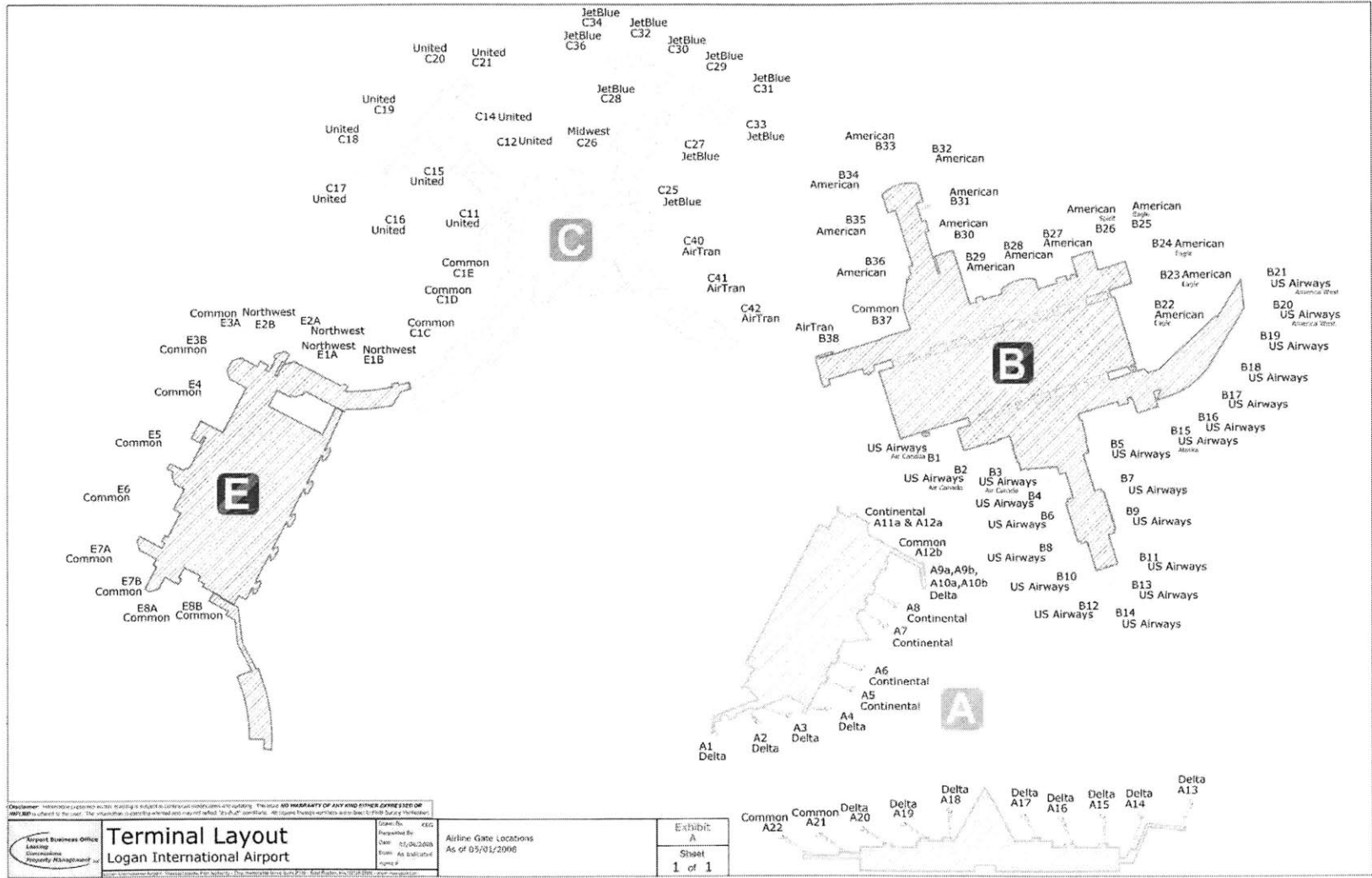


Figure A-5: Allocation of gates to airlines as of May 2008 (courtesy of MASSPORT)

# Appendix B

## Takeoff rate plots

### B.1 John F. Kennedy International Airport(JFK)

#### B.1.1 Visual Meteorological Conditions

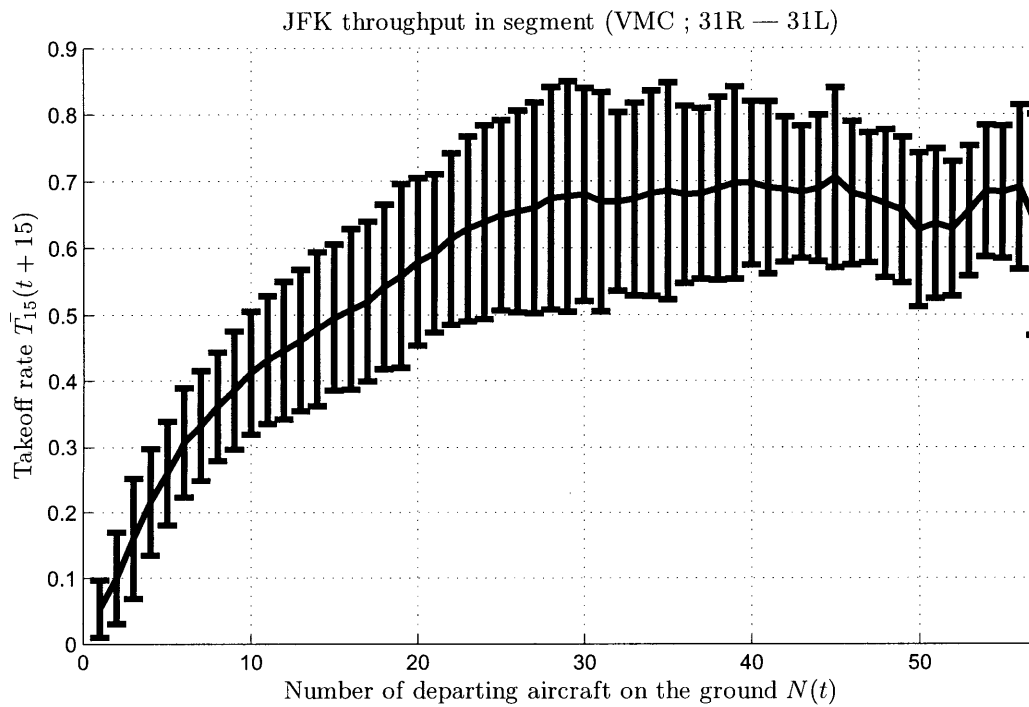
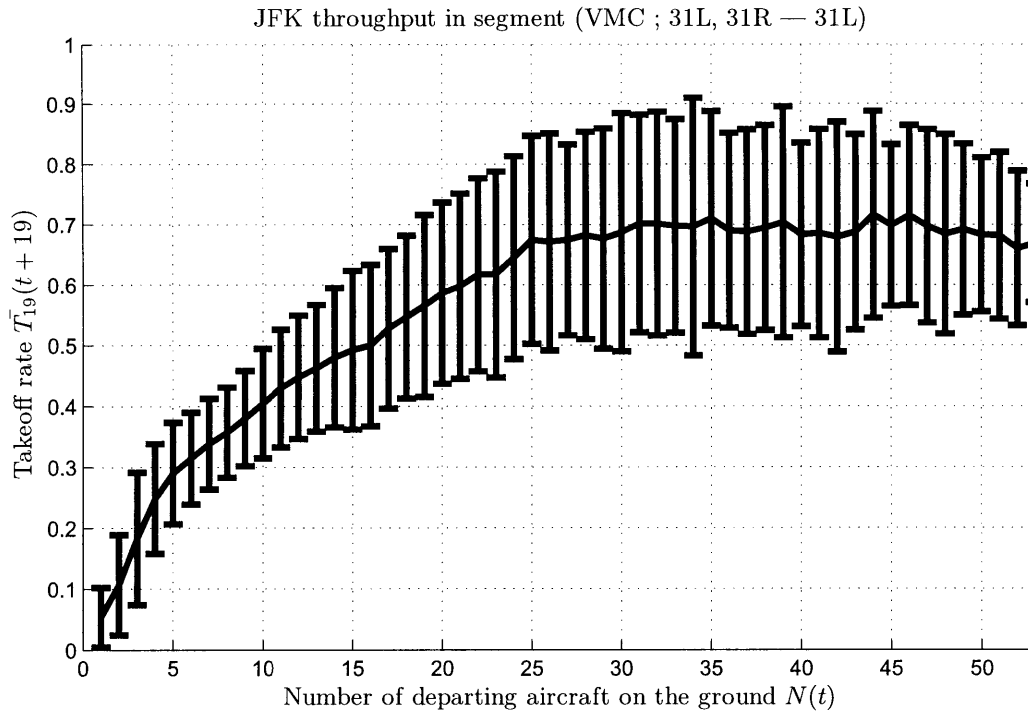
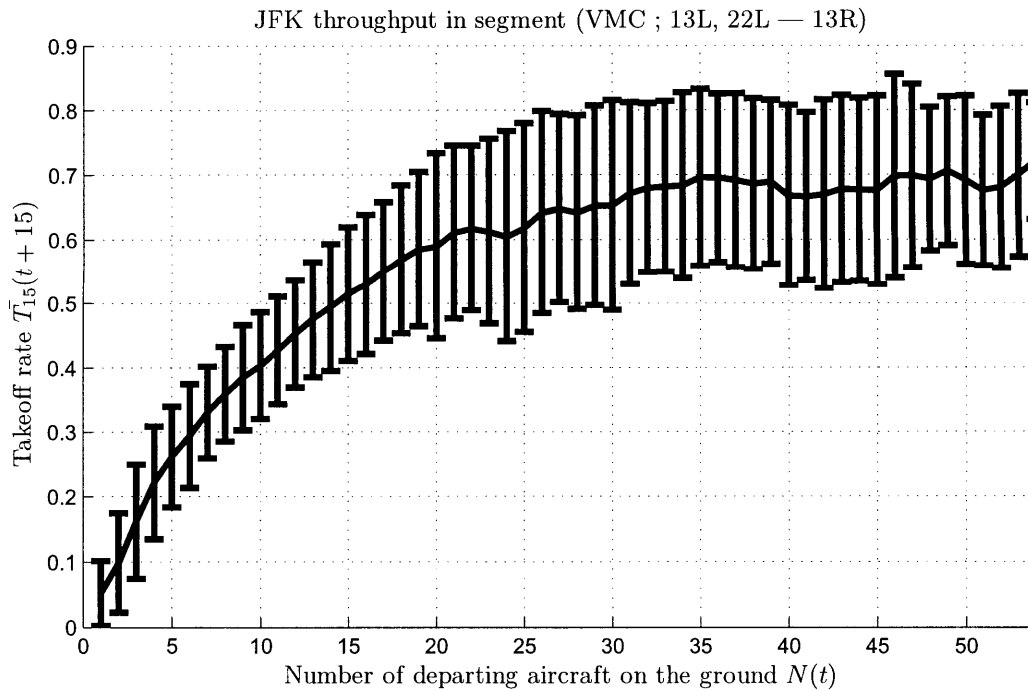


Figure B-1: Takeoff rate as a function of  $N(t)$  in segment (VMC; 31R -31L)



**Figure B-2:** Takeoff rate as a function of  $N(t)$  in segment (VMC; 31L, 31R - 31L)



**Figure B-3:** Takeoff rate as a function of  $N(t)$  in segment (VMC; 13L, 22L - 13R)



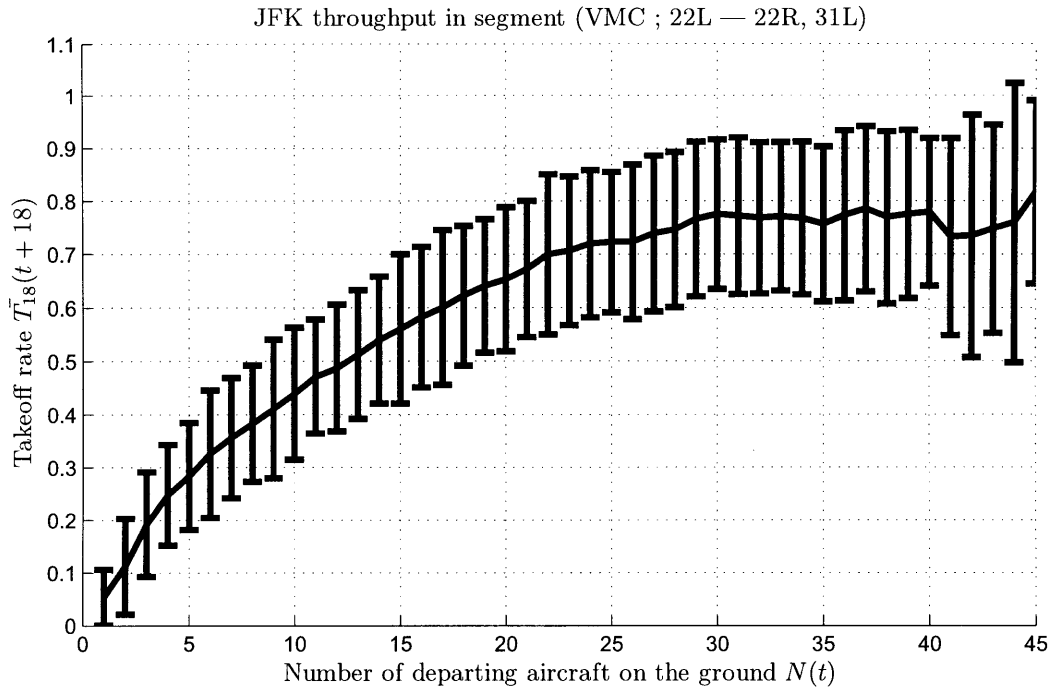


Figure B-4: Takeoff rate as a function of  $N(t)$  in segment (VMC; 22L - 22R, 31L)

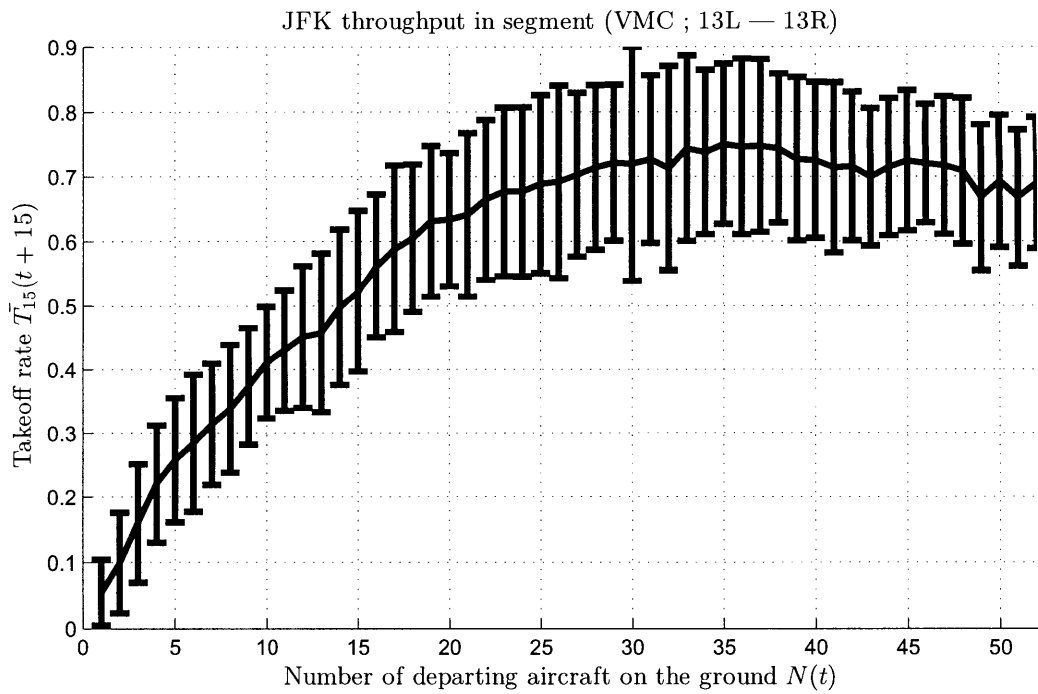
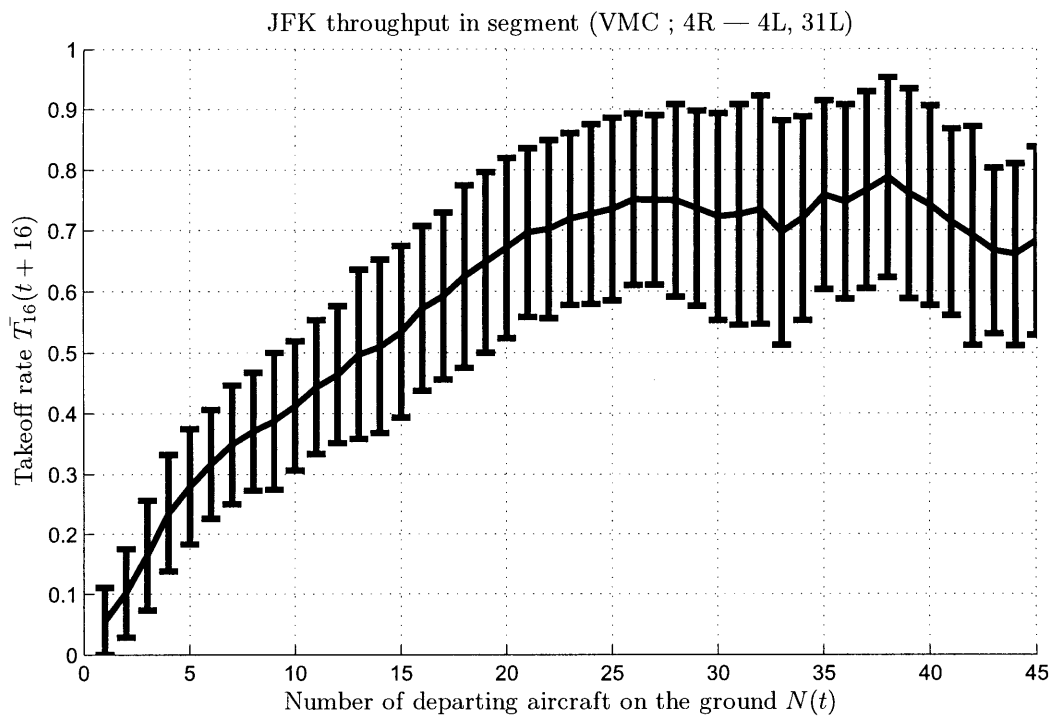


Figure B-5: Takeoff rate as a function of  $N(t)$  in segment (VMC; 13L - 13R)



**Figure B-6:** Takeoff rate as a function of  $N(t)$  in segment (VMC; 4R - 4L, 31L)

### B.1.2 Instrumental Meteorological Conditions

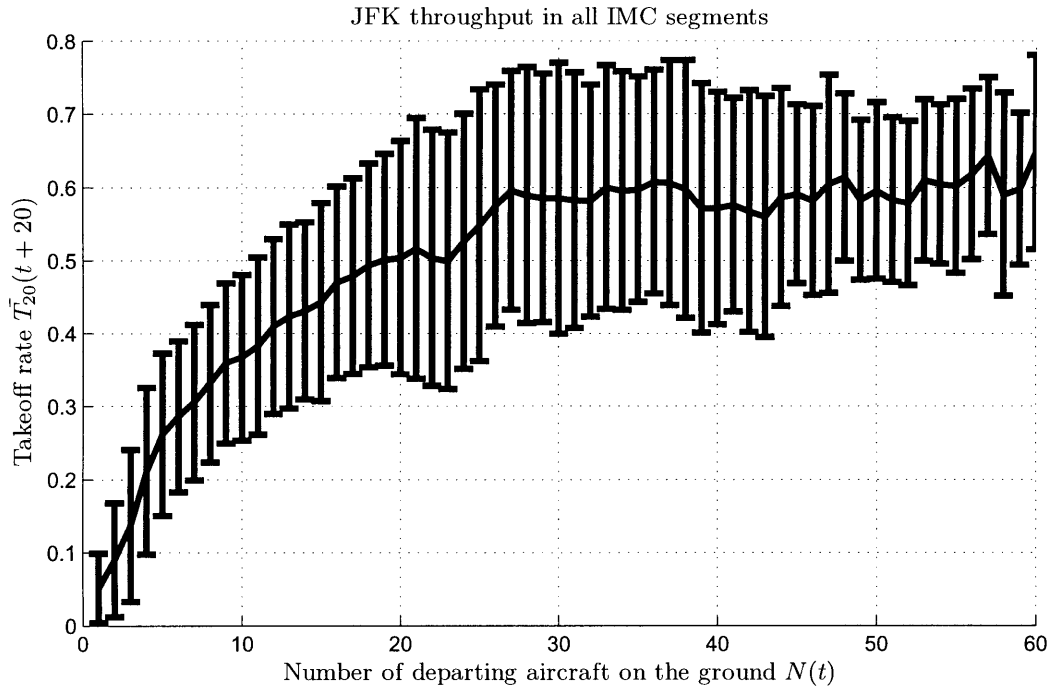
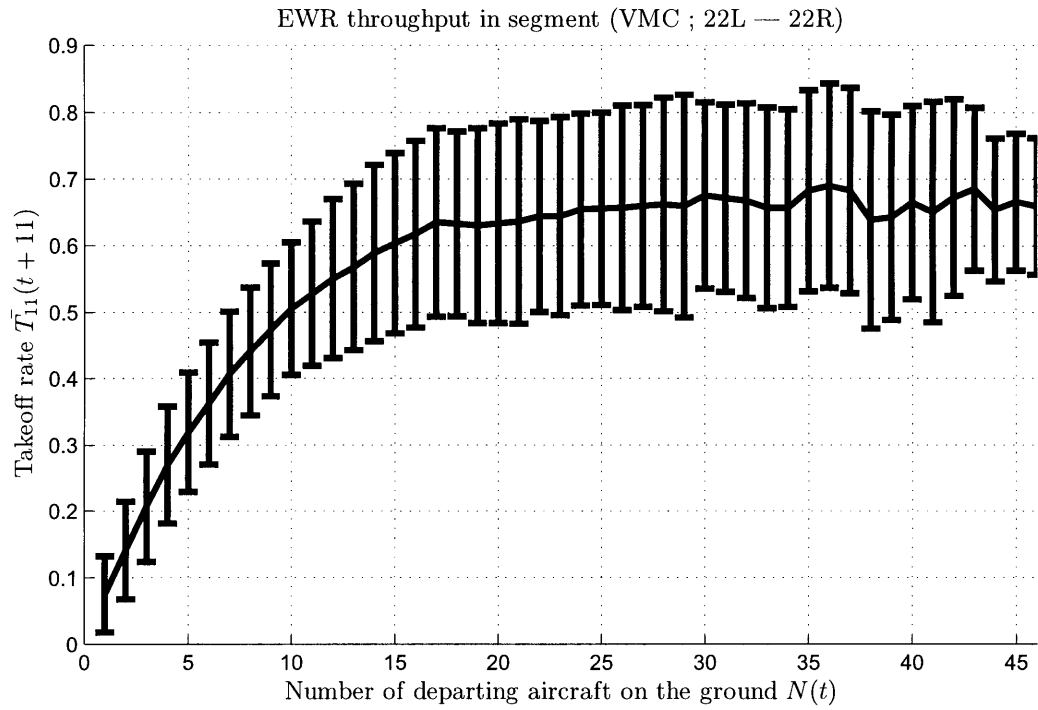


Figure B-7: Takeoff rate as a function of  $N(t)$  in all VMC segments

## B.2 Newark Liberty Airport (EWR)

### B.2.1 Visual Meteorological Conditions



**Figure B-8:** Takeoff rate as a function of  $N(t)$  in segment (VMC; 22L- 22R)

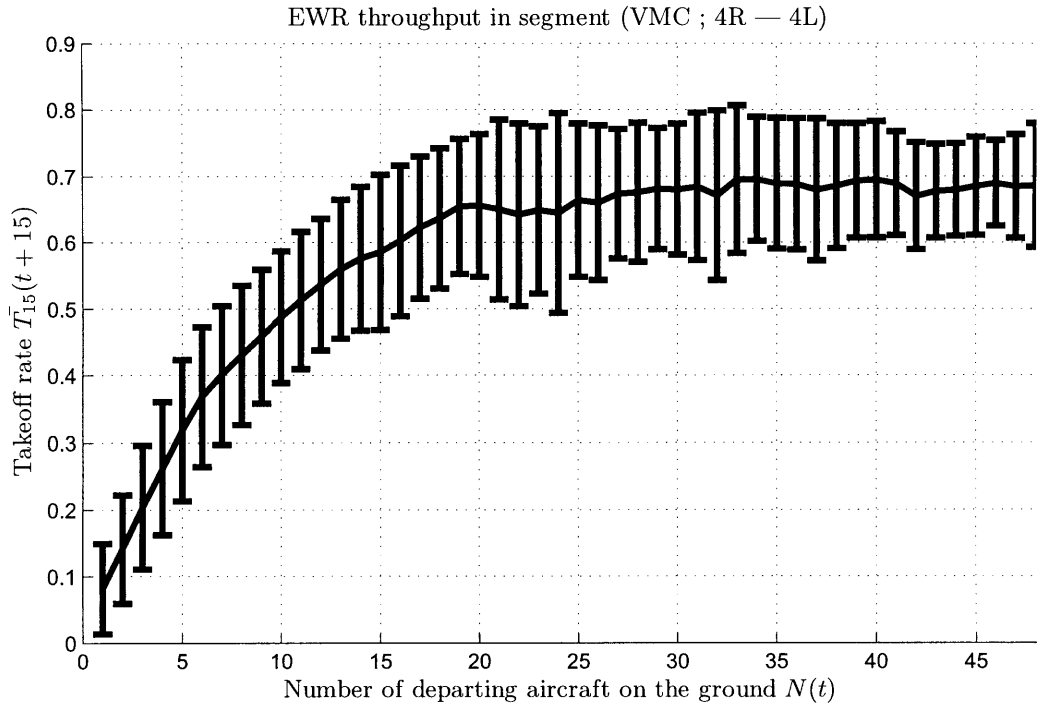


**Figure B-9:** Takeoff rate as a function of  $N(t)$  in segment (VMC; 31L, 4R - 4L)

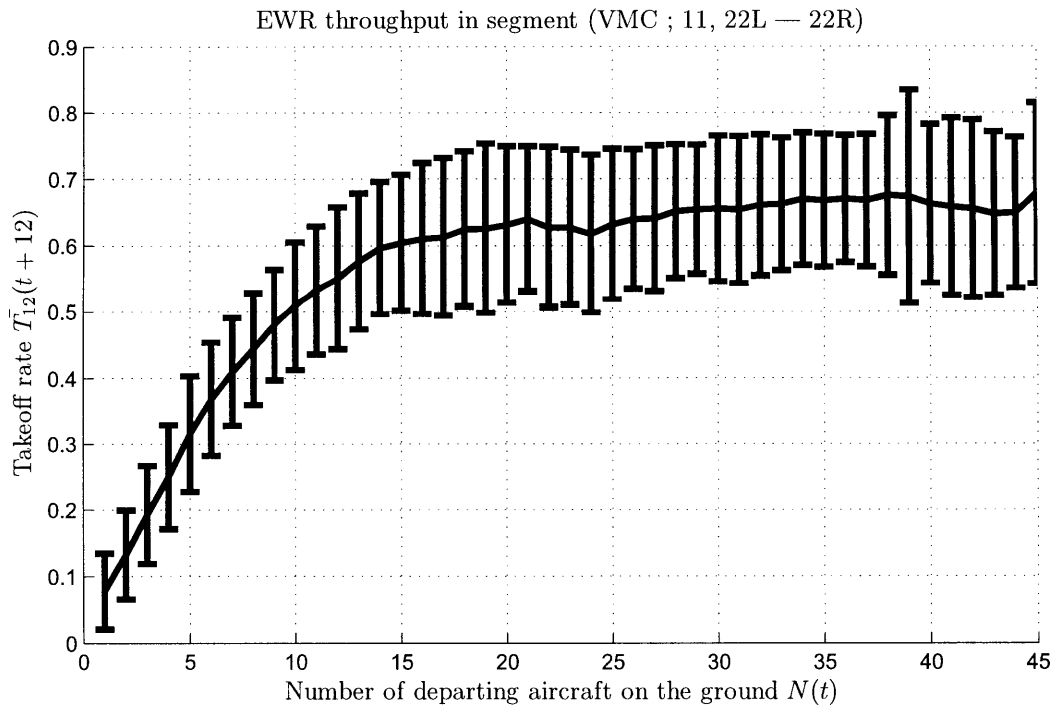


**Figure B-10:** Takeoff rate as a function of  $N(t)$  in segment (VMC; 11, 22L - 22R)

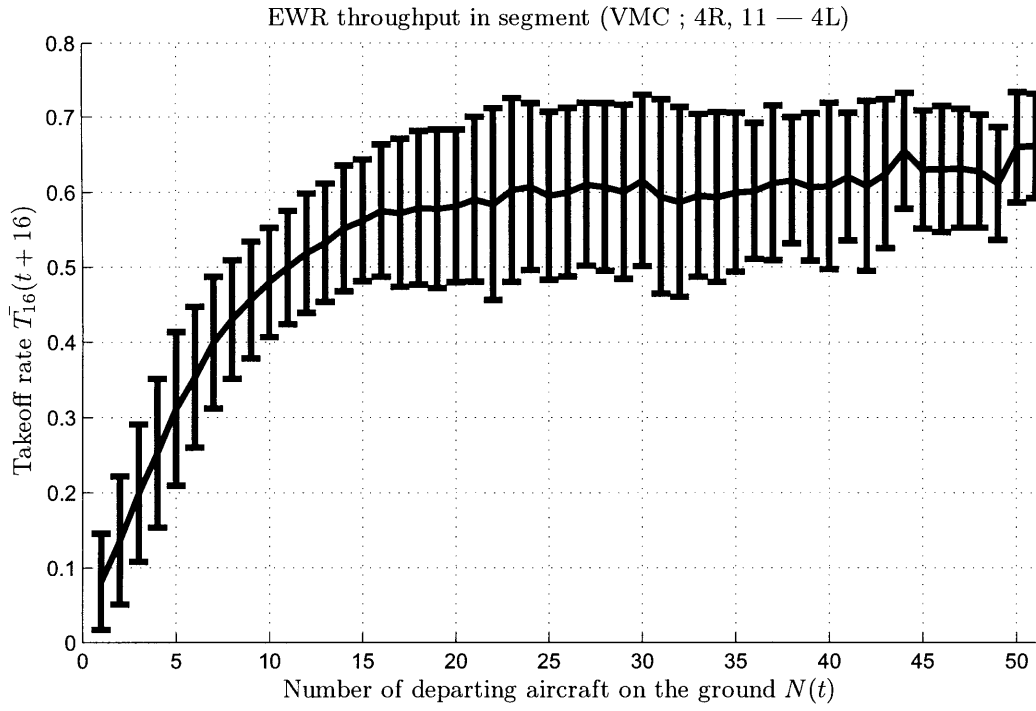


**Figure B-11:** Takeoff rate as a function of  $N(t)$  in segment (VMC; 4R, 11 - 4L)

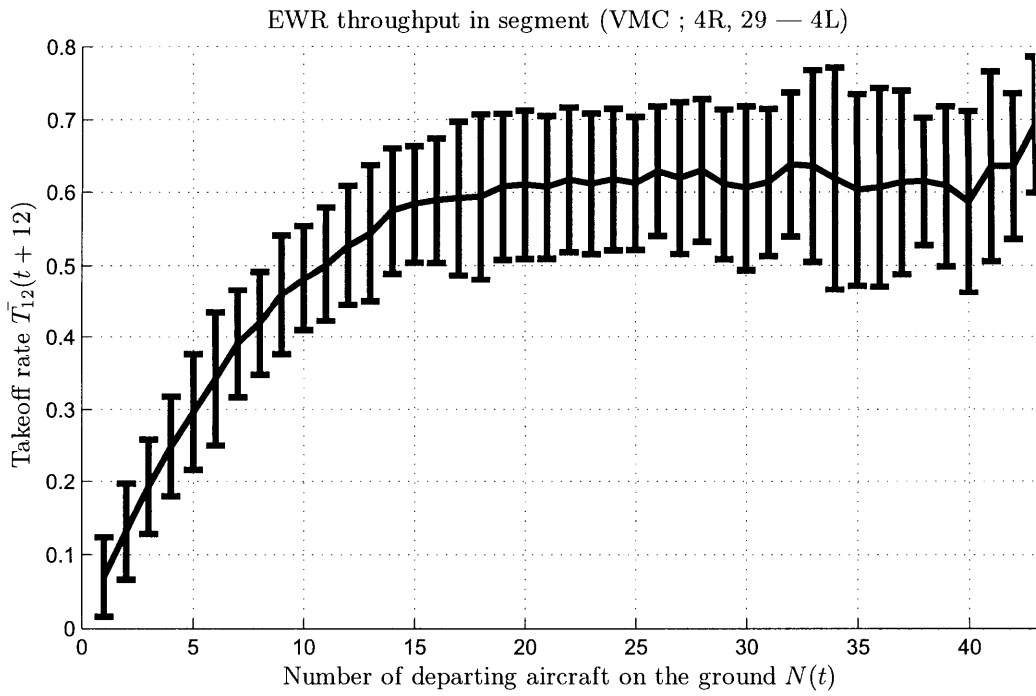


**Figure B-12:** Takeoff rate as a function of  $N(t)$  in segment (VMC; 4R, 29 - 4L)

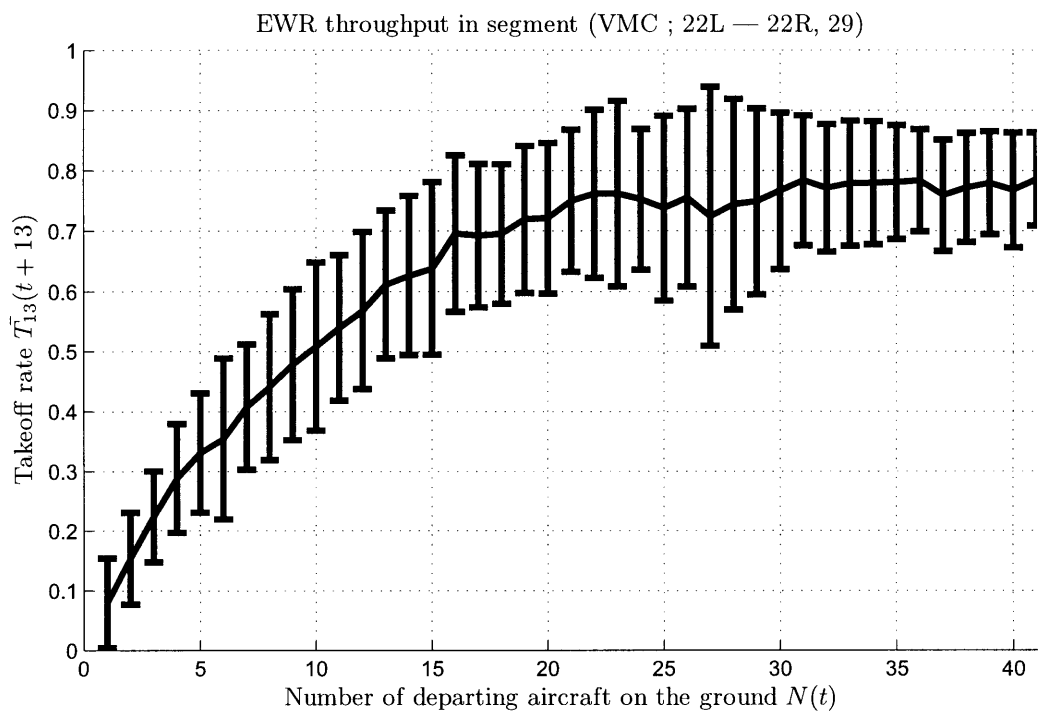


**Figure B-13:** Takeoff rate as a function of  $N(t)$  in segment (VMC; 22L - 22R, 29)

## B.2.2 Instrumental Meteorological Conditions

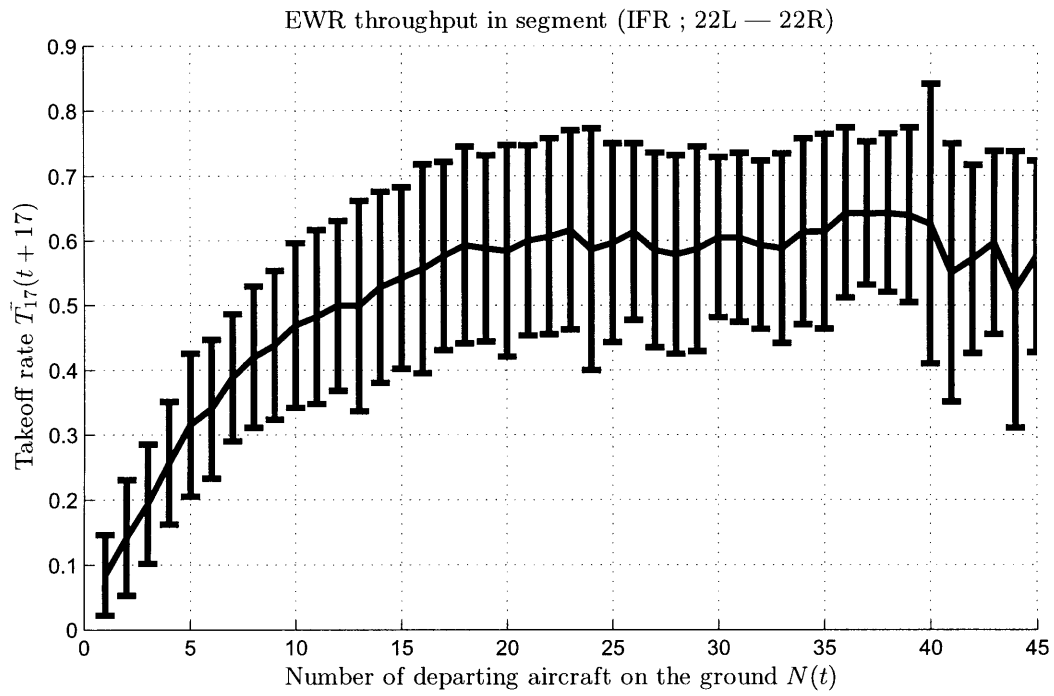
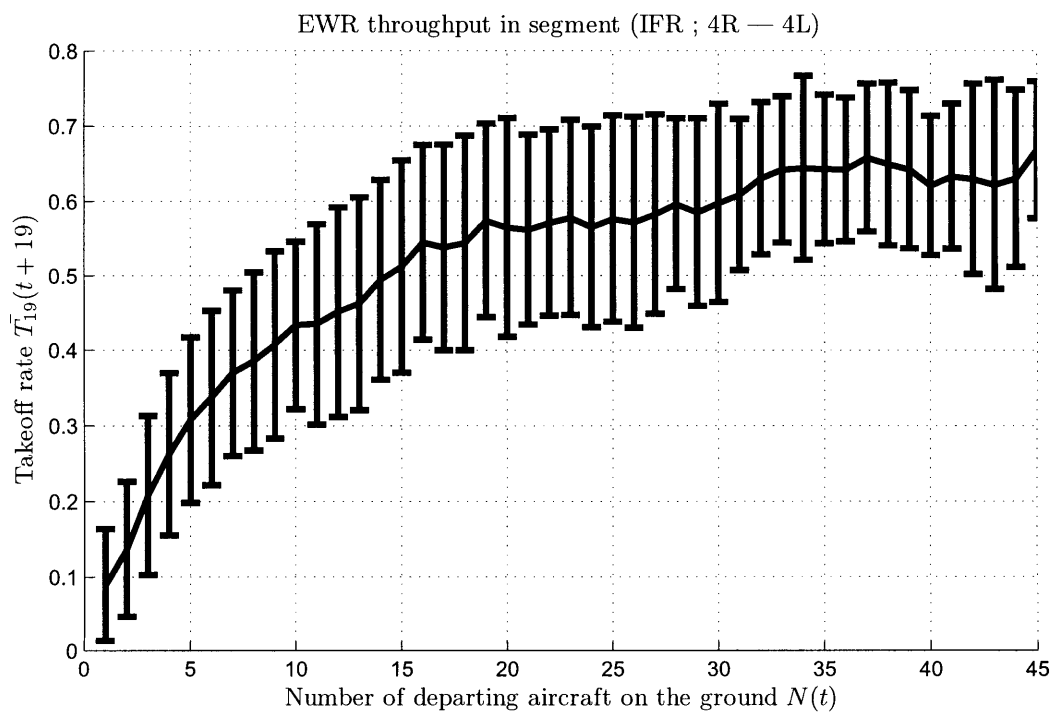


Figure B-14: Takeoff rate as a function of  $N(t)$  in segment (VMC; 22L- 22R)





**Figure B-15:** Takeoff rate as a function of  $N(t)$  in segment (VMC; 4R - 4L)

## B.3 Philadelphia International Airport (PHL)

### B.3.1 Visual Meteorological Conditions

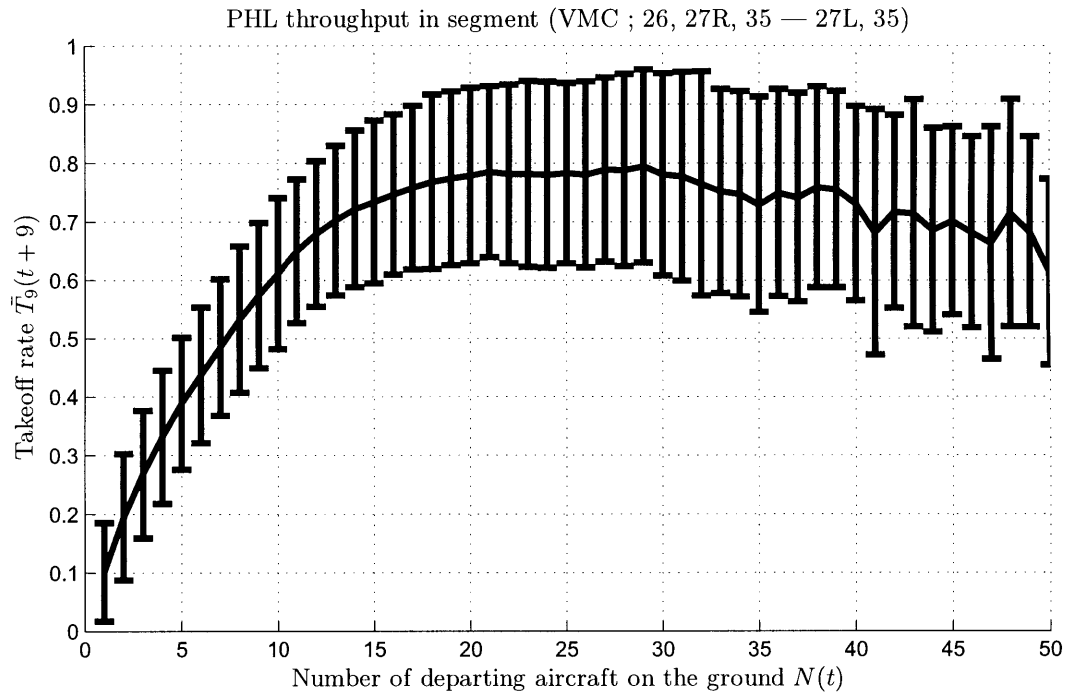
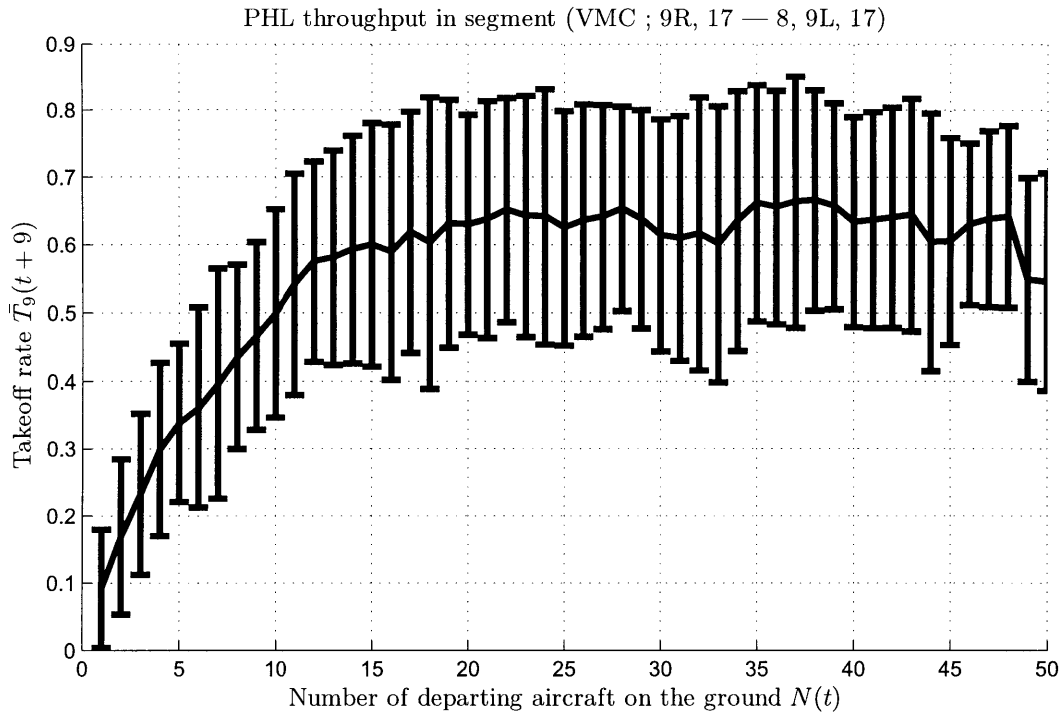
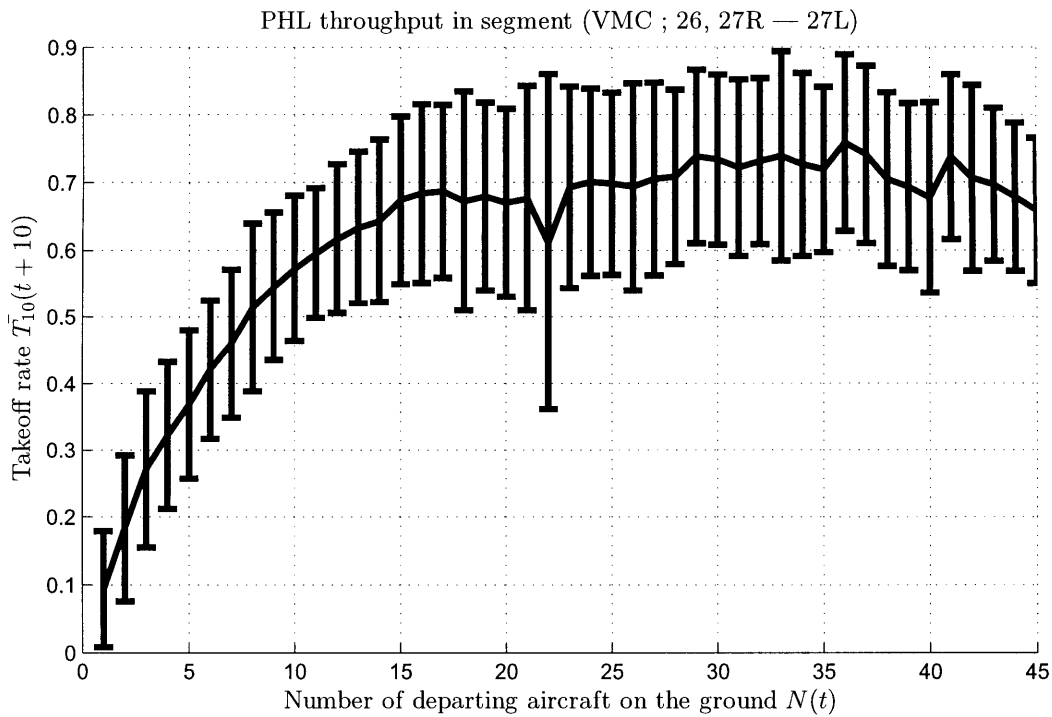


Figure B-16: Takeoff rate as a function of  $N(t)$  in segment (VMC; 26, 27R, 35 - 27L, 35)



**Figure B-17:** Takeoff rate as a function of  $N(t)$  in segment (VMC; 9R, 17 — 8, 9L, 17)



**Figure B-18:** Takeoff rate as a function of  $N(t)$  in segment (VMC; 9R, 35 - 8, 9L, 35)

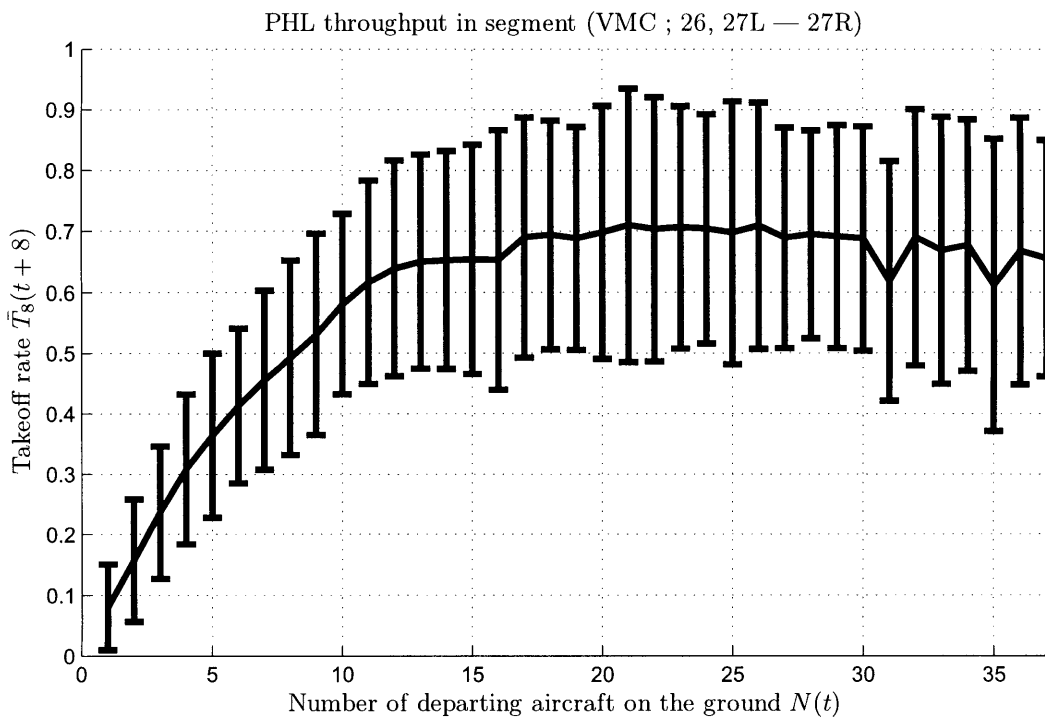


**Figure B-19:** Takeoff rate as a function of  $N(t)$  in segment (VMC; 26, 27R — 27L)

### B.3.2 Instrumental Meteorological Conditions

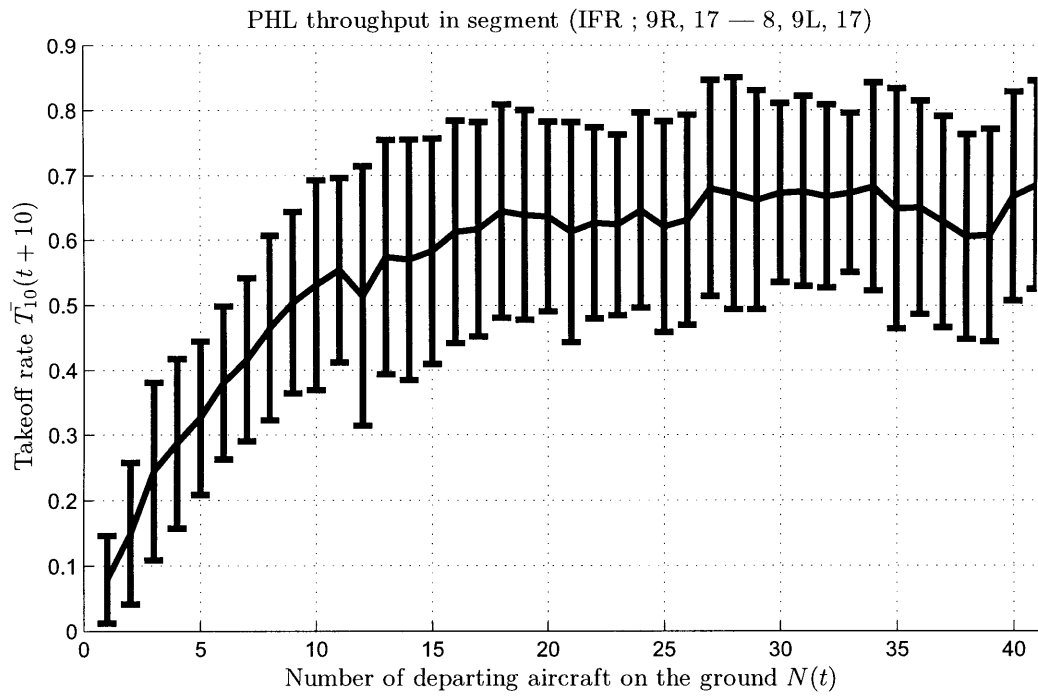
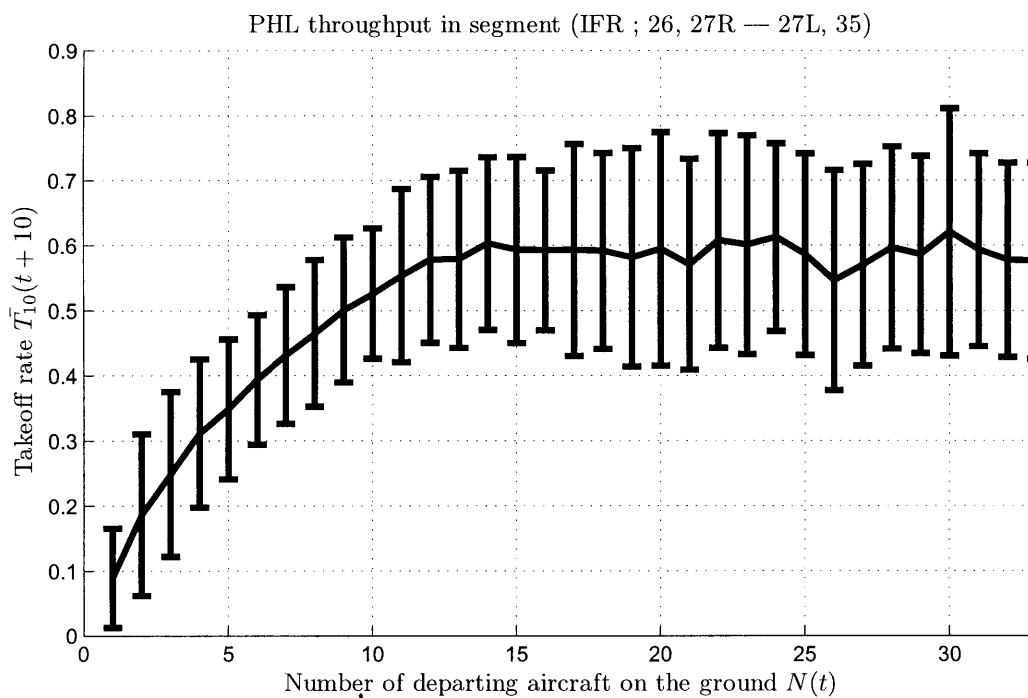


Figure B-20: Takeoff rate as a function of  $N(t)$  in segment (VMC; 9R, 17 - 8, 9L, 17)



**Figure B-21:** Takeoff rate as a function of  $N(t)$  in segment (VMC; 9R - 8, 9L)

# B.4 Boston Logan International Airport (BOS)

## B.4.1 Visual Meteorological Conditions

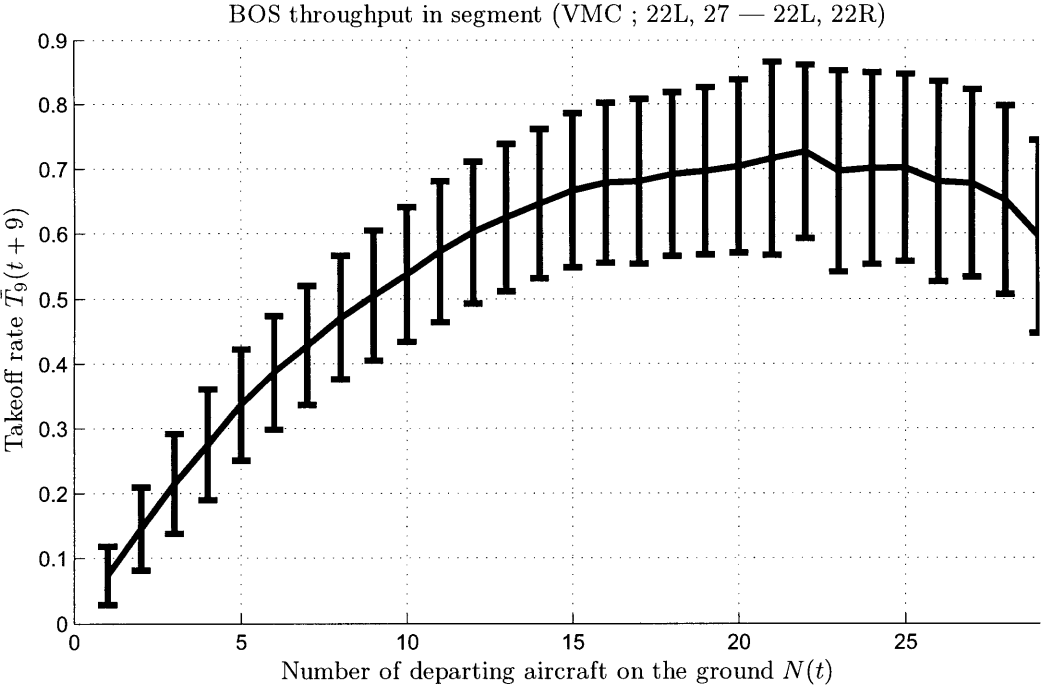


Figure B-22: Takeoff rate as a function of  $N(t)$  in segment (VMC; 22L, 27 — 22L, 22R)

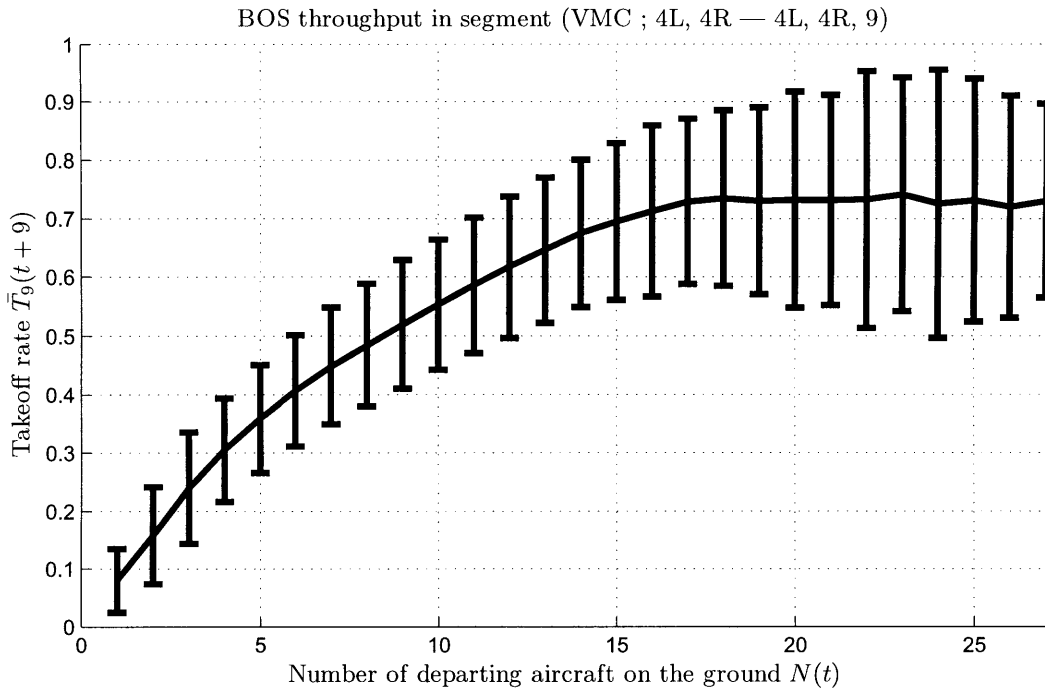


Figure B-23: Takeoff rate as a function of  $N(t)$  in segment (VMC; 4L, 4R — 4L, 4R, 9)

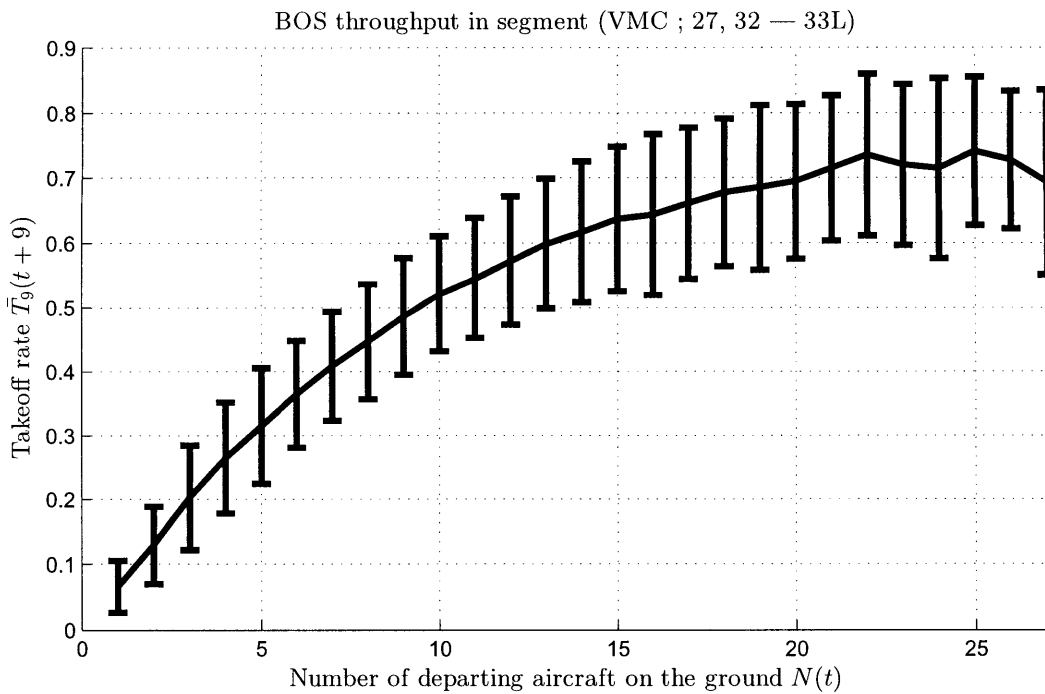


Figure B-24: Takeoff rate as a function of  $N(t)$  in segment (VMC; 27, 32 — 33L)



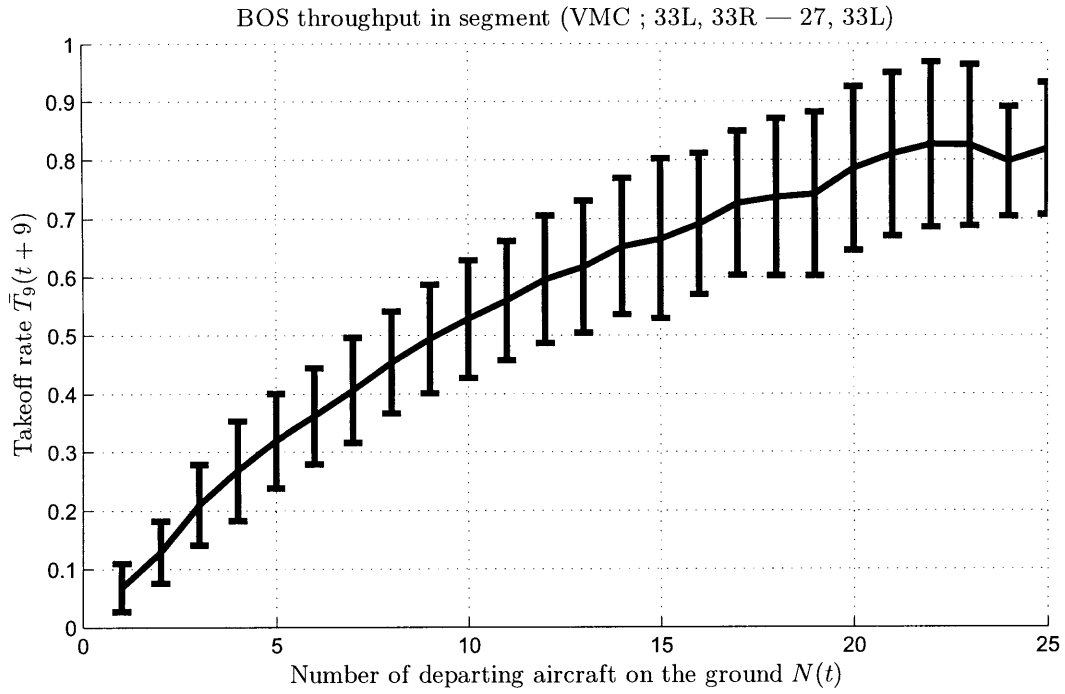


Figure B-25: Takeoff rate as a function of  $N(t)$  in segment (VMC; 33L, 33R — 27, 33L)

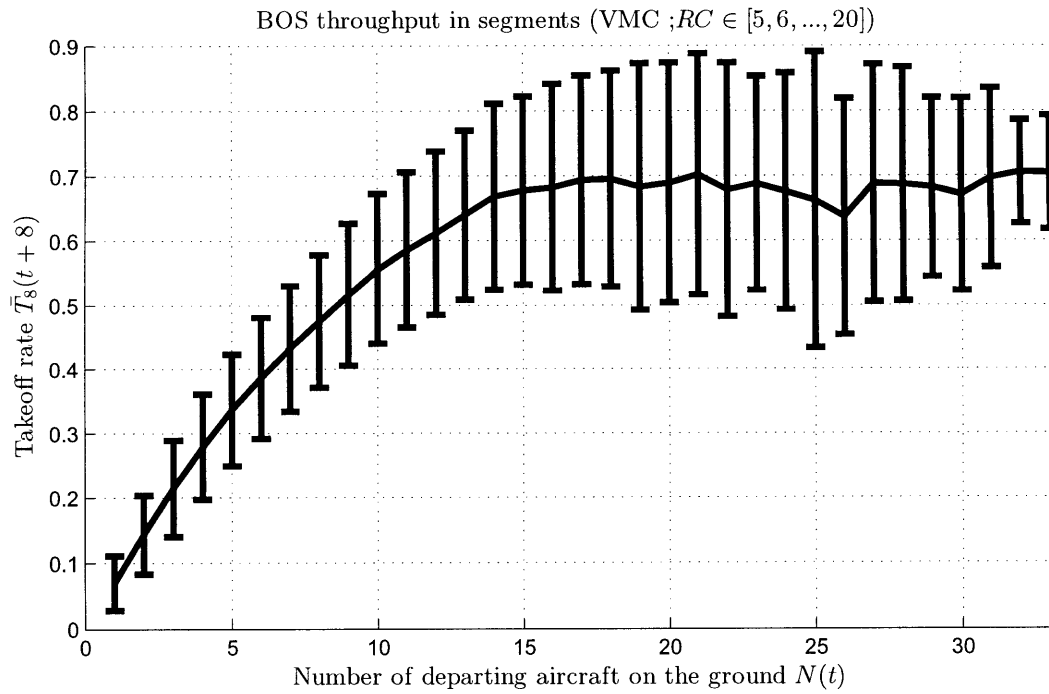


Figure B-26: Takeoff rate as a function of  $N(t)$  in segment (VMC;  $RC \in [5, 6, \dots, 20]$ )

### B.4.2 Instrumental Meteorological Conditions

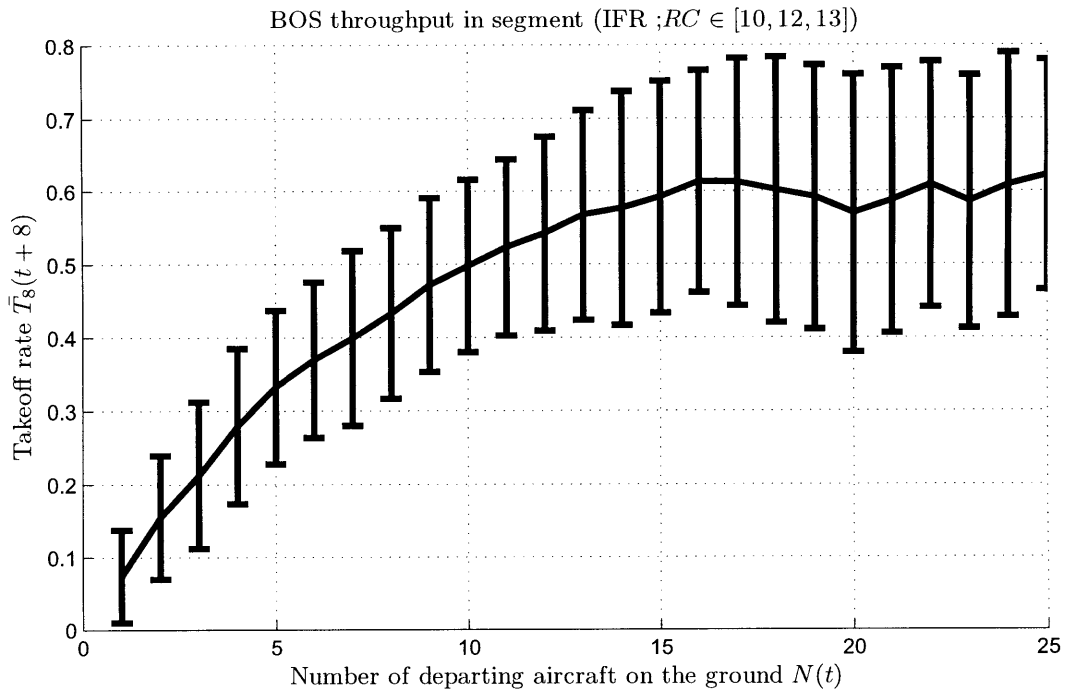


Figure B-27: Takeoff rate as a function of  $N(t)$  in segment (VMC;  $RC \in [10, 12, 13]$ )

# Bibliography

- [1] Airports Council International. Passenger traffic 2007 final, accessed June 2008. <http://www.airports.org/>.
- [2] K. Andersson, F. Carr, E. Feron, and W. Hall. Analysis and modeling of ground operations at hub airports. In *3rd USA/Europe Air Traffic Management R&D Seminar*, 13th-16th June 2000.
- [3] D. P. Bertsekas and J. N. Tsitsiklis. *Introduction to Probability*. Athena Scientific, 2008.
- [4] P. Burgain, E. Feron, J.P. Clarke, and A. Darrasse. Collaborative Virtual Queue: Fair Management of Congested Departure Operations and Benefit Analysis. *Arxiv preprint arXiv:0807.0661*, 2008.
- [5] F. Carr, A. Evans, J.P. Clarke, and E. Feron. Modeling and control of airport queueing dynamics under severe flow restrictions. In *Proceedings of the American Control Conference*, volume 2, 2002.
- [6] F. Carr, A. Evans, E. Feron, and J.P. Clarke. Software tools to support research on airport departure planning. In *Proceedings of the 21st DASC, Irvine CA*, 2002.
- [7] F. R. Carr. *Robust Decision-Support Tools for Airport Surface Traffic*. PhD thesis, Massachusetts Institute of Technology, 2004.
- [8] F.R Carr. Stochastic modeling and control of airport surface traffic. Master's thesis, Massachusetts Institute of Technology, 2001.
- [9] Conductive Technology. Flightstats, accessed September 2008. <http://www.flightstats.com>.
- [10] Christophe Cros and Carsten Frings. Alternative taxiing means – engines stopped. Presented at the Airbus workshop on Alternative taxiing means – Engines stopped, November 2008.
- [11] Richard de Neufville and Amedeo Odoni. *Airport Systems: Planning, Design and Management*. McGraw-Hill, 2003.
- [12] I. Deonandan and H. Balakrishnan. Evaluation of strategies for reducing taxi-out emissions at airports. In *Aviation Technology, Integration, and Operations Conference (ATIO)*, September 2009.
- [13] FAA. Airport capacity benchmark report. Technical report, US Department of Transportation, Federal Aviation Association (FAA), September 2004. <http://www.faa.gov/events/benchmarks>.

- [14] Federal Aviation Administration. Aviation System Performance Metrics, accessed September 2008. <http://aspm.faa.gov>.
- [15] Federal Aviation Administration. Enhanced Traffic Management System Counts, accessed September 2008. <http://aspm.faa.gov/etms>.
- [16] Federal Aviation Administration. The Operations Network, accessed September 2008. <http://aspm.faa.gov/OPSNET>.
- [17] E. R. Feron, R. J. Hansman, A. R. Odoni, R. B. Cots, B. Delcaire, W. D. Hall, H. R. Idris, A. Muharremoglu, and N. Pujet. The Departure Planner: A conceptual discussion. Technical report, Massachusetts Institute of Technology, 1997.
- [18] H. Idris, J. P. Clarke, R. Bhuvva, and L. Kang. Queuing model for taxi-out time estimation. *ATC Quarterly*, 2001.
- [19] H. R. Idris, I. Anagnostakis, B. Delcaire, W. D. Hall, J.-P. Clarke, R. J. Hansman, E. Feron, and A. R. Odoni. Observations of departure processes at Logan airport to support the development of departure planning tools. *Air Traffic Control Quarterly Journal*, 7(4), 1999.
- [20] H. R. Idris, B. Delcaire, I. Anagnostakis, W. D. Hall, N. Pujet, E. Feron, R. J. Hansman, J. P. Clarke, and A. R. Odoni. Identification of flow constraint and control points in departure operations at airport systems. In *AIAA Guidance, Navigation and Control Conference*, August 1998.
- [21] Husni Rifat Idris. *Observation and analysis of departure operations at Boston Logan International Airport*. PhD thesis, Massachusetts Institute of Technology, 2001.
- [22] International Civil Aviation Organization. ICAO Engine Emissions Databank, July 2007.
- [23] Peeter Andrus Kivestu. Alternative methods of investigating the time dependent mngk queue. Master's thesis, Massachusetts Institute of Technology, 1976.
- [24] Kerry Marie Malone. *Dynamic queueing systems : behavior and approximations for individual queues and for networks*. PhD thesis, Massachusetts Institute of Technology, 1995.
- [25] National Aeronautics and Space Administration. Traffic management advisor, accessed June 2008. <http://www.aviationsystemsdivision.arc.nasa.gov/research/foundations/tma.shtml>.
- [26] Federal Aviation Administration Office of Aviation Policy and Plans. Documentation for the aviation system performance metrics: Actual versus scheduled metrics. Technical report, 2002.
- [27] Office of Aviation Policy and Plans, Federal Aviation Administration. Documentation for the Aviation System Performance Metrics (ASPM), May 2002.
- [28] N. Pujet, B. Delcaire, and E. Feron. Input-output modeling and control of the departure process of congested airports. *AIAA Guidance, Navigation, and Control Conference and Exhibit, Portland, OR*, pages 1835–1852, 1999.
- [29] Nicolas Pujet. *Modeling and control of the departure process of congested airports*. PhD thesis, Massachusetts Institute of Technology, 1999.
- [30] Robert Arthur Shumsky. *Dynamic statistical models for the prediction of aircraft take-off times*. PhD thesis, Massachusetts Institute of Technology, 1995.

- [31] M. Terrab and A.R. Odoni. Strategic flow management for air traffic control. *Operations Research*, pages 138–152, 1993.
- [32] U.S. Department of Transportation. Bureau of Transportation Statistics, accessed Sept. 2008. [www.transtats.bts.gov](http://www.transtats.bts.gov).